PHENOTYPIC CHARACTERIZATION OF SELF-ASSEMBLING PROTEIN FRAGMENTS USING NEGATIVE DOMINANCE

A Dissertation

by

ADRIENNE ELIZABETH ZWEIFEL

Submitted to the Office of Graduate Studies of
Texas A&M University
in partial fulfillment of the requirements for the degree of

DOCTOR OF PHILOSOPHY

May 2010

Major Subject: Biochemistry

PHENOTYPIC CHARACTERIZATION OF SELF-ASSEMBLING PROTEIN FRAGMENTS USING NEGATIVE DOMINANCE

A Dissertation

by

ADRIENNE ELIZABETH ZWEIFEL

Submitted to the Office of Graduate Studies of
Texas A&M University
in partial fulfillment of the requirements for the degree of

DOCTOR OF PHILOSOPHY

Approved by:

Chair of Committee,	James C. Hu
Committee Members,	Michael Polymenis
	Donald W. Pettigrew
	Michael Benedik
Head of Department,	Gregory D. Reinhart

May 2010

Major Subject: Biochemistry

ABSTRACT

Phenotypic Characterization of Self-Assembling
Protein Fragments Using Negative Dominance. (May 2010)
Adrienne Elizabeth Zweifel, B.S., University of Missouri-Columbia
Chair of Advisory Committee: Dr. James C. Hu

Protein oligomerization provides a way for cells to modulate function *in vivo*. In this study, self-assembling protein fragments from ParC, DnaX, and proteins of unknown function were used to generate phenotypes in a dominant negative manner. These fragments were expressed as Thioredoxin (TRX) fusions under the control of the inducible *araBAD* promoter. Fragments chosen contain only the oligomerization domain of the protein, lacking the regions necessary for catalytic function.

Fragments of ParC, a subunit of Topoisomerase (Topo) IV, generated fragment-specific phenotypes. Regions that expressed both the oligomerization domain and CTD of ParC (ParC206-752 and ParC332-752) yielded filamentous cells with several different nucleoid segregation phenotypes. Another ParC fragment containing only the oligomerization domain of ParC (ranging from 333-485) yields a *recA*-dependent septation defect in a subset of the population. This phenotype suggests that Topo IV may be inhibiting chromosome dimer resolution.

The overexpression of DnaX247-455, a fragment containing regions of both the tau and gamma subunits of the DNA Polymerase III holoenzyme, led to a severe plating defect. Upon further investigation, this fragment caused filamentation, a nucleoid defect, and induction of *sulA*, similar to the effects seen with the *dnaX* temperature-sensitive alleles.

The overexpression of the various y-protein fragments yielded a variety of media-specific plating defects on over 50% of the proteins tested. The overexpression of the protein fragments yielded effects that were not seen by other overexpression or deletion experiments, even under similar growth conditions. The results presented here show that the overexpression of self-assembling fragments yield a variety of dominant negative phenotypes. Reducing the activity of protein complexes allows for new aspects of the physiological process to be investigated.

NOMENCLATURE

Topo I	Topoisomerase I
Topo III	Topoisomerase III
Topo IV	Topoisomerase IV
CTD	C-terminal domain
TRX	Thioredoxin
CAA	Casamino acids
NO	Nucleoid Occlusion

TABLE OF CONTENTS

LIST OF FIGURES

FIGURE Page

LIST OF TABLES

CHAPTER I

INTRODUCTION

In this dissertation new phenotypes in *Escherichia coli* were characterized in order to bring insight into the biology and regulation of replication, chromosome segregation, and septation as well as identifying conditions under which proteins of unknown function may be studied.

Negative Dominance

Negative dominance is a genetic tool used to investigate function in the context of protein complex assembly. Protein oligomerization is regularly used by cells as a way to modulate protein function *in vivo*-at least 35% of proteins in the cell are predicted to be oligomeric (Goodsell and Olson, 2000). These oligomeric complexes are more stable, allow for more complex structures and finer tuning of regulation than their monomeric counterparts. Transient oligomerization is one way the cell regulates physiological processes. The presence of environmental factors promotes transient oligomerization, promoting specificity and control. Protein interfaces provide unique and stable active and allosteric sites that would be obliterated if oligomerization were disrupted.

Conventional genetic methods used to study protein function usually involve mutagenesis

---

This dissertation follows the style of *Molecular Microbiology*.

or deletion of a gene, which results in a *cis*-acting defect in function. The ability to isolate conditional mutations is a valuable genetic tool that results in the inducible inactivation of protein function. The resulting phenotype allows the processes involving the gene to be characterized. Another method to study *in vivo* function is inhibiting the protein *in trans.* Many studies have used peptide inhibitors to block catalysis at the active site or by blocking allosteric sites.

Negative dominance represents one way to inactivate an oligomeric enzyme or protein complex independent of the gene. In theory, variants of the endogenous protein expressed from a plasmid are presented in excess and therefore interact with a subpopulation of the target in a dominant manner, as shown in Figure 1.1. If these variants were inert with respect to catalysis, then the mutant would give a negative phenotype. The proposed result is a mixture of both functional and inert complexes *in vivo*, thereby knocking down the overall activity of a complex instead of completely obliterating its function. Using this method, overall heterogeneous interactions would be preserved. Essential genes for which conditional mutant alleles have not been isolated would be good targets for use with negative dominance. Since the effect is *in trans*, mutations or disruptions in the gene are not required and inducible expression of the negative dominant effectors allows characterization of intermediate levels of inactivation.

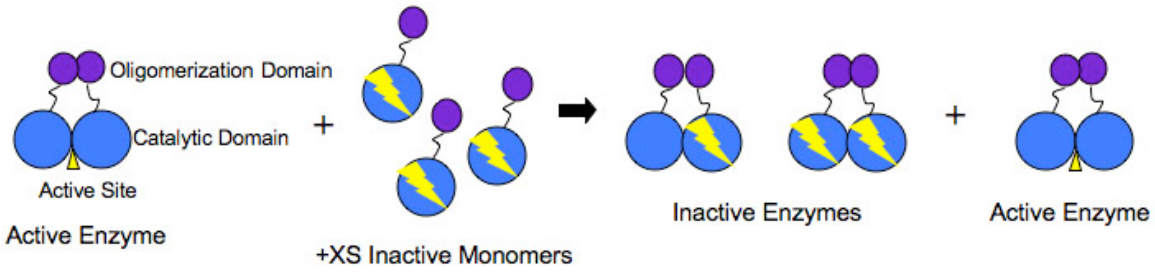

Figure 1.1: Theory of Negative Dominance. In the presence of excess inactive monomers, the population will consist of both inactive enzymes and active ones.

There are several inherent benefits to blocking oligomerization as a means of modulating function. First, the residues at the interface of proteins have a tendency to be slightly more conserved than other residues throughout the protein (Caffrey *et al.*, 2004). This means that it would be less likely for the inhibition provided by the fragment to be overridden by mutations. Second, interrupting oligomerization allows you to define monomeric contribution to the overall function.

A screen identified 232 nonredundant *E. coli* protein fragments that could self-assemble when fused to the DNA-binding domain of the lambda cI repressor (Marino-Ramirez *et al.*, 2004). The majority of these fragments contain the oligomerization domain of the protein, but lack regions required for catalysis. If these fragments reflect the same binding properties as the endogenous full-length protein, then expressing the fragments may produce a negative dominant phenotype by interrupting both homotypic and heterotypic protein interactions.

There are several ways to disrupt complex formation, as shown in Figure 1.2. Fragments supplied in excess bind to the monomer of a homo-oligomeric complex. This is expected to result in a mixture of wild type complexes and heteromultimers between the full-length and the fragment. If function depends upon self-assembly, then the heteromultimers will be inactive, thereby knocking down the overall activity of the complex *in vivo* as modeled in Figure 1.2A.

(A)

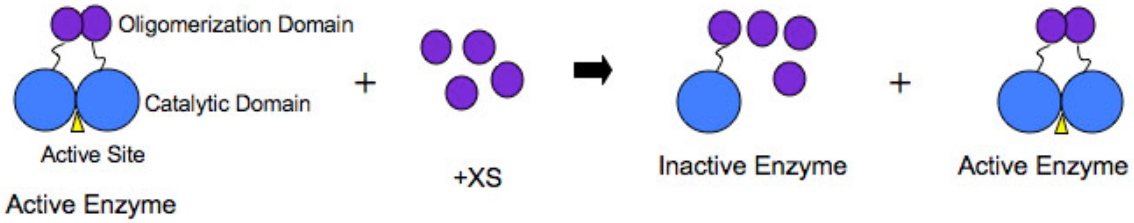

(B)

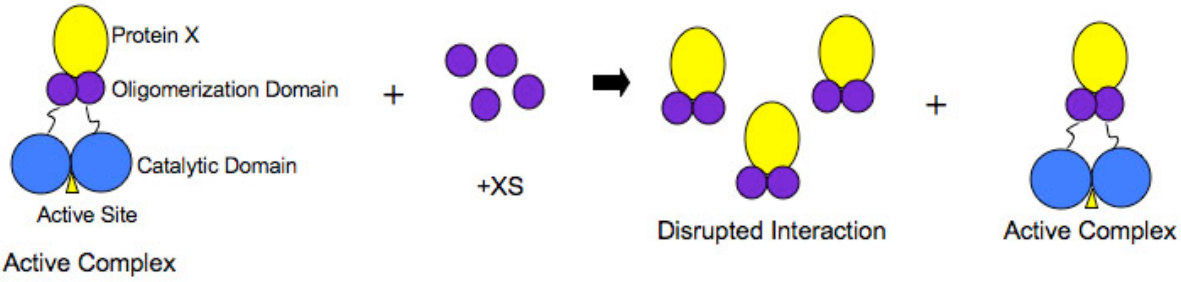

Figure 1.2: Proposed Mechanisms for Negative Dominance Using Oligomerization Domains. (A) Fragments containing oligomerization domains and (B) Protein target X disruption with the self-assembling fragments.

These overexpressed fragments can also interact with other protein targets in the cell, resulting in the disruption of hetero-oligomeric complexes. These interactions allow binding partners of the protein of interest to be identified and mapped onto the structure. This outcome is depicted in Figure 1.2B.

Among the protein fragments identified was the topoisomerase IV subunit ParC. My work in Chapter 3 suggests that it is involved in mediating the septation delay checkpoint that links chromosome segregation to cell division. Here I will review what is known about Topo IV and its roles in the cell.

Chromosomal Maintenance

Escherichia coli (E. coli) is a gram-negative bacterium ranging from 1-2 μm in length whose chromosome is a closed circular ring consisting of 4.6 million base pairs (Blattner *et al.*, 1997; Riley *et al.*, 2006). The chromosome encodes for approximately 4,300 protein-encoding genes that must be organized and accessible such that the cell may alter its expression pattern should changes in its environment arise. In order to be able to still utilize the information encoded within the DNA, the chromosome is supercoiled and folded into structural domains.

Topoisomerases

DNA is a negatively supercoiled, right-handed helix. This level of supercoiling allows for easier strand separation during replication or transcription (Peter *et al.*, 2004; Marians *et al.*, 1986). The topological properties of DNA can be described using a term called the

Linking Number (Lk). Lk is defined as the number of times one strand crosses over the other. It cannot be changed except via a break in the phosphodiester backbone.

The proteins that are responsible for adjusting supercoiling in the cell are called topoisomerases. There are four topoisomerases in *E.coli* as shown in Table 1.1, classified by whether they change the linking number in steps of 1 or 2.

Table 1.1: Four Topoisomerases in *E.coli*.

Name	Gene	Cellular Role	Reference
Type I Topoisomerases			
Topo I	*topA*	Introduction of (+) Supercoils	Zechiedrich et al., 2000
Topo III	*topB*	Recombination	Lopez et al., 2005
		Decatenation	Nurse et al., 2003
Type II Topoisomerases			
DNA Gyrase	*gyrA/ gyrB*	Introduction of (-) Supercoils	Zechiedrich et al., 2000
Topo IV	*parC/ parE*	Decatenation	Adams et al., 1992
		Unknotting	Deibler et al., 2001
		Removal of Precatenanes	Wang et al., 2008
		Introduction of (-) Supercoils	Zechiedrich et al., 2000
		Relaxation of (+) Supercoils	Khodursky et al., 2000

Type I Topoisomerases

There are two type I topoisomerases in *E.coli*, which change the linking number in steps of 1. These are Topoisomerase I (Topo I) and Topoisomerase III (Topo III), encoded by the *topA* and *topB* genes, respectively. These enzymes nick one strand of the duplex, allowing the cleaved strand to swivel around its helical axis 360˚ before sealing the gap. This process changes the linking number in steps of one and does not require ATP. Topo

I acts primarily to relax negative supercoils inserted by DNA Gyrase in order to maintain the general superhelical density of the chromosome (Zechiedrich *et al.*, 2000). Topo III acts in recombination on hemicatenanes and Holliday junctions and can decatenate chromosomes under certain circumstances (Lopez *et al.*, 2005; Nurse *et al.*, 2003)

Type II Topoisomerases

The type II topoisomerases in *E. coli*, DNA Gyrase and Topoisomerase IV (Topo IV) are ATP-dependent enzymes that change the DNA's linking number in steps of two (Bahng *et al.*, 2000; Sugino *et al.*, 1980). These enzymes cut both strands of a single duplex, mediating the passage of a second uncut duplex through the first. The mechanism by which this occurs is displayed in Figure 1.3. Type II Topoisomerases are widely known for being targets of quinolone antibiotics. Binding of the quinolone to either DNA Gyrase or Topo IV results in a poisonous DNA adduct that permanently blocks replication (Chen *et al.*, 1996; Khodursky and Cozzarelli, 1998). However, DNA Gyrase and Topo IV have accumulated quinolone-resistant mutations that allow efficient catalysis even in the presence of quinolone antibacterials (Gruger *et al.*, 2004; Hardy and Cozzarelli, 2003; Zechiedrich *et al.*, 1997).

Figure 1.3: Mechanism of Type II Topoisomerases. The "gate" duplex (pink strand) is cleaved and covalently bound to the topoisomerase (ParC or GyrA). The "transfer" duplex (blue strand) is passed through the gate and released on the other side. This process is ATP-dependent. Picture taken from Corbett *et al.*, 2005.

The two Type II topoisomerases have opposing roles in the cell. DNA Gyrase is a heterotetramer, encoded by *gyrA* and *gyrB*, which introduces negative supercoils into the DNA (Zechiedrich *et al.*, 2000). These negative supercoils are required to counteract the overwinding (increase in positive supercoils) that occurs as a result of strand unwinding during replication and transcription. Failure to resolve these topological issues results in replication fork stalling (Khodursky *et al.*, 2000). Topo IV is also a heterotetramer, encoded by the *parC* and *parE* genes (Kato *et al.*, 1990). Although Topo IV's main role in the cell is decatenating daughter chromosomes at *dif* after replication is complete and unknotting replication intermediates, it also mediates chromosome cohesion and contributes to the maintenance of the superhelical density in the cell by relaxing the negative supercoils introduced by DNA gyrase (Adams *et al.*, 1992; Deibler *et al.*, 2001; Wang *et al.*, 2008; Zechiedrich *et al.*, 2000).

Topoisomerase IV

Temperature-sensitive alleles of both *parC* and *parE* have been identified (*parC1215* and *parE10*). The inactivation of either protein leads to a chromosome-partitioning defect that results in a two populations of cells: filamentous cells with a single centered nucleoid mass in addition to anucleated cells. An example of a filamentous cell with the nucleoid defect is displayed in Figure 1.4. Returning to a permissive temperature allows Topo IV activity to resume and the cells recover (Kato *et al.*, 1990; Kato *et al.*, 1988).

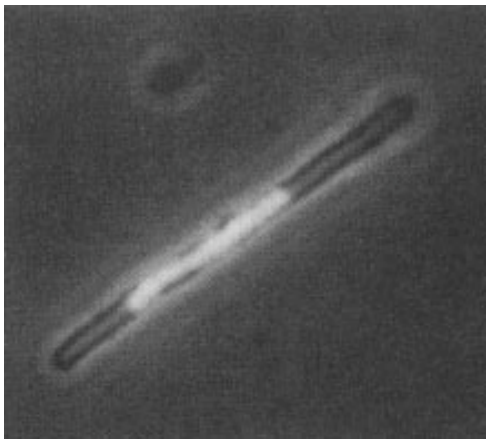

Figure 1.4: *parC1215 (ts)* Nucleoid Partitioning Phenotype. Nucleoid Positioning within the filament at the nonpermissive temperature. Picture taken from Kato *et al*., 1988.

Topoisomerase IV is a heterotetramer consisting of a ParC homodimer and 2 monomers of ParE; the structures of both subunits are shown in Figure 1.6 (Bellon *et al.*, 2004; Corbett *et al.*, 2005; Zechiedrich *et al.*, 1997). Topoisomerase IV has been shown to be very similar to its counterpart in *E.coli*, DNA gyrase, although they each have distinct non-overlapping roles in maintaining the topology of the chromosome (Corbett *et al.*, 2005; Kato *et al.*, 1990).

As noted above and in Figure 1.5, Topo IV has several roles in the cell, more than any other topoisomerase to date. First, its activity is required to unlink the catenated products that form from site-specific recombination or from replication of the chromosome (Figure 1.5A) (Adams *et al.*, 1992; Zechiedrich *et al.*, 1997). Other functions in the cell include the removal of precatenanes that link newly replicated daughter chromosomes together, removal of DNA knots, and general maintenance of supercoiling in the cell (Figure 1.5 B-C) (Deibler *et al.*, 2001; Wang *et al.*, 2008; Zechiedrich *et al.*, 2000). In general maintenance of the superhelical density of the chromosome, Topo IV removes both negative supercoils inserted by DNA gyrase, and positive supercoils that form from overwinding the duplex ahead of the replication fork (Khodursky *et al.*, 2000; Zechiedrich *et al.*, 2000).

Topo IV's role in precatenane removal has been linked to a phenomenon called cohesion. Data from several studies suggest that sister chromosomes are "stuck together" up to 15 minutes after they have been replicated (Bates and Kleckner, 2005; Sunako *et al.*, 2001). The hypothesis for this observation stems from the fact that the sister chromosomes may be topologically linked as precatenanes, or interwound sister DNA duplexes present in a replicating chromosome. Topo IV is said to modulate cohesion by unlinking the precatenanes that keep the loci together, allowing them to be segregated to the appropriate location in the resulting daughter cells. The authors found that

(A)

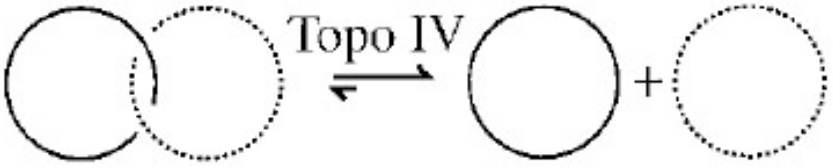

(B)

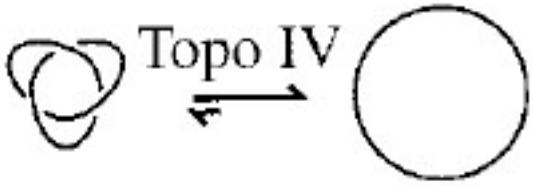

(C)

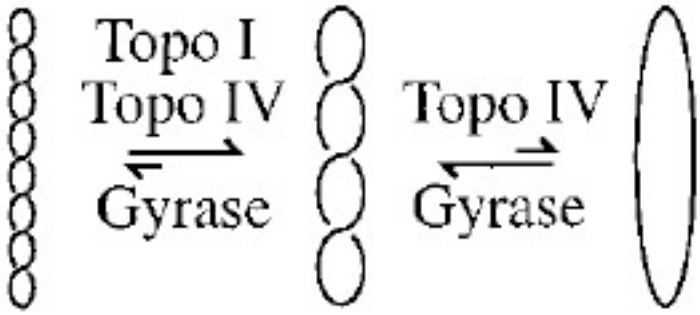

(D)

Figure 1.5: Activities Performed by Topo IV in the Cell. (A) Decatenation, (B) Unknotting, (C) Supercoiling Maintenance, and (D) Precatenane Removal. Figures taken from Deibler *et al*., 2001 and Wang *et al*., 2008.

overexpression of Topo IV leads to decreased cohesion time of the tested chromosomal loci (Wang *et al.*, 2008). The occurrence of nucleoid splitting is delayed upon Topo IV's inactivation, but resumes once Topo IV is active again. This implies that Topo IV's activity is not concentrated at the end of replication, but is needed to separate precatenanes while replication is ongoing.

The mechanism by which Topo IV acts has been well documented. ParC is responsible for substrate specificity via its C-terminal domain (CTD), covalently capturing the DNA after cleavage, strand passage, and religation while the ParE is the ATPase that drives the reaction (Bahng *et al.*, 2000; Corbett *et al.*, 2005).

The ParC crystal structure (Corbett *et al.*, 2005) shows that it contains four domains (Figure 1.6A). The N-terminal CAP domain (residues 1-158) houses the ParE binding domain, a helix-turn-helix motif, and the arginine and tyrosine residues at 119 and 120, respectively, that make up the DNA cleavage site of the protein. The second domain ranges from 159-340 and is termed the "tower." This domain provides structural support and contributes to primary DNA binding. Residues 341-499 make up the dimer interface and connect the tower to the C-terminal domain, ranging from residues 500-753. Corbett *et al*., 2005 suggest that ParC's specificity is dependent on the CTD's ability to discern the topologies of certain DNA crossovers.

(A)

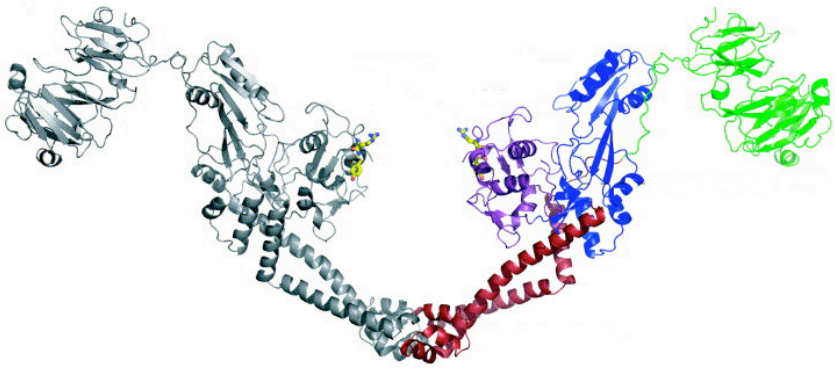

(B)

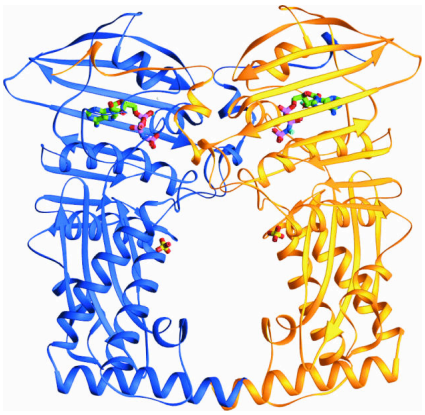

Figure 1.6: Structure of Topo IV Subunits. (A) ParC dimer. The CAP domain is in purple, the tower is in blue, the oligomerization domain is in red and the CTD is in green. (B) ParE dimer. Individual monomers are colored in blue and yellow. The bound adenylyl-imidodiphosphate (ADPNP) molecules are represented as stick figures. Figures taken from Corbett K.D. *et al*., 2005 (A) and Bellon *et al*., 2004 (B).

The crystal structure of ParE's N-terminal domain (Bellon *et al.*, 2004) shows that it binds ATP (Figure 1.6B). Upon binding to ATP, ParE dimerizes into an ATP-operated clamp, which traps the T-segment (colored blue in Figure 1.3) until the gate is opened.

Topoisomerase IV Interactions

In addition to ParC binding to ParE to form the functional Topo IV complex, ParC has been found to have many different binding partners, some of which are listed below.

FtsK

FtsK is a component of the septal ring whose C-terminal domain acts as an ATP-dependent double-stranded DNA translocase to push the replicated chromosomes away from midcell, allowing for final closure of the ring (Saleh *et al.*, 2004). It has been shown to physically interact with the ParC subunit of Topo IV and activate its decatenation activities (Espeli *et al.*, 2003a).

SeqA

SeqA has been shown to specifically interact with Topo IV via the C-terminal domain of ParC and stimulate its decatenation activity (Kang *et al.*, 2003). SeqA's main task in the cell is to bind newly replicated origins at hemimethylated GATC sites, thereby preventing overinitiation at *oriC*. However, SeqA's preference for these hemimethylated sites acts to localize it behind progressing replication forks (Brendler *et al.*, 2000); this may act to concentrate Topo IV activity behind the forks to precatenanes, thereby affecting chromosomal cohesion.

MreB

MreB is another protein that has been shown to physically and functionally interact via the ParC subunit of Topo IV (Madabhushi and Marians, 2009). MreB is an actin homolog whose helical filaments participate in the maintenance of cell shape and the movement and segregation of daughter chromosomes (Kruse *et al.*, 2003). *mreB* mutants appear to be deficient in decatenation, suggesting that Topo IV may be temporally regulated by MreB. The activation or inhibition appears when ParC is bound to MreB filaments or monomers, respectively (Madabhushi and Marians, 2009).

Other ParC Interaction Screens

Several high-throughput protein interaction screens have identified several binding partners of ParC (Arifuzzaman *et al.*, 2006; Butland *et al.*, 2005). Among these were proteins involved in supercoiling and chromosome maintenance, such as GyrA and MukB. Other proteins mainly included ribosomal subunits and lipid biosynthetic proteins.

Chromosome Segregation

In order to provide an accurate, complete copy of the genome to daughter cells upon cell division, the cell must regulate the timing of replication, chromosome segregation, and septation.

Newly replicated daughter chromosomes are connected with both topological and molecular restraints (Figure 1.7). First, normal replication of closed circular

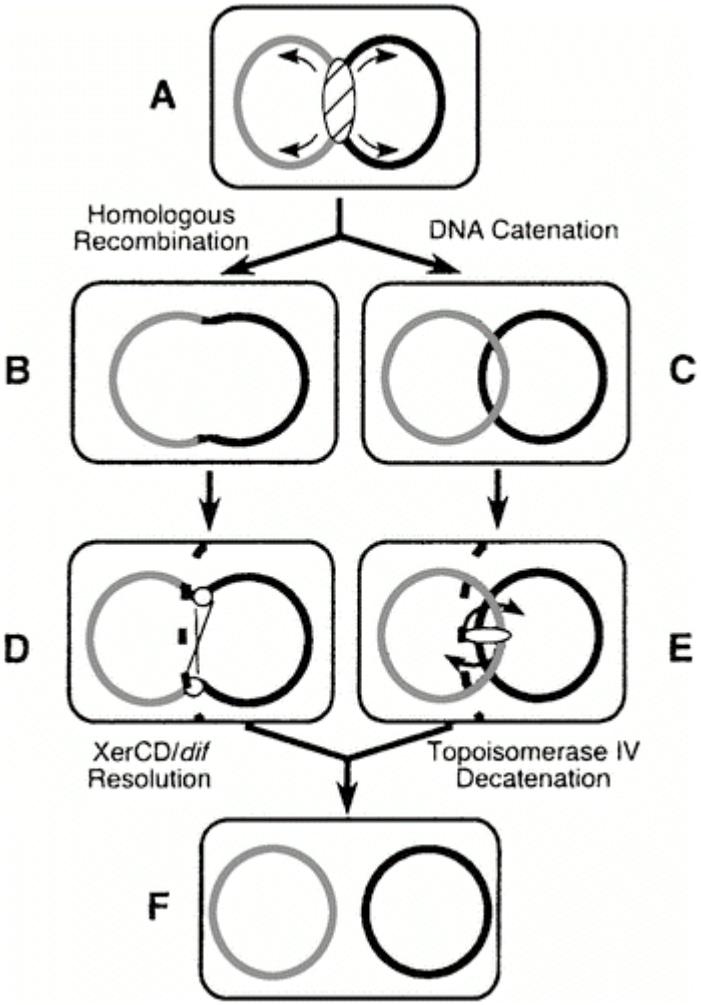

Figure 1.7: Topological Issues Resulting from Replication in *E. coli*. Chromosomes form dimers (B) from uneven numbers of homologous recombination events and must be resolved via XerCD (D). Replication of circular chromosomes leads to the formation of catenanes (C). These are unlinked via Topo IV (E). Figure taken from Gordon and Wright, 2000.

chromosomes results in catenated chromosomes, similar to the links of a chain. Second, uneven numbers of homologous recombination events lead to chromosome dimer formation; this results in two genome equivalents in a single closed circle. In order for cell division to be successful, these topological issues must be resolved so each daughter cell receives a full genome.

Decatenation

First, replication of a closed circular ring results in daughter chromosomes that are topologically connected, depicted as links in a chain in Figure 1.5A. The process of separating the chromosomal links is termed decatenation. If these chromosomes are not unlinked, then the septal ring will cut through them, ultimately leading to the death of the cells. Topo IV acts to unlink the catenanes after replication, modeled by Figure 1.7ACEF. Other proteins, such as Topo III and XerCD, have been shown to decatenate these links under specific conditions, but less efficiently (Grainge *et al.*, 2007; Nurse *et al.*, 2003).

Recombination

Second, during replication, newly replicated sister chromosomes behind the fork undergo recombination. If there are even numbers of these recombination events, then two chromosomes are regenerated and the chromosomes will decatenate and segregate away from the midcell. However, if that number is uneven, then the result is a chromosome dimer, where the two genome equivalents are joined as one big circle as modeled in Figure 1.7B (Blakely *et al.*, 1991). In order to resolve this situation, the cell employs the

site-specific recombinase XerCD heterodimer to resolve the dimer into catenated monomers (Blakely *et al.*, 1993; Zechiedrich *et al.*, 1997). Chromosome dimer resolution also requires both active cell division and the C-terminal domain of FtsK (Steiner *et al.*, 1999; Steiner and Kuempel, 1998a).

Terminal dif Site

The site at which both Topo IV decatenation and XerCD-mediated dimer resolution occurs is called *dif* (deletion induced filamentation) because cells lacking this terminal region form a subpopulation of filamented cells with aberrant nucleoid structures (Kuempel *et al.*, 1991). The area flanking this *dif* site contains repeated DNA sequences termed KOPS, for FtsK-orienting polar sequences (Bigot *et al.*, 2006; Bigot *et al.*, 2005). FtsK's DNA translocation activity centers *dif* at midcell (Lowe *et al.*, 2008), where it is the substrate for both Topo IV and XerCD. XerCD has recently been shown to interact with the FtsK CTD already bound to *dif* (Graham *et al.*, 2010). The interaction with FtsK then promotes dimer resolution.

Septation

The process by which an *E.coli* cell divides into two independent cells is called septation and proceeds by concurrent furrowing of the inner and outer membranes and the peptidoglycan layer. In order to ensure this goes smoothly, the cell division process contains 3 parts.

Selection of the Division Site

As the chromosome is being replicated, the cell must choose location of the division site. In order to equally divide the cellular contents into the corresponding daughter cells, the cell must ensure that the septum be close to the middle. To this end, the cell uses two systems to select the division site: the Min system and Nucleoid Occlusion reviewed in Figure 1.8 (RayChaudhuri *et al.*, 2000). First, the *minB* operon consists of three proteins: MinC, MinD, and MinE (Jaffe *et al.*, 1988). MinC and MinD form a dimer, which binds to FtsZ, inhibiting its polymerization (Hu and Lutkenhaus, 2000). The MinCD complex oscillates between poles, its high polar concentration inhibiting Z ring formation there (Raskin and de Boer, 1999). This allows FtsZ to polymerize only when the MinCD concentration is low, which is somewhere in the middle of the cell. The cell also employs a process called nucleoid occlusion (NO). This process inhibits Z-ring formation in regions that contain DNA and involves SlmA (Bernhardt and de Boer, 2005; Woldringh *et al.*, 1991). Bernhardt and de Boer, 2005 found that SlmA directly interacts with FtsZ, thereby inhibiting its polymerization.

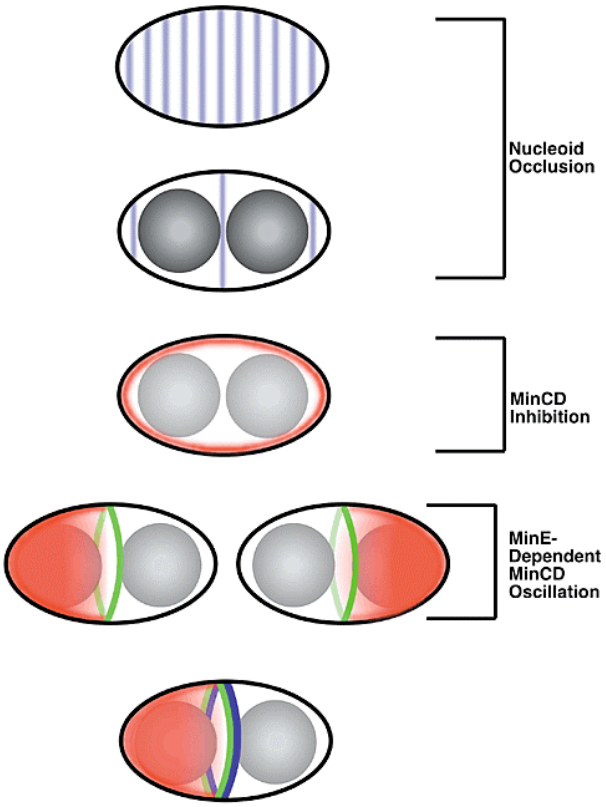

Figure 1.8: NO- and Min-Dependent Division Site Selection. Figure taken from RayChaudhuri *et al*., 2000.

Assembly of the Ring

Once the division site is selected, proteins are recruited in an FtsZ-dependent sequential manner to form a complex known as the septal ring. This linear recruitment pathway is shown in Figure 1.9. FtsZ, the bacterial homologue of tubulin, polymerizes around the inside of the membrane at midcell. Afterwards, ZipA (for FtsZ interacting protein A) and FtsA (homologue to actin) are added to the ring, anchoring the ring to the membrane (Pichoff and Lutkenhaus, 2002). In all, about a dozen cytoplasmic and membrane

anchored proteins are recruited to form the fully functional ring.

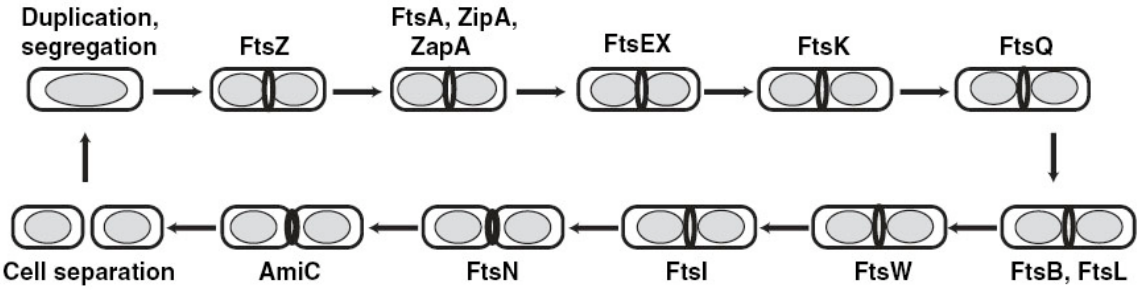

Figure 1.9: Linear Recruitment Pathway of Septal Ring Components. Figure taken from Geissler & Margolin, 2005.

At some critical concentration of FtsZ, hydrolysis of the GTP initiates the constriction of the ring, which also promotes increased curvature of the membrane (Osawa *et al.*, 2009; Scheffers *et al.*, 2002). Some proteins attached to the ring coordinate invagination of the membrane with the synthesis/ degradation of new peptidoglycan for the cell wall (FtsI), while others help to segregate the chromosome away from midcell (FtsK) (Pisabarro *et al.*, 1986; Yu *et al.*, 1998).

Constriction and Cell Separation

A balance of peptidoglycan (PG) synthesis and degradation occurs throughout the cell cycle. There are two types of enzymes responsible for synthesizing PG: lytic transglycosylases (i.e. MltA or Slt) and transpeptidases (i.e. PBP3). Lytic transglycosylases are responsible for breaking the disaccharide chains so that new PG can be inserted. FtsI (Penicillin binding protein 3) encodes for the essential membrane-bound

transpeptidase involved in synthesizing PG at the "new pole," by inserting multiple strands side by side during constriction of the ring (Ishino *et al.*, 1986; Ursinus and Holtje, 1994).

The Tol/Pal complex couples the inner membrane constriction with that of the PG and outer membrane (Gerding *et al.*, 2007). This complex consists of five proteins: TolA, TolQ, and TolR, which reside in the inner membrane, TolB in the periplasm, and Pal with the outer membrane. All proteins in this complex localize to the division site and that localization requires the septal ring protein FtsN. The various interactions amongst these proteins allow for the complex to span the length of the entire envelope. Mutations in any of the genes exhibit discordant invagination of the outer membrane, resulting in "OM blebs," where the outer membrane becomes detached from the PG and bulges out.

Separation of the daughter cells is the final step in cell division. As the septal ring constricts the inner membrane (IM), the peptidoglycan layer (PG) and outer membranes (OM) must narrow as well. This is done by several means.

The final step of cell division involves completely separating the daughter cells from one another. This task is completed by the muramidases AmiABC and murein hydrolase EnvC (Bernhardt and de Boer, 2004; Heidrich *et al.*, 2001; Priyadarshini *et al.*, 2007). Deletion of several of these genes leads to a septation defect, where cells fail to separate and form chains, ranging in length from 3 up to 24 cells (Bernhardt and de Boer, 2003; Priyadarshini *et al.*, 2006).

Segregation-Septation Checkpoint

In order to ensure that the daughter cells inherit the full chromosome after each division, the cell sets up checkpoints at various stages within the cell cycle. It must be able to postpone septation if replication or decatenation has not finished. The septal ring protein that mediates this important checkpoint function is FtsK (Bigot *et al.*, 2004). As shown above in Figure 1.9, FtsK is recruited early in the ring construction, however it doesn't act until late in the septation process (Wang and Lutkenhaus, 1998). FtsK has an N-terminal domain, which tethers the protein to the membrane, and a C-terminal domain, which is actually an ATP-dependent translocase that interacts with DNA (Begg *et al.*, 1995). The purpose of this translocation property functions not only to direct *dif* to the septum where Topo IV and Xer Resolvase reside, but also to simplify DNA topology in the terminus (Grainge *et al.*, 2007). FtsK forms a hexameric ring as the septum constricts, forming around the DNA (Lowe *et al.*, 2008). The terminus region of the chromosome contains repeated sequences called FtsK Orienting Polar Sequences (KOPS), which act to orient the terminus region's movement towards *dif* (Capiaux *et al.*, 2002). There are several mechanisms set up involving FtsK, Topo IV, and XerCD that allow for the implementation of a septation checkpoint, should one be necessary.

First, the subunits of Topo IV are temporally and spatially regulated during active replication. It has been shown that the ParC subunit of Topo IV localizes with the replisome while the ParE subunit is localized to the DNA-free regions of the cell (Espeli *et al.*, 2003b). When replication is complete, the holoenzyme dissociates, allowing ParC to interact with ParE. This also allows for Topo IV to be active near *dif*, which is the

preferred cleavage site for Topo IV during decatenation (Hojgaard *et al.*, 1999). Also, a physical interaction mediated by the ParC subunit of Topo IV with the C-terminal domain of FtsK has been shown to activate Topo IV's decatenation activity (Espeli *et al.*, 2003a). This allows the unlinked daughter chromosomes to be pumped away from the septal plane.

Next, FtsK is required for XerCD-mediated resolution of chromosome dimers (Steiner *et al.*, 1999). A physical and functional interaction between FtsK CTD and XerD stimulates site-specific recombination at *dif* (Bonne *et al.*, 2009; Recchia *et al.*, 1999; Yates *et al.*, 2006). The XerCD recombinase is thought to bind to *dif* as FtsK translocates the terminus region (Graham *et al.*, 2010). The interaction between FtsK and XerCD may serve as the signal to stop the translocation. In this way resolution is spatially regulated by the XerCD interaction with FtsK.

Once *dif* is at the junction between cells, FtsK stimulates both Topo IV and XerCD activities so that Xer may resolve chromosome dimers and the chromosome may be topologically unlinked. The results in Chapter III indicate that the Topo IV and XerCD may bind on the same region of FtsK, potentially inhibiting XerCD.

Replication of the Chromosome

In order to ensure that an accurate, complete copy is available to segregate into daughter cells, the chromosome must first be replicated. The doubling time for *E.coli* growing aerobically is around 20 minutes in rich media. However, bidirectional replication takes

40 minutes to complete at 37ºC. This timing issue is resolved by having multiple replication forks actively replicating the chromosome at any point in the bacteria's life cycle. Under normal conditions, bidirectional replication is accomplished by the DNA Polymerase III holoenzyme. This multiprotein complex contains at least 9 protein components, listed in Table 1.2. There are three stages to replication: initiation, elongation, and termination.

Initiation

During initiation, the DNA Polymerase III holoenzyme assembles onto the origin of replication (*oriC*). The DnaA protein is responsible for unwinding this region such that the primosome loader DnaC can bind to load the primosome (Carr and Kaguni, 2002; Marszalek and Kaguni, 1994; Seitz *et al.*, 2000). *dnaA* mutants cannot separate the strands of the origin, therefore progressive rounds of replication cannot be initiated (Takata *et al.*, 2000). Once the pre-priming complex is present and the holoenzyme is assembled, the complex begins the elongation phase of the cycle. The DNA Polymerase III core consists of α, ε, and θ. The accessory protein τ is responsible for dimerizing the core, thereby coordinating leading and lagging strand synthesis (Kodaira *et al.*, 1983; Maki *et al.*, 1988). γ, δ, δ', χ, ψ are members of the gamma clamp loader involved in loading the β sliding clamp onto the DNA (Jeruzalmi *et al.*, 2001a).

Table 1.2: Subunits of the DNA Polymerase III Holoenzyme.

Protein	Function	Gene
α	Polymerase	*dnaE*
ε	3'-5' exonuclease	*dnaQ*
θ	Unknown	*holE*
τ	Dimerizes cores	*dnaX*
	Protect β from Removal	*dnaX*
γ	Clamp Loader	*holA*
δ	Clamp Loader	*holB*
δ'	Clamp Loader	*holB*
χ	Clamp Loader	*holC*
φ	Clamp Loader	*holD*
β	Sliding clamp	*dnaN*

Elongation

In order to synthesize both strands of the DNA simultaneously, the two core polymerases dimerize via an interaction with the C-terminal domain of τ (Studwell-Vaughan and O'Donnell, 1991). It is through this interaction that τ coordinates leading and lagging strand synthesis. The interactions made by the domains of both τ and γ is shown in Figure 1.10.

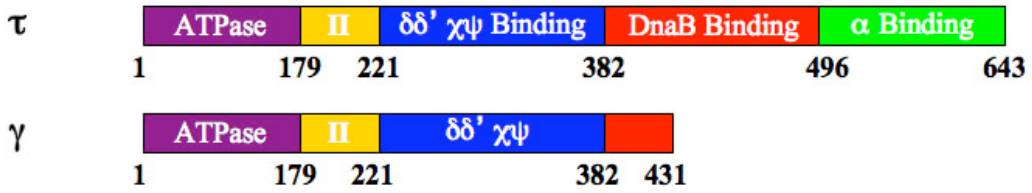

Figure 1.10: DnaX Domain Regions and Interactions.

The essential *dnaX* gene produces two polypeptides, τ and γ, due to a ribosomal frameshift at codons 429-430 (Flower and McHenry, 1990). Both products are members of the DNA Polymerase III holoenzyme and are involved in the DNA elongation step of replication, but only τ is essential (Blinkova *et al.*, 1993; Kodaira *et al.*, 1983). Two conditional mutations, *dnaX36* and *dnaX2016*, have been isolated and characterized *in vivo*. At the restricted temperature, these alleles are defective in DNA replication and as a result, the cells filament (Filip *et al.*, 1974; Henson *et al.*, 1979). This filamentation is due to induction of the SOS response and it is presumed that the inactivation of the tau/ gamma destabilize the replication fork, leading to double stranded breaks (Skovgaard and Lobner-Olesen, 2005).

The γ subunit contains the first two-thirds of the τ polypeptide (from residues 1-431), but lacks τ's C-terminal domain. It has been shown that the gamma subunit is the main component of the β clamp loader. Although both τ and γ contain domain III, only γ is bound to χ, ψ and δ, δ' *in vivo* (Glover and McHenry, 2000; Jeruzalmi *et al.*, 2001a).

Replication Fork Stalling

Replication fork progression rarely continues unimpeded-blocks are present approximately 18% of the time under normal conditions (Maisnier-Patin *et al.*, 2001). Upon encountering DNA lesions, the replication fork will stall while the cell tries to repair the damage. In addition to induced DNA damage from sources such as UV, spontaneous DNA damage can occur in an aerobically growing cell from the action of hydroxyl radicals (Keyer *et al.*, 1995). Replication forks may also stall at bound proteins, unusual DNA structures, and pause sites within the DNA (Hyrien, 2000; Michel, 2000; Rothstein *et al.*, 2000). In order to salvage the round of replication, origin-independent restart must occur. This may be done either by restarting the existing holoenzyme, or disassembling the original and building anew (Courcelle *et al.*, 1997).

Termination

The bidirectional replication forks converge in a region called the terminus. DNA sequences called *ter* sites are bound by Tus proteins (Kamada *et al.*, 1996). Tus interacts with the helicase subunit of the holoenzyme in a polar fashion, thereby inhibiting its DNA translocation and unwinding activities (Hiasa and Marians, 1992; Neylon *et al.*, 2000).

Proteins of Unknown Function

It was found that of the 4,300 protein-encoding genes annotated in *E. coli*, approximately 1,700 genes encoded proteins of unknown function (Blattner *et al.*, 1997; Ito *et al.*, 2005; Riley *et al.*, 2006). Several genome-scale attempts have been made to elucidate the

functions of these proteins (encoded by genes termed y-genes) (Baba *et al.*, 2006; Gerdes *et al.*, 2003).

Large-scale phenotypic screens seek to identify conditions under which these functions are required for growth. Previous attempts to generate conditional media-dependent phenotypes have been rather successful. Gerdes *et al*., 2003 used transposon mutagenesis to identify genes essential for growth in LB. They found 620 proteins of unknown function to be essential, but 3,126 were dispensable for growth when deleted. Also, Ito *et al*., 2005 used phenotypic microarrays to test whether 1400 deletions metabolize 95 different carbon sources. Of the 700 deletions that encoded proteins of unknown functions, approximately 230 showed metabolic defects on at least one carbon source. Using the protein fragments, we will try to generate media-specific phenotypes that can be studied further.

A subset of fragments from proteins of unknown function was found to exhibit media-specific plating defects. The overexpression of the protein fragments yielded effects that were not seen by other overexpression or deletion experiments, even under similar growth conditions (Baba *et al.*, 2006; Kitagawa *et al.*, 2005).

CHAPTER II

LONG ParC FRAGMENTS

Topoisomerase (Topo) IV, a type II topoisomerase, is a heterotetramer consisting of two monomers of ParC and two monomers of ParE (Peng and Marians, 1993). Topo IV plays multiple roles in the cell (Figure 2.1). First, its activity is required to unlink the catenated products that form from site-specific recombination or from replication of the chromosome, as depicted in Figure 2.1A (Adams *et al.*, 1992; Zechiedrich *et al.*, 1997). Other functions in the cell, shown in Figure 2.1B-D include the removal of precatenanes that link newly replicated daughter chromosomes together, removal of DNA knots, and general maintenance of supercoiling in the cell (Deibler *et al.*, 2001; Wang *et al.*, 2008; Zechiedrich *et al.*, 2000). In general maintenance of the superhelical density of the chromosome, Topo IV both removes negative supercoils inserted by DNA gyrase, and positive supercoils that form from overwinding the duplex ahead of the replication fork (Khodursky *et al.*, 2000; Zechiedrich *et al.*, 2000).

(A)

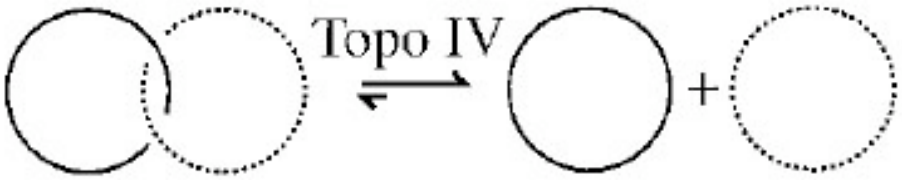

(B)

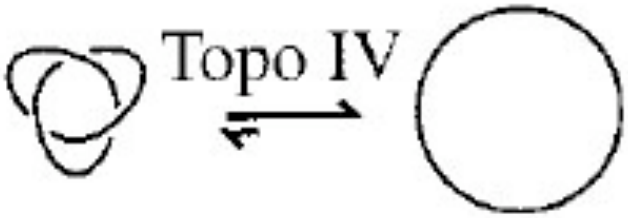

(C)

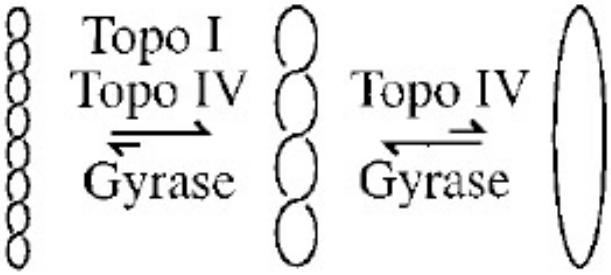

(D)

Figure 2.1: Topological Issues Resolved by Topo IV. (A) Decatenation, (B) Unknotting, (C) Supercoiling Maintenance, and (D) Precatenane Removal. Figures taken from Deibler *et al*., 2001 (A-C) and Wang *et al*., 2008 (D).

Temperature-sensitive alleles of both *parC* and *parE* have been identified. The inactivation of either protein leads to a chromosome-partitioning defect that results in a two populations of cells: filamentous cells with a single, centered nucleoid mass in addition to anucleated cells (Kato *et al.*, 1990; Kato *et al.*, 1988). Cells deficient in Topo IV cannot decatenate replicated chromosomes and therefore form septa at the DNA-free poles rather than at midcell.

The *parC1215 (ts)* allele that caused this partitioning defect is a single nucleotide substitution of G2199A, which corresponds to a D703G substitution (Kato *et al.*, 1990). Assuming that the *ts* allele represents a complete loss of Topo IV activity at the restrictive temperature, isolating individual functions becomes complicated due to the lethality. The requirement for Topo IV at multiple stages in the cell cycle makes studying its individual functions challenging.

The ParC crystal structure (Corbett *et al.*, 2005) shows that it contains four domains (Figure 2.2A). The N-terminal CAP domain (residues 1-158) houses the ParE binding domain, a helix-turn-helix motif, and the arginine and tyrosine residues at 119 and 120, respectively, that make up the DNA cleavage site of the protein. The second domain ranges from 159-340 and is termed the "tower." This domain provides structural support and contributes to primary DNA binding. Residues 341-499 make up the dimer interface and connect the tower to the C-terminal domain, ranging from residues 500-753. Corbett *et al*., 2005 suggest that ParC's specificity is dependent on the CTD's ability to discern the topologies of certain DNA crossovers.

(A)

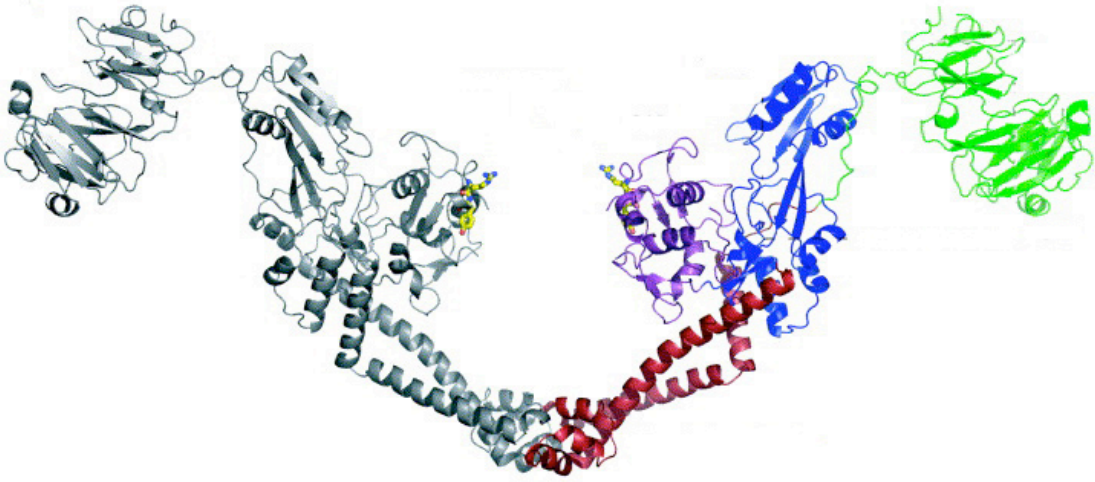

(B)

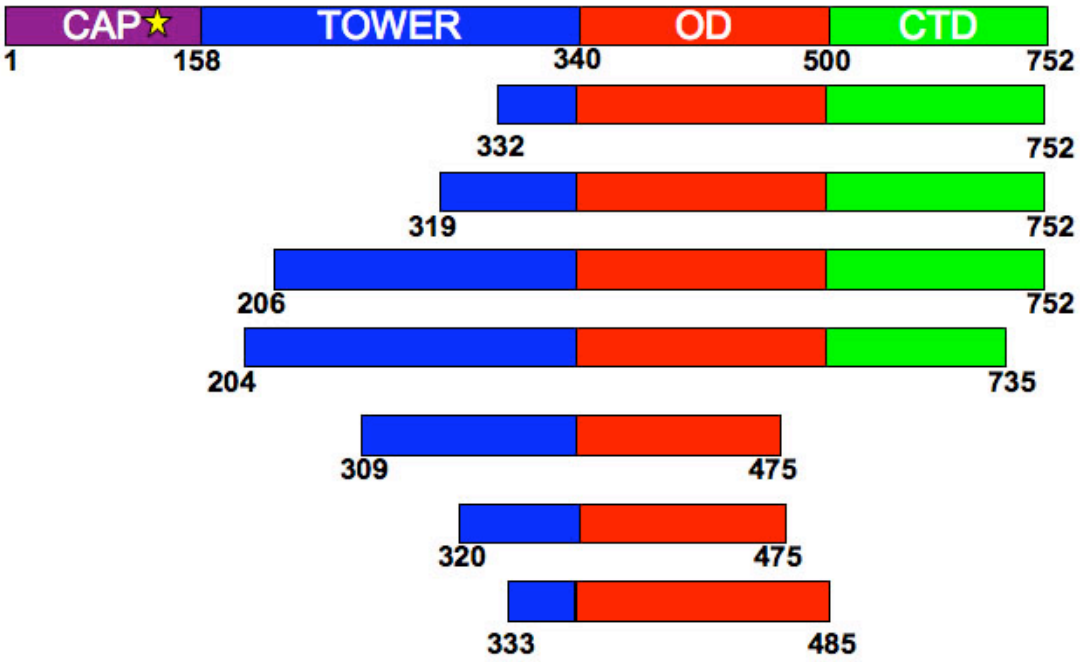

Figure 2.2: Domains of ParC Used in Negative Dominance. (A) ParC Structure taken from Corbett *et al*., 2005. (B) ParC fragments overexpressed from Marino-Ramirez *et al*., 2004. This chapter will focus on the ParC206-752 and ParC332-752 fragments while Chapter III will focus on ParC333-485.

Negative Dominance of Topo IV Fragments

The catalytic function of ParC within the Topo IV complex relies on its ability to form a homodimer, with symmetrical active site residues located on each monomer. These residues are covalently bonded to the broken DNA strands of the substrate. The ParC dimer pivots to allow the transfer segment of DNA (blue) to pass through the gate (pink) as shown in Figure 2.3. All the fragments being expressed contain the oligomerization domain, so the subset of Topo IV complexes containing the fragments will be catalytically inert. The fragment may also be interacting with another protein target X.

Because these fragments do not include the full length ParC subunit, we hypothesize that overexpression of the ParC fragments shown in Figure 2.2B would have a detrimental effect on cell growth. In theory, a subset of the endogenous full-length ParC will participate in functional Topo IV complexes while another subset will interact with ParC truncations.

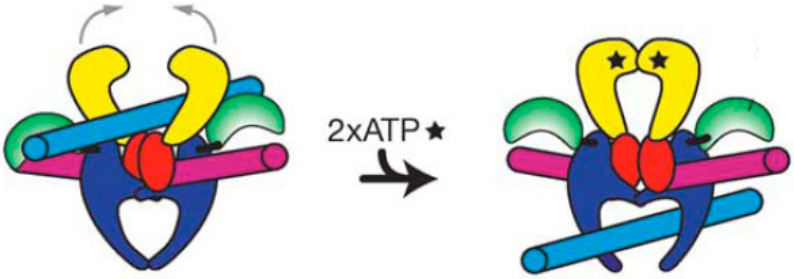

Figure 2.3: Mechanism of Topo IV. The "gate" duplex (pink strand) is cleaved and covalently bound to the ParC subunit. The "transfer" duplex (blue strand) is passed through the gate and released on the other side. The ParE ATPase (shown in yellow) hydrolyzes the ATP needed to fuel this reaction. Figure taken from Corbett *et al.*, 2005.

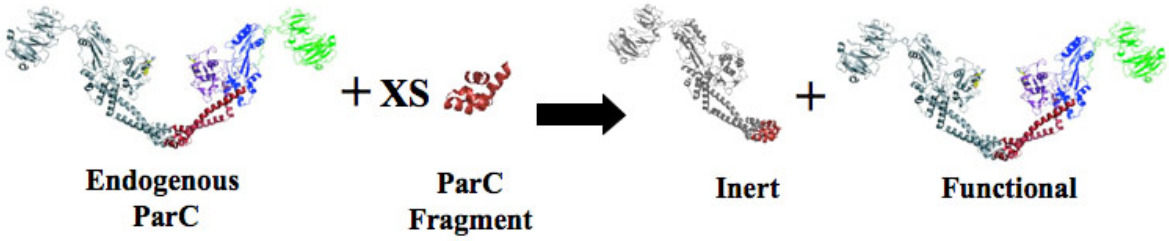

Figure 2.4: Theoretical Negative Dominant Effect from ParC Fragment Overexpression. ParC interacts with endogenous full-length ParC.

Materials and Methods

Bacterial Strains and Plasmids

Table 2.1: Bacterial Strains Used in Chapter II.

Strain	Genotype	Reference
MG1655	F-, λ^-, *rph-1*	Blattner *et al*., 1997
AZ766	MG1655/ pAZ696	this study
AZ767	MG1655/ pAZ697	this study
AZ768	MG1655/ pAZ698	this study
AZ769	MG1655/ pAZ699	this study
AZ770	MG1655/ pAZ700	this study
AZ771	MG1655/ pAZ701	this study
AZ1141	MG1655/ pAZ804	this study
AZ1142	MG1655/ pAZ854	this study
AZ1143	MG1655/ pAZ855	this study
AZ1144	MG1655/ pAZ856	this study
AZ1145	MG1655/ pAZ857	this study
AZ1146	MG1655/ pAZ858	this study
AZ1147	MG1655/ pAZ859	this study
AZ1148	MG1655/ pAZ860	this study
AZ1149	MG1655/ pAZ861	this study
AZ1177	MG1655*parC1215 metC::Tn10*	this study

Table 2.2: Plasmids Used in Chapter II.

Plasmid Name	Description	Relevant Marker	Reference
pAZ696	**ParC503-752** in pJM198	tetracycline	this study
pAZ697	**ParC553-752** in pJM198	tetracycline	this study
pAZ698	**ParC603-752** in pJM198	tetracycline	this study
pAZ699	**ParC653-752** in pJM198	tetracycline	this study
pAZ700	**ParC703-752** in pJM198	tetracycline	this study
pAZ701	**ParC723-752** in pJM198	tetracycline	this study
pAZ804	**ParC1-752** in pJM198	tetracycline	this study
pAZ854	**ParC319-752** in pJM198	tetracycline	this study
pAZ855	**ParC204-735** in pJM198	tetracycline	this study
pAZ856	**ParC332-752** in pJM198	tetracycline	this study
pAZ857	**ParC309-475** in pJM198	tetracycline	this study
pAZ858	**ParC206-752** in pJM198	tetracycline	this study
pAZ859	**ParC333-485** in pJM198	tetracycline	this study
pAZ860	**ParC320-475** in pJM198	tetracycline	this study
pAZ861	**DnaX247-455** in pJM198	tetracycline	this study
pJM185	**Gcn4 LZ** in pJM198	tetracycline	this study
pJM198	P_{BAD}- His Patch Thioredoxin pACYC origin- destination vector	tetracycline	this study

Growth Conditions

Overnight cultures were grown for about 16 hours in 2 ml LB + 20 µg/ml tetracycline + 0.1% D-fucose in a rollerdrum rotating at 37˚C. Bacterial strains and plasmids used in this study are listed in Tables 2.1 and 2.2, respectively. The overnights were diluted 1:1000 into 10 ml LB + 20 µg/ml tetracycline in 125 ml Erlenmeyer flasks at 37˚C at a shaker speed of 6 (~210 rpms) in a New Brunswick Scientific Gyrotory Water Bath Shaker Model G76. The cultures were induced at OD_{600} = 0.2 to a final concentration of 0.2% L-arabinose for cultures overexpressing the target and 0.1% D-fucose for the control. Microscopy and OD samples were taken every 30 minutes to document the growth of the culture.

For plating dilutions, M9 plates (Miller, 1972) containing 20 µg/ml tetracycline + either 0.2% L-arabinose (inducer) or 0.1% D-fucose (anti-inducer) were used for plating dilutions. Overnight cultures grown in M9 + 20 µg/ml tetracycline + 0.1% D-fucose were serially diluted 1:10 into 1x M9 salts using multichannel pipettes. Cells were spotted onto the plates using a 48-or 96-pronged replicator (Boekel). This instrument applies about 5 µl of culture per spot to the plates. Plates were allowed to dry and were incubated at 37˚C overnight. Both colony morphology and plating efficiency were documented for these experiments.

Cloning Procedures

parC gene fragments were amplified from the plasmids described in Marino *et al*., 2004 using the PCR primers *forward-attB1* (GGGGACAAGTTTGTACAAAAAAGCAGGC-

TACAAGGACGACGATGACAAG) and *reverse-attB2* (GGGGACCACTTTGTACA-AGAAAGCTGGGTCTTTCGGGCTTTGTTAGCAG). The DNA fragments were cloned into the expression vector pJM198 using the Gateway Cloning Technology (Invitrogen).

Microscopy

Cell Fixation

Cells were fixed by adding 0.19 volumes of 16% paraformaldehyde to aliquots of culture. Cells were allowed to stand at room temperature for 30 minutes and placed on ice for up to 3 hours. Samples were then pelleted gently at 3.3xg (6,000 rpm) in a tabletop centrifuge for 3 minutes. The supernant was removed and the cells were washed 3 times in ice-cold 1x PBS. After the final wash, the pellet was resuspended in 250-500 µl of 1x PBS (dependent upon the size of pellet) and stored at 4˚C in the dark.

Fluorescence

Coverslips were coated with 0.01% poly-L lysine and washed 3 times with MilliQ water. They were then rinsed with 100% ethanol and dried. 30 µl of fixed culture was added to the coverslip and allowed to set for 3 minutes. Dabbing the edge of the coverslip to a paper towel and dipping the coverslip into 1x PBS removed the excess culture. The coverslips were allowed to dry for 5 minutes on a paper towel (side with the sample facing up). 3 µl of DAPI (3 µg/ml) was applied and the coverslips were immediately inverted onto slides with 3 µl Anti-Fade mounting media (Invitrogen).

Images were captured using a Zeiss AxioPhot microscope at 100x magnification using both the DIC and the DAPI filters for phase contrast (exposure time ~50 ms) and DNA (exposure time ~110 ms), respectively.

Results

Negative Dominance of ParC fragments

The ParC fragments were cloned into a low copy number vector such that expression of the fragments as C-terminal fusions to a mutant thioredoxin (TRX) was under control of the *araBAD* promoter. Plating efficiency of cells expressing these fusions was compared to cells overexpressing the similar fusions of Gcn4 LZ and DnaX247-455, protein fragments also known to self-assemble (Figure 2.5A). Although the expression of DnaX247-455 is lethal at high copy (Chapters III and IV) its expression on a low copy number plasmid does not affect growth.

All of the ParC fragment fusions that extend to the C-terminus exhibit a diminished ability to form colonies: ParC 332-752, 319-752, and mostly severely 206-752. Fragments that dimerize in the lambda repressor fusion assay, but lack the C-terminal region of the protein (i.e. ParC 204-735) are no more toxic than fusions to the full length ParC protein. Comparing ParC 332-752 to ParC333-485 or ParC206-752 to ParC204-735 is consistent with a requirement for the C-terminal domain of the protein for a strong plating phenotype.

(A)

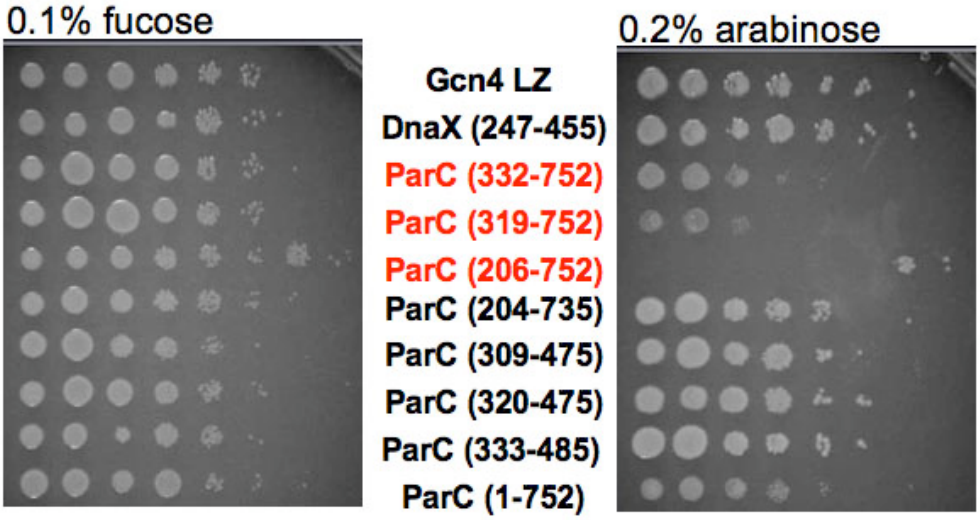

(B)

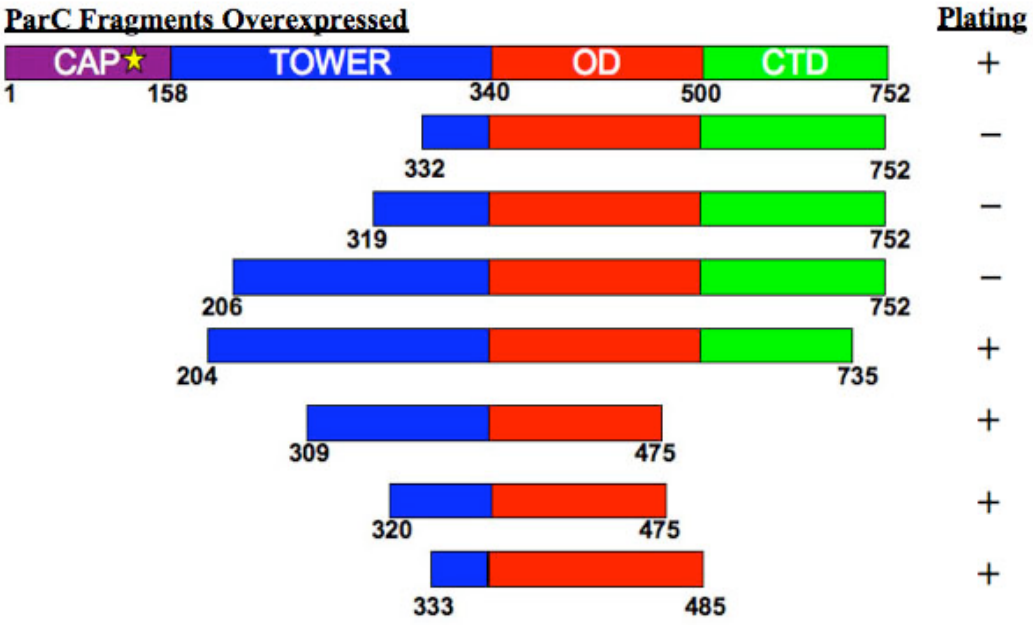

Figure 2.5: Plating Results of the Isolated ParC Fragments. (A) Plating efficiency comparison of different ParC fragments. (B) Summary of the plating results from (A).

Although overexpression of the oligomerization domain 333-485 alone was not sufficient to elicit a reduced plating effect, all of the toxic constructs contained the dimerization domain by virtue of how they were initially isolated. Additional N-terminal ParC deletions were made to determine whether the C-terminal domain alone was sufficient to cause the reduced plating phenotype (Figure 2.6).

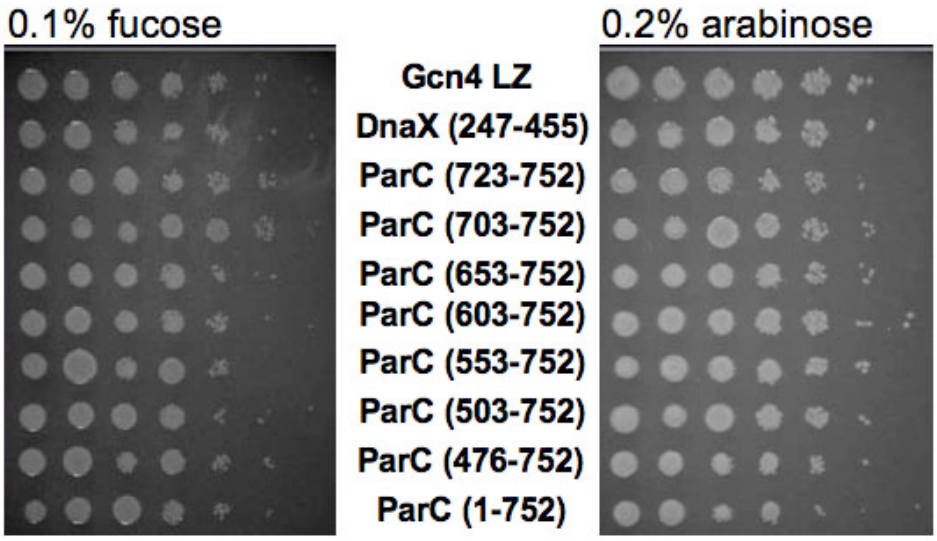

Figure 2.6: Plating Efficiency of ParC N-terminal Deletions.

The plating efficiency of all strains overexpressing the C-terminal region alone was comparable to the uninduced control. Therefore both the oligomerization domain and the C-terminal domain of ParC are required for the plating phenotype.

Morphology of Cells Expressing ParC Fragments

The essentiality of ParC was established from the conditional lethal phenotype of the temperature-sensitive parC1215 allele (Kato *et al.*, 1988). At the nonpermissive temperature, cells with this allele become deficient in segregating their chromosomes and as a result, filament and are therefore unable to form colonies. Since the overexpression of ParC fragments described above was toxic, we examined the morphologies of cells overexpressing two of the toxic fragments, ParC206-752 and ParC332-752, as well as the morphology of cells expressing the nonlethal fragment Par333-485, which is shown in Figure 2.7. Overexpression of the two lethal fragments led to filamentation. In contrast, expression of ParC333-485 did not lead to filamentation. However, overexpression of the nonlethal fragment did lead to a partial defect in septation. The phenotypes of ParC333-485 are further characterized in Chapter III. In this chapter, I will focus on the properties of the lethal fragments.

DNA Segregation Phenotypes

The filamentous cells were further classified based on DNA organization within the cell. Similar to the trend of one fragment yielding several different cellular morphologies, these same fragments also affected chromosome segregation to different degrees. Within each population of mutants, there were several different aberrant DNA configurations. In order to assess the severity of the phenotype, nucleoid morphology was grouped into 6 distinct classes.

(A)

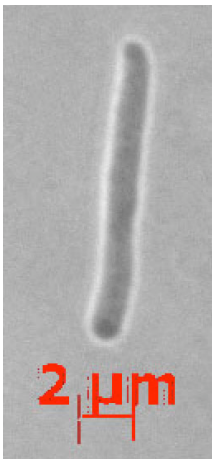

(B)

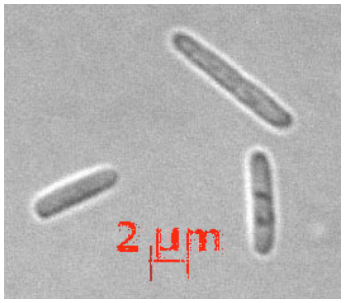

(C)

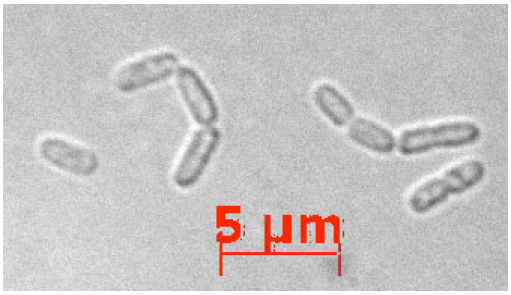

Figure 2.7: Cellular Morphologies of ParC Fragment Overexpression. The different regions of the ParC protein overexpressed include ParC332-752 (A), ParC206-752 (B), ParC333-485 (C).

Table 2.3: Examples of Nucleoid Classes.

Class	Description	Example
1	**Regularly spaced, small, condensed nucleoids (mainly non- filamentous cells)**	
2	**One central nucleoid mass at center (most similar to *parC1215* phenotype)**	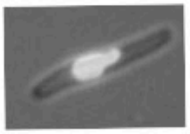
3	**Multiple separated nucleoids evenly distributed about the center of the cell**	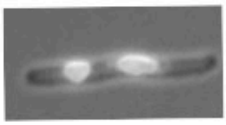
4	**Multiple nucleoids connected by strands of DNA distributed about cell center**	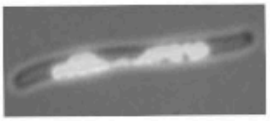
5	**Nucleoids localized to the pole due to guillotining by septation**	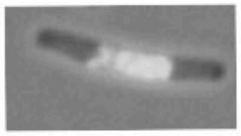
6	**Large nucleoids that take up the majority of cell volume**	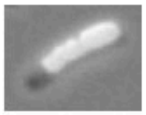

There are six classes into which cells were grouped based on their nucleoid structure. An overview of these classes along with examples is shown in Table 2.3. The first class of nucleoid segregation represents the wild type nucleoid segregation pattern. This consists of regularly spaced, condensed nucleoids completely separated from each other. This class mainly consists of cells that are not filamentous and show no deviant nucleoid localization patterns. Small, condensed nucleoids localizing to the poles would be

included in this class. The second class consists of cells containing one nucleoid mass located at cell center. This class may be most similar to that of the *parC1215 (ts)* phenotype, but the size of the nucleoid mass may vary. The third class contains cells with multiple nucleoids that are evenly distributed about the center and are not connected by strands of DNA, which brings us to the fourth class. In this class, cells possess multiple nucleoid structures that are connected by one or two strands of DNA. The fifth class consists of cells with nucleoids localized to the pole region of the cell. It should be noted that these cells occur due to the septation over the nucleoid, which may mean a malfunctioning of the *min* system, or the nucleoid mass extends unilaterally towards one pole. For classes 2-5, the DNA generally occupies less than 50% of the total cell volume of the filament. In the last class (class 6), the nucleoid staining of these cells consumes the majority of the cell volume, suggesting a severe segregation phenotype or decondensation of the nucleoid. It should be noted that anucleate cells were placed in class 7. Representative samples of these phenotypes are also shown in the table. The distributions of cells in each class for those producing lethal ParC fragments or the Gcn4 LZ control are shown in Figure 2.8.

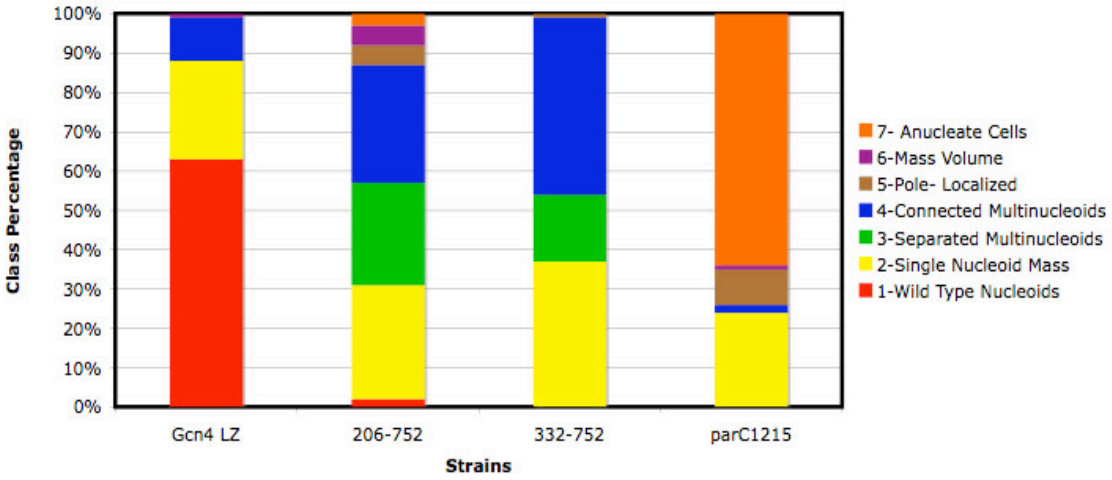

Figure 2.8: Nucleoid Class Distribution. The class distributions are shown for Gcn4, ParC206-752, ParC332-752, and *parC1215 (ts)* 150 minutes after arabinose induction.

The non-filamentous Gcn4 LZ control sample consisted of mainly three types of nucleoid configurations. 63% of the cells in this sample contain two small, condensed nucleoids that are localized at the poles of the cells. This is consistent with the hypothesis that daughter nucleoids segregate away from midcell after replication. 11% of the cells from this strain show a dumbbell-like nucleoid segregation pattern, consistent with daughter chromosomes caught actively separating after replication is complete. The strands that remain connecting the two nucleoids may represent connections in the form of catenanes and/or chromosome dimers. Once Topo IV acts to decatenate the chromosomes or Xer recombinase acts to resolve chromosome dimers the nucleoids will exist as separate entities until septation. 25% of the cells contain a single small nucleoid mass in the center of the cell. These cells may have recently undergone cell division, and are young with respect to the replication process. Once replication is

close to completion the nucleoids will migrate away from the septal plane.

The filaments overexpressing the longer ParC fragment have several different nucleoid organization patterns. Cells expressing the ParC332-752 fragment show a strong preference for the single nucleoid mass (Class 2-37%) and the conjoined nucleoids (Class 4-45%), with multiple separated nucleoids trailing behind (Class 3-17%). Cells expressing the longer ParC206-752 fragment contain equivalent numbers of cells containing a single nucleoid mass (Class 2-29%), and cells containing both separated and conjoined nucleoids (Classes 3-26% and 4-30%, respectively). For the cells containing a single nucleoid mass, the mass is centered within the filament and displays a positioning pattern closest to that of the *parC1215 (ts*) phenotype.

Although some of the nucleoids in cells expressing the ParC fragments are in classes seen in cells overexpressing Gcn4 LZ, the Gcn4 nucleoids are generally smaller and more compact. This may reflect the smaller average size of the Gcn4-expressing cells, which are between 2-4 μm in length as expected for wild-type *E. coli* growing under these conditions.

Cells containing the *parC1215 (ts)* allele were also characterized 150 minutes after they were shifted to 37˚C for comparison. Consistent with Kato *et al*., 1988, the majority of cells consisted of anucleate cells as well as filamented cells with a single nucleoid (Figure 2.8). Only a subset of the cells expressing the ParC fragments has the published

partitioning phenotype and there are very few, if any anucleate cells.

The appearance of the partitioning phenotype occurs more rapidly with the *parC1215 (ts)* allele than with that of the fragment; this difference may be due to the kinetics of the induction. The endogenous ParC protein is presumed to be inactivated within minutes of temperature shift in the *parC1215 (ts)* strain whereas the ParC fragments must first accumulate to a critical concentration before a reduction of Topo IV activity in the cell is noticed. Therefore, earlier timepoints after the temperature shift of the *parC1215 (ts)* may mimic later timepoints of the ParC fragment overexpression phenotype. To that end, cells containing the *parC1215 (ts)* allele were grown at the non-permissive temperature for 60 minutes and nucleoid structure was characterized; these results are shown in Figure 2.9.

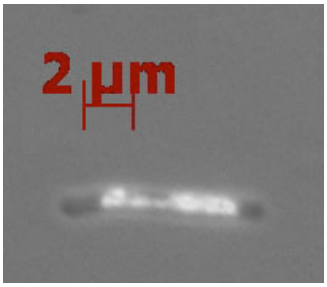

Figure 2.9: *parC1215* Partitioning Phenotype at an Early Timepoint. The figure shown was taken 60 minutes after shifting to the nonpermissive temperature.

Although the cells are not as filamented as the ParC206-752 or ParC332-752 samples, a small portion of cells containing the *parC1215 (ts)* allele do have similar nucleoid

structures after 60 minutes of growth at the restrictive temperature. This indicates that filaments with connected nucleoids seen in the ParC206-752 and ParC332-752 samples may be defective in Topo IV activity.

Discussion

The overexpression of ParC206-752 and 332-752 led to a heterogeneous DNA segregation pattern, with the nucleoid morphology falling into six distinct classes. Four classes of mechanisms may explain this phenotype, but since a combination of any of the mechanisms may be occurring, it is difficult to distinguish between them.

1st Mechanism: Endogenous ParC Interaction

First, endogenous ParC protein could be the primary target; oligomerization of the fragments with full-length ParC could reduce the formation of active Topo IV complexes. This is consistent with the fact that the fragments contain the oligomerization domain and truncations lacking the oligomerization domain relieve the plating deficiency; this interaction would result in a reduction of Topo IV activity. Since a partial loss phenotype for *parC* has not been described, the decrease may manifest itself in decatenation, cohesion, unknotting, or supercoiling maintenance.

If this explanation were sufficient, then one would expect the phenotype to closely resemble that of the *parC1215 (ts)*. The observation that some of the *parC1215 (ts)* cells exhibit conjoined nucleoids at 60 minutes after the shift to 37˚C suggests that the ParC

truncations may in fact be interfering with Topo IV activity in a subset of the cells at least. However, the terminal phenotypes of the *ts* mutation and the fragment expression are distinct. This might reflect the kinetics of inhibition. The speed with which the phenotype appears in the *parC1215 (ts)* strain is much faster than that of the ParC fragment. Upon temperature shift of the *parC1215 (ts)* allele, the effect on Topo IV is almost immediate because existing complexes as well as new complexes are disrupted. In contrast, the ParC fragment must accumulate to a certain concentration in order to render its effect and preexisting Topo IV might not be affected by the truncations. The ability of residual complexes to continue to act might lead to a different spectrum of terminal phenotypes than is seen in the *ts* mutant.

2nd Mechanism: Interaction with Protein X

Second, the fragments may be mimicking intact ParC's interaction with another protein. If this is the case, then the phenotype described above would represent a complete or partial inactivation of the target protein. Not only is this true in theory, but it has been shown that the ParC subunit of Topo IV interacts with multiple proteins including, but not limited to DnaX, FtsK, MreB, and SeqA, which may contribute to the phenotype (Espeli *et al.*, 2003a; Espeli *et al.*, 2003b; Kang *et al.*, 2003; Madabhushi and Marians, 2009).

If the fragments were interacting with another target protein in the cell, then the phenotype would be due to an inability to localize or activate Topo IV. The native

functions of the Protein X may be affected as well, although its catalytic domains or binding sites to other proteins may remain unhindered. The effect may manifest as a partial mutant or a combination of different phenotypes. ParC has been shown to interact with a multitude of proteins from several different processes (Butland *et al.*, 2005). Due to the sheer number of characterized interactions, determining which protein target is involved would be most difficult to illustrate. Considering the phenotype described above, proteins involved in replication, septation, and chromosome stability/ maintenance would be likely candidates.

For instance, FtsK is an essential protein that has been shown previously to physically and functionally interact with ParC (Espeli *et al.*, 2003a). The C-terminus of FtsK is a DNA binding motor domain that directs replicated chromosomes into daughter cells as the septum constricts. Additionally, this domain stimulates not only Topo IV's decatenase activity, chromosome dimer resolution via XerCD, but it also simplifies chromosomal topology in the terminal region of the chromosome (Aussel *et al.*, 2002; Espeli *et al.*, 2003a; Grainge *et al.*, 2007). If the ParC fragments interfere with the CTD of FtsK, this would affect decatenation, dimer resolution, and chromosome topology.

MreB is another protein that has been shown to physically and functionally interact via the ParC subunit of Topo IV (Madabhushi and Marians, 2009). MreB is an actin homolog whose helical filaments participate in the maintenance of cell shape and the movement and segregation of daughter chromosomes (Kruse *et al.*, 2003). *mreB*

mutants appear to be deficient in decatenation, suggesting that Topo IV may be temporally regulated by MreB. The activation or inhibition appears when ParC is bound to MreB filaments or monomers, respectively (Madabhushi and Marians, 2009). If the ParC fragments block endogenous Topo IV from binding to MreB, then replicated chromosomes may be partitioned before Topo IV is fully active.

Lastly, SeqA has been shown to specifically interact with the C-terminal domain of ParC (Kang *et al.*, 2003). SeqA's main task in the cell is to bind newly replicated origins at hemimethylated GATC sites, thereby preventing overinitiation at *oriC*. However, SeqA's preference for these hemimethylated sites acts to localize it behind progressing replication forks (Brendler et al., 2000); this may act to localize Topo IV activity behind the forks to precatenanes, thereby affecting chromosomal cohesion. If ParC fragments block binding to SeqA, the endogenous Topo IV would not be able to bind. This may result in its inability to relax DNA or resolve precatenanes.

In addition to the proteins described above, ParC interacts with a multitude of other proteins, either genetically or physically. There are two proteins that interact with ParC genetically, acting as high-copy suppressors of the *parC1215 (ts)* allele: *setB* and *topB* (Espeli *et al.*, 2003c; Nurse *et al.*, 2003). Also, Espeli *et al.*, 2003 demonstrated that the ParC protein colocalized with the replication machinery via an interaction with DnaX; a mutation in the DnaX protein resulted in the loss of that colocalization (Espeli *et al.*, 2003b). Finally, ParC has been shown to interact with over 15 different partners from a

high-throughput 2-hybrid screen (Butland *et al.*, 2005).

3rd Mechanism: Substrate Binding

Thirdly, the fragments may be interfering with Topo IV binding to its DNA substrate. If the fragments were able to bind, they would reduce the number of free sites for functional Topo IV, reducing Topo IV function *in trans*. The C-terminal domain of the ParC protein is responsible for substrate specificity of the complex and truncations with both the oligomerization domain and the CTD may bind to right-handed DNA crossovers (Corbett *et al.*, 2005). A fragment lacking the C-terminal region might lower the binding affinity of the complex to bind to its substrate, since the functional enzyme contains two of these motifs instead of only one. Since the fragments still lack the domains necessary for ParE binding and covalent catalysis, the fragment could be reducing the number of binding sites accessible to a fully functional Topo IV complex (Peng and Marians, 1993; Yokochi *et al.*, 1996). In the end, the Topo IV complex will function when bound to DNA, but substrate binding may be the rate-limiting step due to the overwhelming presence of inert ParC fragment dimers.

Finally, the phenotype may be a combination of options described above. Due to ParC's promiscuity and the sheer excess of fragment expressed, several of the mechanisms described may be acting concurrently.

Loss of specific functions of Topo IV may not be easy to detect during fragment expression; other proteins in the cell are able to compensate for the partial loss of Topo

IV. For example, DNA gyrase inserts negative supercoils into DNA while Topo IV and Topo I maintain positive supercoiling. If Topo IV activity was reduced, Topo I would still function to counter DNA Gyrase (Zechiedrich *et al.*, 2000). Likewise, Topo IV is not the only decatenase in the cell. Both Topo III and XerCD have been shown to decatenate the chromosome in the absence of Topo IV (Grainge *et al.*, 2007; Nurse *et al.*, 2003). Decantenation by these proteins may be too inefficient to meet the cell's needs. In fact, we believe that ParC contributes to XerC's own resolution activities, which will be discussed in Chapter III. Another process involving Topo IV is cohesion. It was shown that mild increases in Topo IV activity reduce sister chromosome cohesion time by removing precatenanes that form between them. The authors go on to show that impairment of Topo IV does not inhibit chromosome migration or chromosome segregation (Wang *et al.*, 2008). The only role that Topo IV plays that may not be redundant is its ability to remove knots that form due to normal cellular functions such as recombination and replication. However, although it is expected that failure to resolve knots *in vivo* is lethal, this has never been demonstrated (Deibler *et al.*, 2001).

CHAPTER III

CHARACTERIZATION OF THE ParC333-485 PHENOTYPE

Newly replicated daughter chromosomes are connected with both topological and molecular restraints (Figure 3.1). First, normal replication of closed circular chromosomes results in catenated chromosomes, similar to the links of a chain. Second, uneven numbers of homologous recombination events lead to chromosome dimer formation; this results in two genome equivalents in a single closed circle. In order for cell division to be successful, these topological issues must be resolved so each daughter cell receives a full genome.

Catenanes form naturally by replicating a closed circular chromosome. Before they may be partitioned into each daughter cell, they must be unlinked; Topo IV decatenates linked chromosomes (Adams *et al.*, 1992; Zechiedrich *et al.*, 1997). Topo IV is an essential enzyme composed of a dimer of ParC and two monomers of ParE (Peng and Marians, 1993). Decatenation occurs in the DNA terminus region at the chromosomal locus *dif* and is temporally regulated by the DNA translocase motor domain of FtsK, a component of the septal ring (Espeli *et al.*, 2003a; Hojgaard *et al.*, 1999).

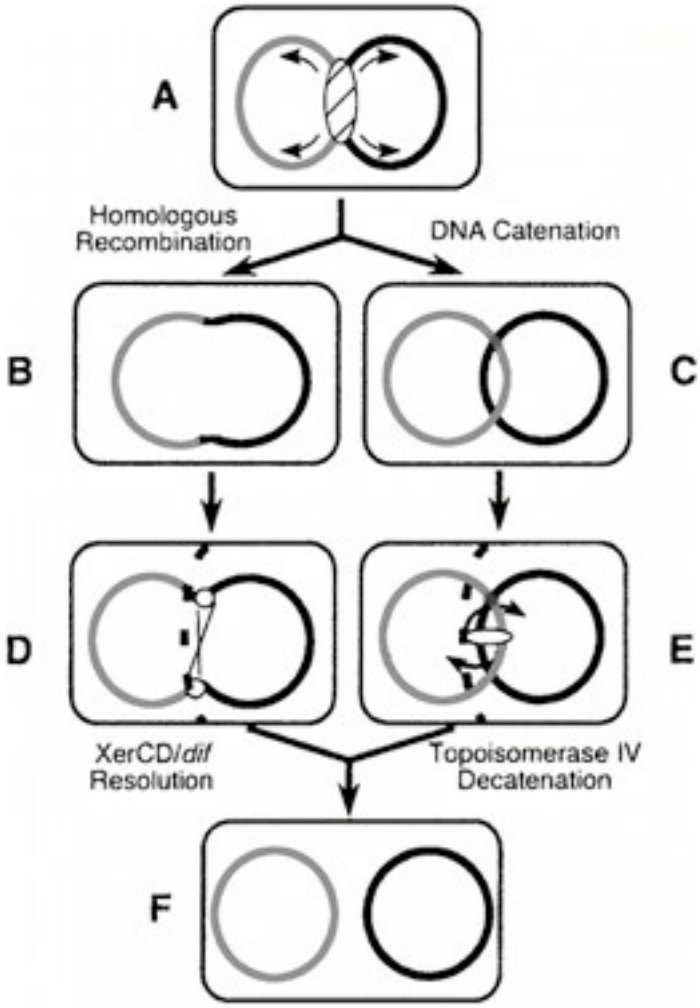

Figure 3.1: Chromosome Topology during Replication. Figure taken from Gordon and Wright, 2000.

Not only does Topo IV decatenate daughter chromosomes, it also acts in other aspects of DNA topology, such as supercoiling maintenance, unknotting, and cohesion. Temperature sensitive alleles for both subunits have been identified (*parC1215* or *parE10*) and growth at the restrictive temperature generates filamentous cells containing

a single mass of intertwined chromosomes as well as anucleated cells that arise from polar division events (Kato *et al.*, 1988).

For resolution of the chromosome dimers, *E. coli* employs XerCD, a site-specific recombinase. This complex also acts at *dif* to separate the genome equivalents into catenated monomeric chromosomes, which Topo IV will subsequently unlink (Kuempel *et al.*, 1991; Zechiedrich *et al.*, 1997). The process of chromosome dimer resolution acts only as cell division occurs and similar to Topo IV's decatenation activity, XerCD activity is also regulated by the C-terminal domain of FtsK (Steiner *et al.*, 1999).

Mutants deficient in *xerC* have an excess of cells at the two-cell stage due to the inefficiency at which these chromosome dimers resolve (Blakely *et al.*, 1991). Inactivating *recA* inhibits the formation of the dimers, thereby eliminating the requirement for XerCD. Once chromosome dimers and catenanes are resolved, FtsK finishes the translocation of the chromosomes into the daughter cells and the septum closes.

ParC333-485 Fragment

In Chapter II, I showed that overexpression of ParC fragments containing the oligomerization domain and the C-terminal domain resulted in lethal plating defects. In this chapter, I will describe the functional characterization of a ParC fragment that produces a less severe phenotype. The fragment corresponding to the oligomerization

domain of ParC, ranging from residue 333 to residue 485 was found previously in a screen that identifies protein fragments that self-assemble (Marino-Ramirez *et al.*, 2004). The boxed region shown in Figure 3.2A highlights the region identified in the screen.

(A)

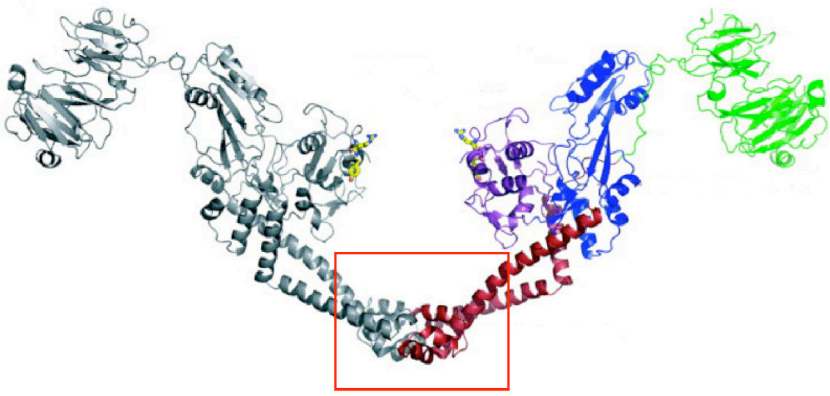

(B)

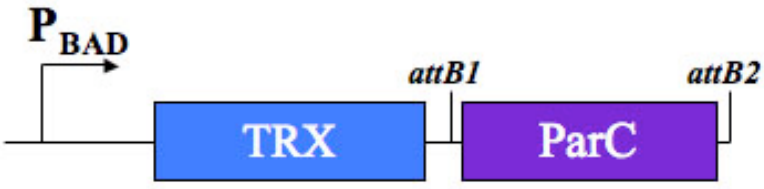

Figure 3.2: Construct Overexpression of ParC333-485. (A) Mapping of the ParC333-485 region identified in the screen described in Marino-Ramirez *et al*., 2004 onto the structure published in Corbett *et al*., 2005. (B) Expression construct for the ParC fragments.

Expression of the TRX-ParC333-485 was induced and the resultant phenotype was characterized. Upon overexpression, ParC333-485 could potentially interact with two kinds of protein targets in the cell, as depicted in Figure 3.3. First, since the fragment contains the oligomerization domain of ParC, an interaction with the endogenous Topo IV may occur. Since the interference is predicted to only affect a subset of ParC in vivo, the efficiency with which Topo IV functions would be reduced. Second, ParC333-485 may interact with Protein X, a protein that interacts with Topo IV (Figure 3.3B). If this former occurs, the fragment will be acting in a negative dominant manner, thereby affecting any or all of the functions performed by Topo IV. However, if the latter occurs, then the fragment would be acting as an inhibitor. The phenotype seen would mirror a full or partial inactivation of the target protein (Herskowitz, 1987).

To that end, the 333-485 region of ParC identified in the screen was fused to a His-patch Thioredoxin (HP-TRX) tag and put under the control of the inducible arabinose promoter, P_{BAD}, as shown in Figure 3.2B. Upon its induction, a subset of cells within the population exhibits a *recA*-dependent chaining defect. This phenotype is unique to Topo IV because its known mutant alleles (i.e. *parC1215* or *parE10*) cause filamentous cells deficit in nucleoid partitioning or completely anucleate cells (Kato *et al.*, 1988).

(A)

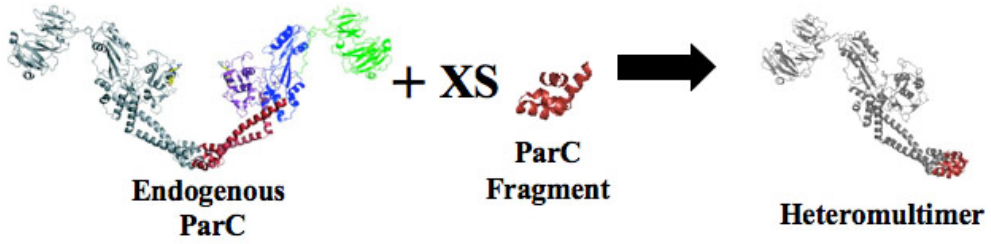

(B)

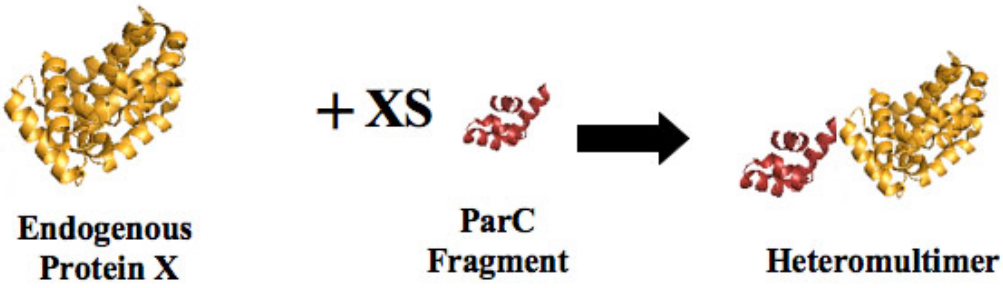

Figure 3.3: Putative Overexpression Targets. Predicted Interactions of the ParC fragment with Endogenous Topo IV (A), or another endogenous protein, X (B). This approach affects protein function in a post-translational manner.

Materials and Methods

Bacterial Strains and Plasmids

Table 3.1: Bacterial Strains Used in Chapter III.

Strain	Genotype	Reference
MG1655	F-, λ⁻, *rph-1*	Blattner et al., 1997
RY15076	MG1655 *lacI*^{q} *lacZ*::*Tn5*	Ry Young
AZ1289	MG1655 *recA- srl::Tn10*	this study
AZ49	MG1655/ pJM187	this study
AZ102	MG1655/ pAZ9	this study
AZ107	MG1655/ pAZ13	this study
AZ1177	MG1655 *parC1215 metC::Tn10*	this study
AZ1249	RY15076/ pJM185 + pDSW207-FtsN	this study
AZ1269	RY15076/ pAZ859 + pDSW207-FtsN	this study
AZ1289	MG1655 *recA- srl::Tn10*	this study
AZ1290	MG1655 *recA- srl::Tn10*/ pJM187	this study
AZ1291	MG1655 *recA- srl::Tn10/* pAZ13	this study
AZ1389	MG1655 *lexA3 malF::Tn10*/ pJM187	this study
AZ1390	MG1655 *lexA3 malF::Tn10*/ pAZ13	this study

Table 3.2: Plasmids Used in Chapter III.

Plasmid Name	Description	Relevant Marker	Reference
pJM187	**Gcn4** LZ in pBAD-DEST49	ampicillin	this study
pAZ9	**DnaX247-455** in pBAD-DEST49	ampicillin	this study
pAZ13	**ParC333-485** in pBAD-DEST49	ampicillin	this study
pJM198	P_{BAD}- His Patch Thioredoxin destination vector/ pACYC origin	tetracycline	this study
pJM185	**Gcn4 LZ** in pJM198	tetracycline	this study
pAZ859	**ParC333-485** in pJM198	tetracyline	this study
pDSW207-FtsN	P_{lac}- FtsN-GFP	ampicillin	Wissel and Weiss, 2004
pBAD-DEST49	P_{BAD} His-Patch Thioredoxin Gateway vector/ pUC origin	ampicillin	Invitrogen

Growth Conditions

Overnight cultures were grown for about 16 hours in 2 ml LB with 200 µg/ml ampicillin and 0.1% D-fucose in a roller drum rotating at 37˚C. The bacterial strains and plasmids used in this study are listed in Tables 3.1 and 3.2, respectively. The overnight cultures were diluted 1:1000 into 10 ml LB + 200 µg/ml ampicillin in 125ml Erlenmeyer flasks at and incubated at 37˚C in a New Brunswick Gyrotory Water Bath Shaker model G76 at a shaker speed of 6 (~210 rpms). When the cultures reached an OD_{600} = 0.05, L-arabinose was added (final concentration 0.2%) to induce expression of the fragments. For control cultures, D-fucose (final concentration 0.1%) was added instead of L-arabinose. Samples for microscopy and to measure optical density were taken every 30 min for 180 min to document the growth of the culture. To maintain the cells in exponential phase, 90 min after induction cultures were diluted 1:10 into fresh prewarmed LB with 200 µg/ml ampicillin and L-arabinose (0.2%) or D-fucose (0.1%) and grown for an additional 90 minutes.

LB plates containing 200 µg/ml ampicillin + either 0.2% L-arabinose (inducer) or 0.1% D-fucose (anti-inducer) were used to test the various strains in dilution assays. Overnight cultures grown as described above were serially diluted 1:10 into 1x M9 salts using a multichannel pipettor. Cells were spotted onto the plates using a 48-or 96-pronged replicator (Boekel). This instrument applies 5-10 µl of culture onto the plates. Plates were allowed to dry and then incubated at 37˚C overnight. Both colony morphology and plating efficiency were documented for these experiments.

Cloning Procedures

parC gene fragments were amplified from the plasmids described in Marino *et al*., 2004 using the PCR primers *forward-attB1* (GGGGACAAGTTTGTACAAAAAAGCAGG-CTACAAGGACGACGATGACAAG) and *reverse-attB2* (GGGGACCACTTTGTAC-AAGAAAGCTGGGTCTTTCGGGCTTTGTTAGCAG). The DNA fragments were cloned into the expression vector pBAD-DEST49 or pJM198 using the Gateway Cloning Technology (Invitrogen).

Microscopy

Cell Fixation

Cells were fixed by adding 0.19 volumes of 16% paraformaldehyde to aliquots of culture. Cells were allowed to stand at room temperature for 30 minutes and then placed on ice for up to 3 hours. Cells were then pelleted gently at 3.3xg in a tabletop centrifuge for 3 minutes. The supernant was removed and the cells were washed 3 times in ice-cold 1X PBS. After the final wash, the pellet was resuspended in 250-500 µl of 1x PBS (dependent upon the size of pellet) and stored at 4˚C in the dark.

Fluorescence

Coverslips were coated with 0.01% poly-L-lysine, washed 3 times with MilliQ water, then rinsed with 100% ethanol and dried. Cells (30 µl) were placed on the coverslip and allowed to sit for 3 minutes. Dabbing the edge of the coverslip to a paper towel and dipping the coverslip into 1x PBS removed the excess culture. The coverslips with the sample facing up were allowed to air dry for 5 minutes on a paper towel. 3 µl of DAPI (3 µg/ml) was added before the coverslips were inverted onto slides with 3 µl Anti-Fade mounting medium (Invitrogen).

Images were captured using a Zeiss AxioPhot 2 microscope at 100x magnification. Phase contrast, DNA, and GFP were visualized using 20-50 ms, 110-200 ms, and 5-6 s exposure times, respectively.

Quantification of Cell Length

The cells were measured with a ruler in cm and converted to μm by multiplying the value by (4.5 cm/2 μm). This value was obtained by averaging measurements of the scale bar. In addition to chain length, the number of cells/ chain, and the number of apparent nucleoids were reported.

Results

Characterization of the Plating Phenotype

In order to examine whether the phenotypes of cells expressing the short fragment affected growth, I compared the plating efficiency of the cells expressing the fragment to cells expressing other oligomerizing protein fragments. The plating efficiency of the ParC333-485 fragment was similar to that of the Gcn4 control in the presence or absence of inducer, while overexpression of DnaX247-455 was lethal when plated on arabinose (Figure 3.4).

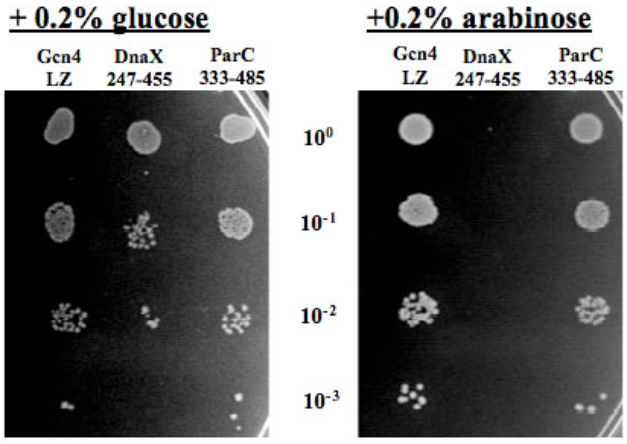

Figure 3.4: Plating Dilution of the ParC333-485 Fragment. This fragment was compared to other proteins known to self-assemble.

Although the plating efficiency was comparable, the individual colonies expressing the ParC333-485 were mucoid. The majority of mucoid phenotypes (*lon, capRS*) are due to an overproduction of capsular polysaccharide, although the implications of this phenotype are not clear (Bush and Markovitz, 1973). Thus, unlike the longer ParC fragments, *E.coli* tolerates expression of the shorter ParC fragment.

Characterization of ParC333-485 Overexpression in Liquid Culture

Growth Rate

I compared the growth of cells overexpressing the short ParC fragment in liquid culture (Figure 3.5). ParC333-485 expressing cultures have comparable doubling times measured by turbidity to those grown in fucose (data not shown) and the Gcn4 LZ control.

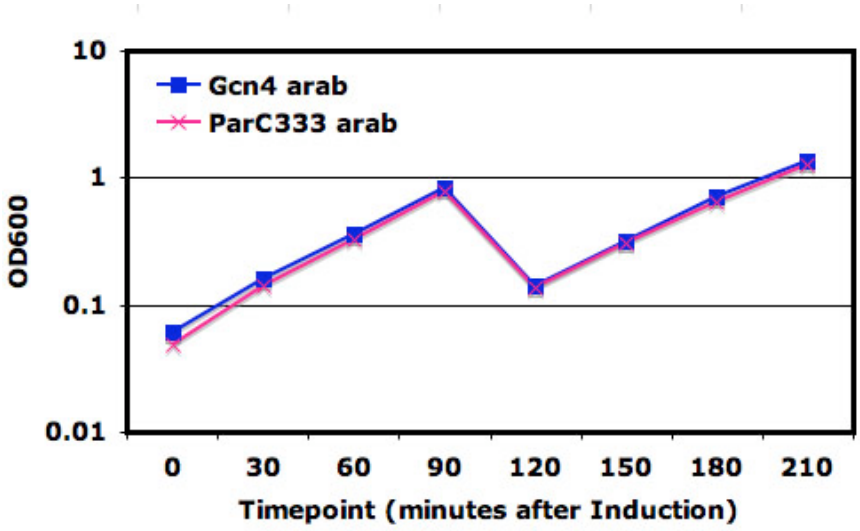

Figure 3.5: Growth Rate of Cells Expressing the ParC333-485 Fragment. Growth rate of cells expressing ParC333-485 was compared to those expressing the Gcn4 LZ control.

Microscopy

Although the ParC333-485 expression has not been consistent with known phenotypes of conditional *parC1215 (ts)* allele, the mucoid appearance of the colonies may indicate a lesser defect. In order to determine the whether this was the case, cells expressing ParC333-485 were viewed under the microscope (Figure 3.6).

(A)

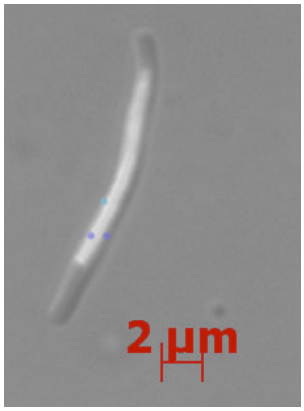

(B)

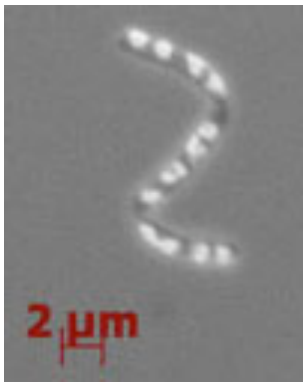

Figure 3.6: Morphological Comparison between ParC333-485 and *parC1215 (ts)*. Cell morphology and nucleoid organization were compared in cells harboring the *parC1215 (ts)* allele (A) grown at the restrictive temperature and cells expressing the ParC333-485 fragment (B). Pictures were taken 150 minutes after temperature shift (A) or induction (B).

Microscopy revealed that the ParC333-485 overexpression phenotype is completely different to that of the *parC1215 (ts)* in two ways. First, the fragment appears to have an effect on cell division whereas the *parC1215 (ts)* produces smooth filaments. Second, there appears to be only minor nucleoid partitioning defects (if any) in the ParC fragment phenotype. This is in contrast to the ts allele that contains a single mass of intertwined chromosomes centered within the filament. Figure 3.7 quantifies the chaining phenotype as a function of time. Unlike the typical partitioning phenotype seen with a *parC* or *parE* mutant, the cells expressing ParC333-485 form incompletely separated chains of three or more cells with visible septa

As the induction progresses, individual cells in the TRX-ParC333-485 sample form chains while cells in the Gcn4 LZ control divide and separate normally. Figure 3.7B shows that the cells expressing ParC333-485 exhibit an arabinose-dependent chaining defect in a subset of the population while the Gcn4 LZ control cells exhibit consistent populations of single and double cells (Figure 3.8A). The cell chaining begins 60 minutes after induction and increases for about 60 minutes before decreasing.

The cell chaining only occurs in a subset of the population and the relative numbers of chains vs. doublets vs. single cells is inconsistent compared to the Gcn4 LZ control. These results are graphed in Figure 3.8

(A)

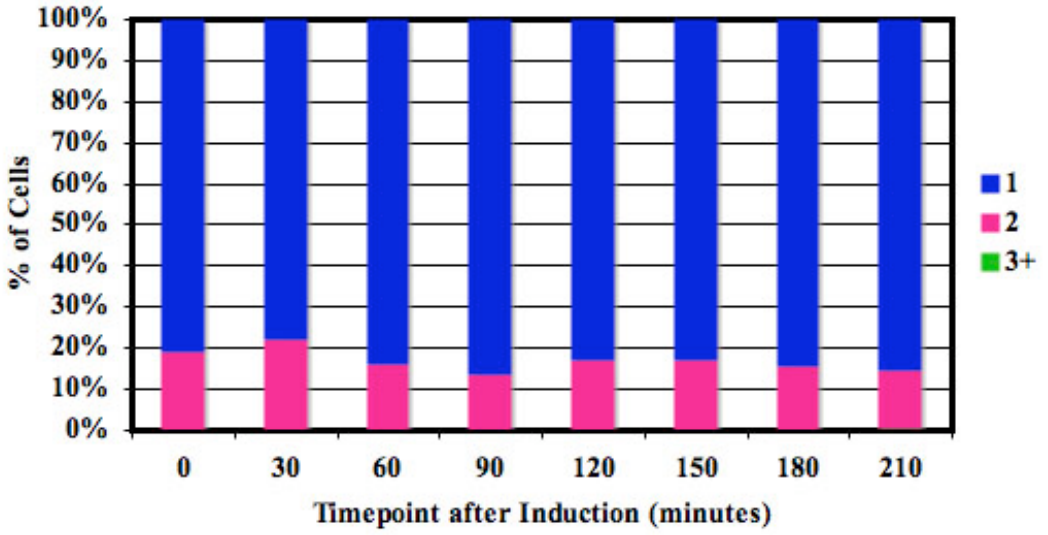

(B)

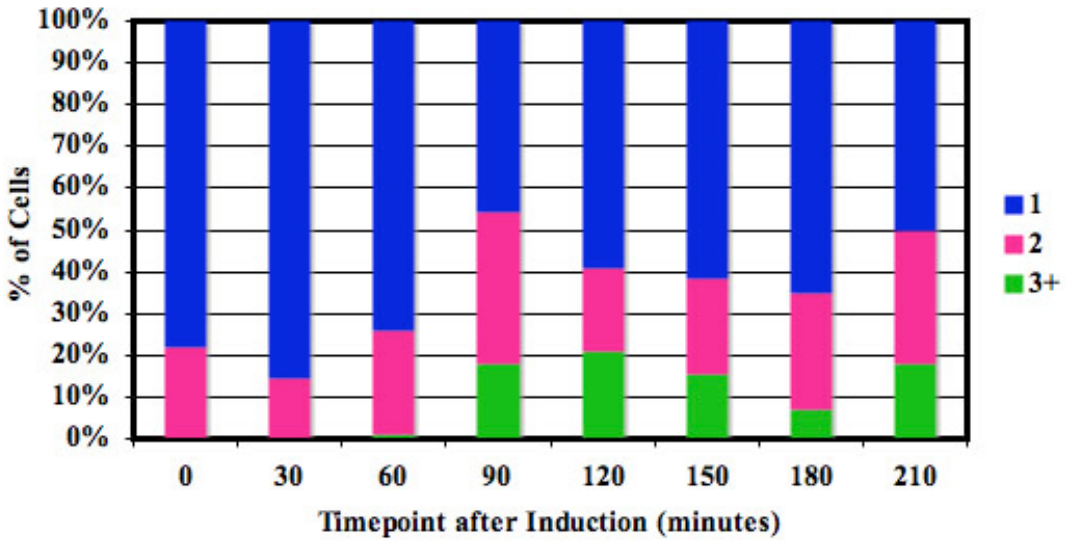

Figure 3.7: Quantification of the Chaining Phenotype. A comparison is made between the Gcn4 LZ control (A), and cells expressing the ParC333-485 fragment (B). The "1", "2", and "3+" are indicative of single cells, doublets, and chains with 3 or more cells per chain respectively.

(A)

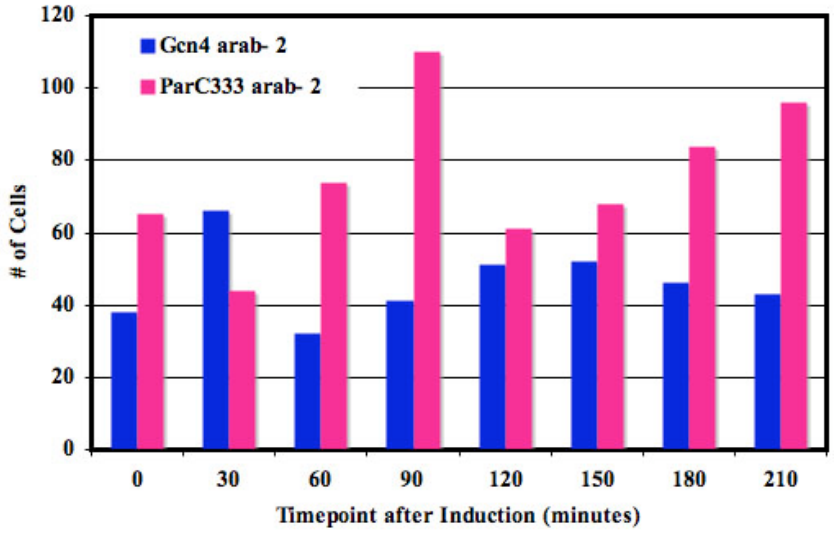

(B)

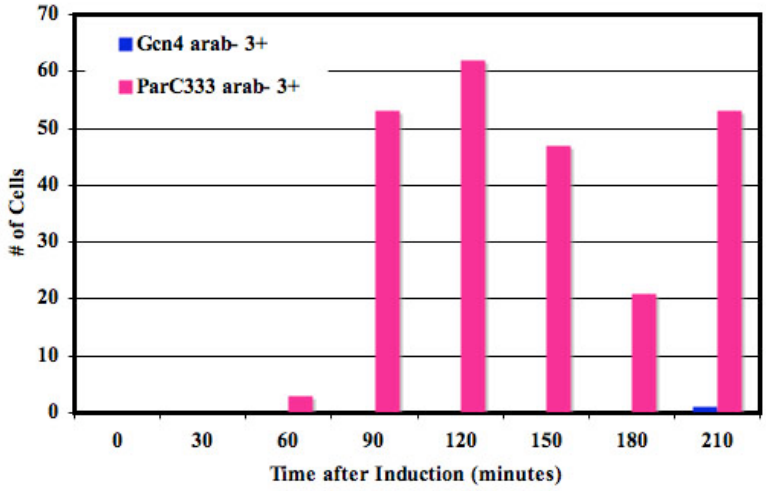

Figure 3.8: Comparison of Multi-Cell Chains. The number of doublets (A) and longer chain (B) from Gcn4 LZ-and ParC333-485-expressing cells were compared throughout the duration of the induction. Notice that in (A), the Gcn4 sample has a consistent number of doublets while those cells vary in the ParC333-485 sample.

The cells seem to grow and divide in exponential phase, however, the number of cells per chain starts to increase as the cells approach an $OD_{600} = 0.8$. Cultures were diluted into fresh media in an effort to increase the number of cells participating in the chains, but the chains shortened until the OD reached 0.8 again.

Characterization of the Septation Phenotype

A cell chaining phenotype linked to either subunit of Topo IV has never been reported. Chaining has been seen in mutants of genes involved in chromosome segregation and cell division, such as *ftsK*, *ami*AC, *tat*A (due to the mislocalization of the *ami* genes), *xerC* among others (Bernhardt and de Boer, 2003; Blakely *et al.*, 1991; Priyadarshini *et al.*, 2006). If the ParC333-485 interferes with any of these proteins *in vivo*, the cell chaining phenotype may be explained.

Presence of the Septal Ring Components

One reason the cells overexpressing ParC333-485 are defective in septation may be that the fragment is interfering with recruitment of the necessary proteins to the septal ring.

A visible constriction indicates that at least some of the ring proteins are present and functional (Bernhardt and de Boer, 2003). However, in order to determine whether the chaining is due to the absence or malfunction of a late recruit to this pathway, I examined localization of FtsN.

FtsN is one of the last proteins to be recruited to the ring, and its recruitment is dependent upon localization of FtsZ and FtsA and the function of FtsI and FtsQ (Hale and de Boer, 2002; Mercer and Weiss, 2002; Wissel and Weiss, 2004). Therefore, correct localization of FtsN means all necessary proteins up to FtsI are present and functional. According to previous FtsN localization studies, foci of GFP-tagged FtsN may be visualized in ~50% of normal cells undergoing division (Addinall *et al.*, 1997).

Consistent with previous studies, GFP-FtsN foci occurred in close to 45% of cells with either a single septum or for chaining cells, in at least one of the septa. Most chains containing 3-4 cells showed at least one GFP-FtsN foci as seen in Figure 3.9B, while chains of four or more cells contained two GFP foci.

(A)

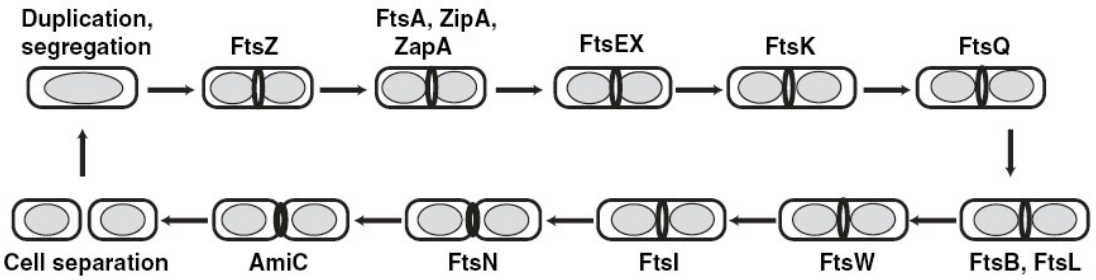

(B)

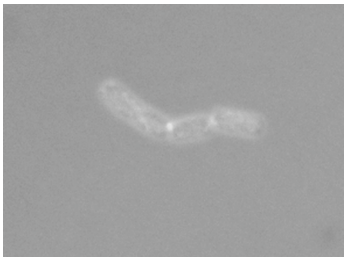

(C)

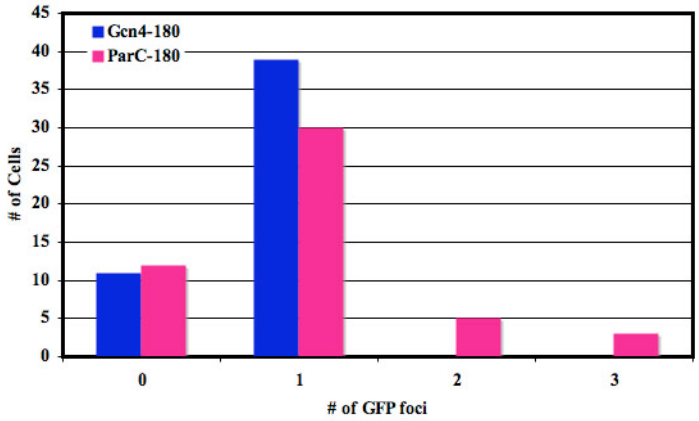

Figure 3.9: Recruitment and Localization of GFP-FtsN. (A) Septal ring recruitment pathway taken from Geissler and Margolin, 2005, (B) DIC and GFP overlay of a chain containing 2 foci of GFP-FtsN, and (C) Histogram of GFP-FtsN foci seen in cells expressing ParC333-485.

Tests for Synthetic Effects

Since the chaining phenotype of cells overexpressing ParC333-485 is relatively mild, additional mutations were introduced in an attempt to make the phenotype more severe. These additional mutations were chosen based on synthetic effects seen with proteins involved with either chromosomal positioning, segregation, or septation.

ΔmukB

MukB is a chromosomal maintenance protein involved in chromosome folding and DNA condensation (Cui *et al.*, 2008). *mukB* mutants are defective in chromosome segregation and as a result, form filaments with irregularly space nucleoids (Niki *et al.*, 1991).

It has been shown previously that a Δ*mukBftsK1::cat* double mutant is synthetically lethal (Yu *et al.*, 1998). If the ParC333-485 fragment interferes with the FtsK C-terminal domain, then the chaining phenotype might be exacerbated. However, combining the Δ*mukB* deletion with the overexpression of ParC333-485 does not make the phenotype more severe. This suggests that ParC333-485 is not interfering with the CTD of FtsK.

ΔminC/ΔslmA

Both proteins SlmA and MinC have roles in nucleoid occlusion. SlmA and MinC (together with MinD) inhibit septal ring formation in regions of the cell where DNA resides and at the poles respectively (Bernhardt and de Boer, 2003; Hu and Lutkenhaus,

2000). A *ΔslmAΔminC* double mutant is synthetically lethal, so if TRX-ParC333-485 interferes with either of these proteins in the absence of the other, then a lethal phenotype should occur (Bernhardt and de Boer, 2005). However, combining either of these mutations with ParC333-485 expression has no effect on the efficiency of plating.

XerCD Resolvase

The cultures overexpressing the ParC333-485 fragment are enriched for cells at the two-cell stage and greater, similar to a *xerC* mutant phenotype. Both XerCD recombinase and Topo IV function to resolve topological issues after replication has been completed (Adams *et al.*, 1992; Blakely *et al.*, 1993). Also, published literature suggests that both complexes act at the same chromosomal locus (*dif*) and are activated by FtsK (Espeli *et al.*, 2003a; Hojgaard *et al.*, 1999; Kuempel *et al.*, 1991; Recchia *et al.*, 1999; Steiner *et al.*, 1999). If the ParC333-485 fragment interferes with XerCD's ability to resolve chromosome dimers, then deleting *xerC* would eliminate the target.

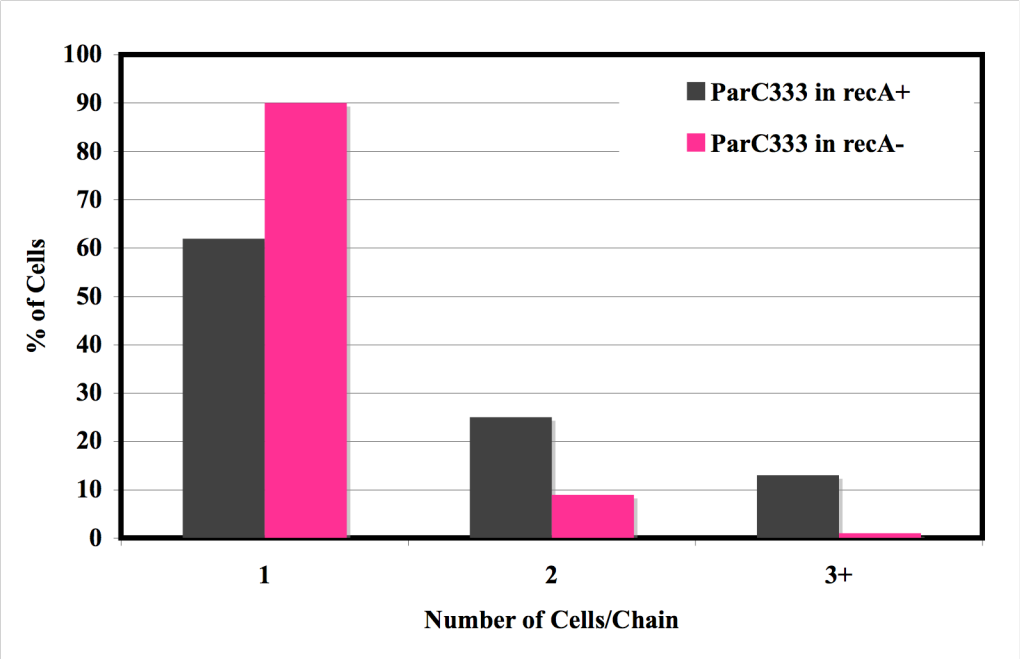

Figure 3.10: *recA* Dependence of the Chaining Phenotype. There are fewer cells present as doublets or chains in the absence of *recA*.

Rec-Dependence

The excess of cells at the two-cell stage in a *xer* mutant is due to the cell's inability to resolve chromosome dimers, the product of uneven numbers of homologous recombination events. The compensatory mutation in *recA*⁻ eliminates the presence of these dimers, thereby suppressing the *xerC* phenotype (Blakely *et al.*, 1991). If overexpression of ParC333-485 is affecting this same process, then its chaining phenotype should also be *recA*-dependent. As shown in Figure 3.10A, the mutation in *recA* suppresses the ParC333-485 chaining phenotype. There is a drastic reduction in the number of cells at the two-cell stage and above in the *recA*⁻ strain background. This effect is also shown in Figure 3.10B, where the distribution of cells expressing the ParC333-485 is comparable to that of the Gcn4 LZ control. RecA is widely known for its role in recombination and is linked to both formation of chromosome dimers and induction of the SOS response by DNA damage.

ParC333-485 expression did not induce *sulA*, the SOS-dependent protein that inhibits Z ring formation (data not shown) and previous studies show that *parC1215* filamentation is *sulA*-independent at the non-permissive temperature. Although chaining is not a typical SOS phenotype, the *recA*⁻ dependence of the ParC333-485 phenotype warranted a second look at its induction.

(A)

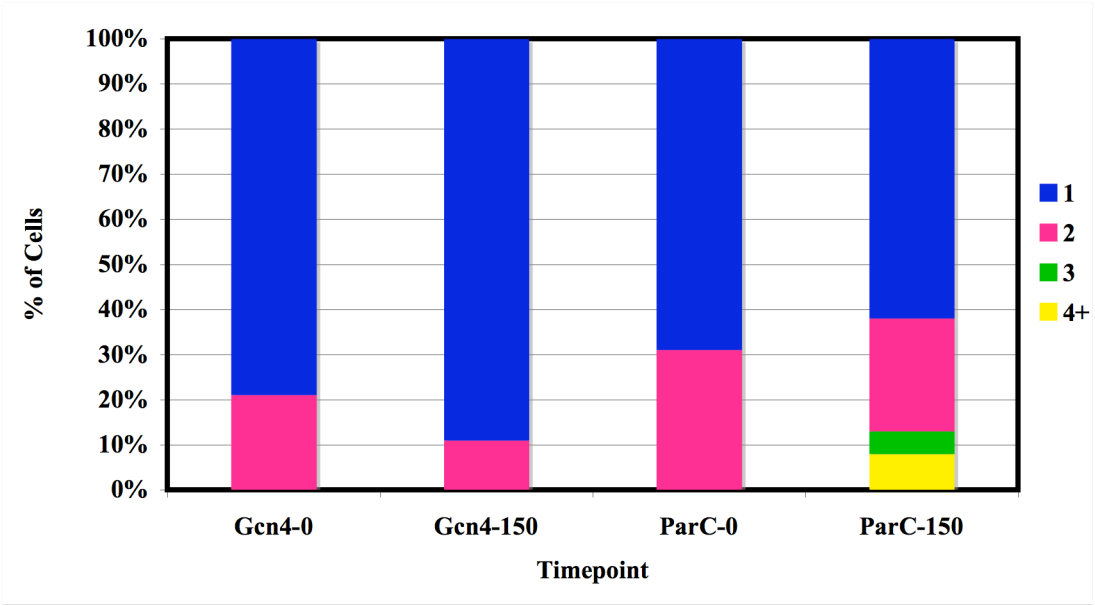

(B)

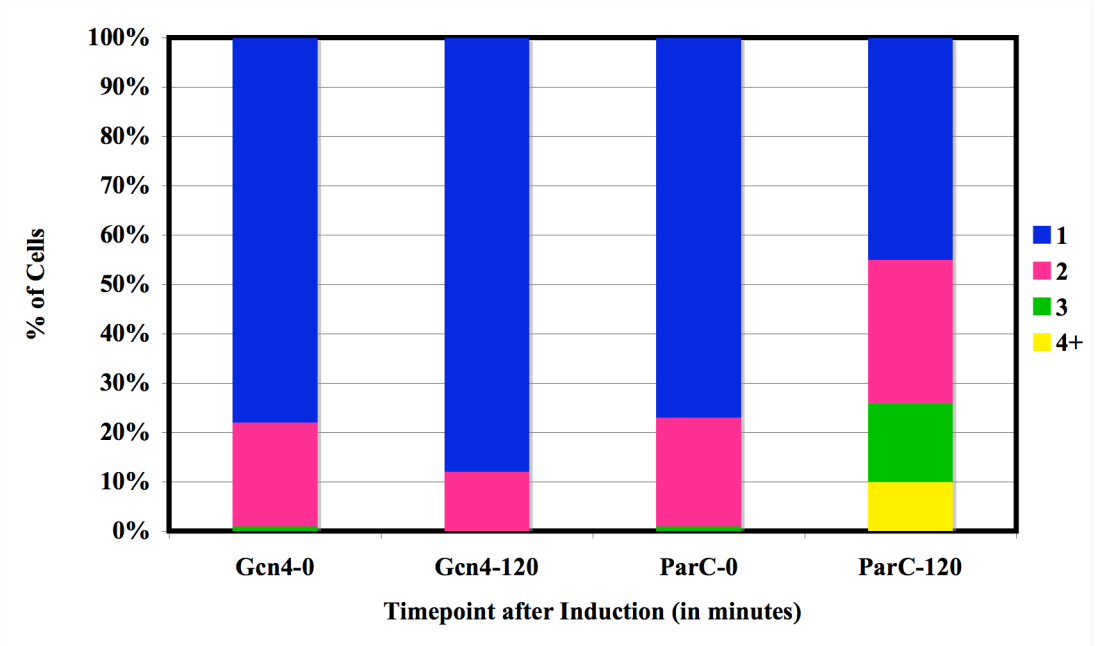

Figure 3.11: Effect of *lexA3* on the ParC333-485 Chaining Phenotype. Chaining phenotype in the *lexA*$^{+}$ strain background (A) and in the *lexA3* strain background (B) 0 or 150 minutes after Gcn4 LZ or ParC333-485 induction. Single cells are represented in blue, doublets in pink, 3 cell-chains in green, and chains of 4 or more cells are yellow.

SOS Response

To determine whether the *recA*$^-$dependence of the chaining defect is due to the induction of the SOS response, the overexpression of ParC333-485 was examined in a *lexA3* (*Ind*$^-$) strain background. The LexA repressor controls the expression of over 30 genes involved in the SOS response. Upon DNA damage, such as UV irradiation, LexA cleavage derepresses over 30 genes involved in the SOS reponse, including *sulA, umuCD*, and *recA* (Fernandez De Henestrosa *et al.*, 2000).

If the chaining were due to SOS induction, the *lexA3* mutation would alleviate the ParC333-485 overexpression phenotype. However, after 5 doublings the chains persist, indicating that the *recA*-dependence of the ParC333-485 phenotype is SOS-independent, and thereby due to *recA*'s role in homologous recombination/ chromosome dimer formation (Figure 3.11).

Discussion

Overexpression of ParC's oligomerization domain ranging from residues 333-485 yield a mild chaining phenotype in a subset of the overall population, even though the fragment should be uniformly present in all cells. Similar chaining phenotypes have been reported previously with septal ring components *ami*C and *ftsK* (CTD-dependent), although the chains are generally longer and they occur in a higher percentage of the population (Bernhardt and de Boer, 2003; Diez *et al.*, 1997; Priyadarshini *et al.*, 2006).

The chains of cells induced by ParC333 overexpression are shorter than would be

expected if the fragment immediately and irreversibly blocked septation while growth continued. Two models could account for this. First chaining could be reversible. A temporary block may be preventing complete septum formation and once the issue is resolved, septation continues. Failure to segregate chromosomes properly will trigger a "checkpoint" that delays septum closure. Alternatively, chaining could be terminal but cells might be limited to maximum length before they die. If the latter is occurring, the lethality must involve something other than inhibition of septation per se, because such limits are not observed with *amiC* and *ftsK* mutants.

The distribution of short chain lengths at different times after ParC333 induction suggests that a subset of the population is continuously initiating chains. The short chains of cells and their distribution within the population is reminiscent of the phenotype seen in a *xerC* mutant (Blakely *et al.*, 1991). *xerC* encodes one subunit of a site-specific recombinase that resolves chromosome dimers as septation occurs. Chromosome dimers form when there is an uneven number of homologous recombination events between sister DNA strands during replication. These dimers pose a problem for chromosome segregation and must be resolved before the septum closes (Hendricks *et al.*, 2000). The XerCD recombinase catalyzes site-specific recombination at *dif*, a site near the terminus of replication, which resolves the dimers into catenated monomers, which get unlinked through the action of Topo IV (Blakely *et al.*, 1991; Zechiedrich *et al.*, 1997). After decatenation, the chromosomes are finally partitioned

into the daughter cells. These chromosome dimers only occur in about 10-15% of the cells in a population, so XerCD activity is not required for segregation all the time (Perals *et al.*, 2000; Steiner and Kuempel, 1998b).

In *xerC* mutants, the excess of cells at the two-cell stage due to the cell's inability to resolve these dimers is therefore *recA*-dependent (Blakely *et al.*, 1991). If overexpression of ParC333 is affecting this same process, then the chaining phenotype should also be *recA* dependent, which is what we observe. RecA is also involved in the DNA damage-inducible SOS response (Fernandez De Henestrosa *et al.*, 2000). If the chaining was caused by DNA damage such as double-stranded breaks, then overexpressing ParC333 in a SOS-deficient strain would alleviate the phenotype. We investigated ParC333 overexpression in such a strain and found the same trends in chaining persist, indicating that a product of homologous recombination is responsible for the chaining phenotype. These results, together with what is known about Topo IV suggest that overexpression of the 333-485 fragment is affecting XerCD activity or lowering the efficiency with which the cell segregates its chromosome.

There are multiple ways in which ParC333-485 might affect XerCD activity. First, the ParC333 fragment could be interfering with XerCD through a direct interaction. Due to the interdependence of chromosome dimer resolution, decatenation, and septation, a "supercomplex" containing FtsK, XerCD and Topo IV has been discussed (Bigot *et al.*, 2007). However, an interaction between either subunit of Topo IV with either subunit

of the Xer recombinase has not been shown in either of two genome-wide screens for interacting proteins (Arifuzzaman *et al.*, 2006; Butland *et al.*, 2005). In an alternative mechanism, the ParC333 fragment could be interfering with XerCD indirectly via its interaction with FtsK. It has been reported that FtsK's C-terminal motor domain is required for chromosome dimer resolution and physically interacts with both XerCD and the ParC subunit of Topo IV (Espeli *et al.*, 2003a; Recchia *et al.*, 1999; Steiner *et al.*, 1999). Cells harboring a deletion of this domain fail to correctly segregate the chromosome, resulting in a severe cell chaining phenotype (Geissler and Margolin, 2005) that masks the chaining phenotype from the ParC333 overexpression (data not shown).

If excess ParC333-485 blocks the FtsK/ XerCD interaction, then the rate of chromosome dimer resolution would be reduced and septation would be completely blocked or delayed. The two ways by which a triggered septation checkpoint can act to inhibit septation are to either block septal ring assembly or block septal ring closure. The presence of the GFP-FtsN foci at the multiple septa within the ParC333-485 chains is consistent with published work (Addinall *et al.*, 1997). This indicates that FtsN is present at the septum and the constriction indicates that it is functioning properly. In fact, chains of the ParC333-485 sample consisting of 3 or more cells are repeatedly seen with GFP-FtsN foci at multiple septa within the chain, indicating that multiple septa make it all the way through the assembly.

Septum closure may be delayed due to a non-functional component of the ring or incomplete segregation of the daughter chromosomes. The fact that the periplasmic domain of FtsN must be functional for visible constriction of the septum to occur indicates that at least the late recruits are functioning properly (Bernhardt and de Boer, 2003). These results suggest that the ParC333-485 chains fail to close the ring due to inefficient chromosome segregation, specifically resolution of chromosome dimers by the XerCD recombinase.

CHAPTER IV

PHENOTYPES OF OTHER PROTEIN FRAGMENTS

Negative Dominance

Conventional genetic methods to study protein function usually involve mutagenesis or deletion of a gene, which results in a *cis*-acting defect in function. Another way to study *in vivo* function is inhibiting the protein *in trans.* Many studies have used peptide inhibitors to block catalysis at the active site or by blocking allosteric sites.

Negative dominance represents one way to inactivate an oligomeric enzyme or protein complex *in trans*. In theory, variants of the endogenous protein expressed from a plasmid are presented in excess and therefore interact with a subpopulation of the target in a dominant manner. If these variants are inert with respect to catalysis, then the mutant would give a negative phenotype. The proposed result is a mixture of both functional and inert complexes *in vivo*, thereby knocking down the overall activity of a complex instead of completely obliterating its function. Essential genes for which conditional mutant alleles have not been isolated would be good targets for use with negative dominance. Since the effect is *in trans*, mutations or disruptions in the gene are not required and inducible expression of the negative dominant effector allows characterization of intermediate levels of inactivation. Using this method, overall heterogeneous interactions would be preserved.

Protein oligomerization is used by cells as a way to modulate protein function *in vivo*-at least 35% of proteins in the cell are predicted to be oligomeric (Goodsell and Olson, 2000). These oligomeric complexes are more stable, allow for more complex structures and finer tuning of regulation than their monomeric counterparts. Transient oligomerization is one way the cell regulates physiological processes. The presence of environmental factors promotes transient oligomerization, promoting specificity and control (Nooren and Thornton, 2003). Protein interfaces provide unique and stable active and allosteric sites that would be obliterated if oligomerization were disrupted.

There are several inherent benefits to blocking oligomerization as a means of modulating function. First, the residues at the interface of proteins have a tendency to be slightly more conserved than other residues throughout the protein (Caffrey *et al.*, 2004). This means that it would be less likely for this type of inhibition to be overridden by single mutations. Second, interrupting oligomerization allows you to define monomeric contribution to the overall function.

A screen identified *E. coli* protein fragments that could self-assemble when fused to the DNA-binding domain of the lambda cI repressor (Marino-Ramirez *et al.*, 2004). The majority of these fragments contain the oligomerization domain of the protein, but lack regions required for catalysis. If these fragments reflect the same binding properties as the endogenous full-length protein, then expressing the fragments may produce a negative dominant phenotype by interrupting both homotypic and heterotypic protein

interactions.

Fragments of the endogenous protein were overexpressed and used to disrupt protein function by blocking the formation of active protein complexes. There are several ways to disrupt complex formation, as shown in Figure 4.1. Fragments supplied in excess bind to the monomer of a homo-oligomeric complex. This is expected to result in a mixture of wild type complexes and heteromultimers between the full-length and the fragment. If function depends upon self-assembly, then the heteromultimers will be inactive, thereby knocking down the overall activity of the complex *in vivo* as modeled in Figure 4.1A.

These overexpressed fragments can also interact with other protein targets in the cell. These interactions allow binding partners of the protein of interest to be identified and mapped onto the structure. This outcome is depicted in Figure 4.1B. In this chapter, the DnaX247-455 fragment will be discussed as well as novel growth phenotypes for a subset of proteins with unknown functions.

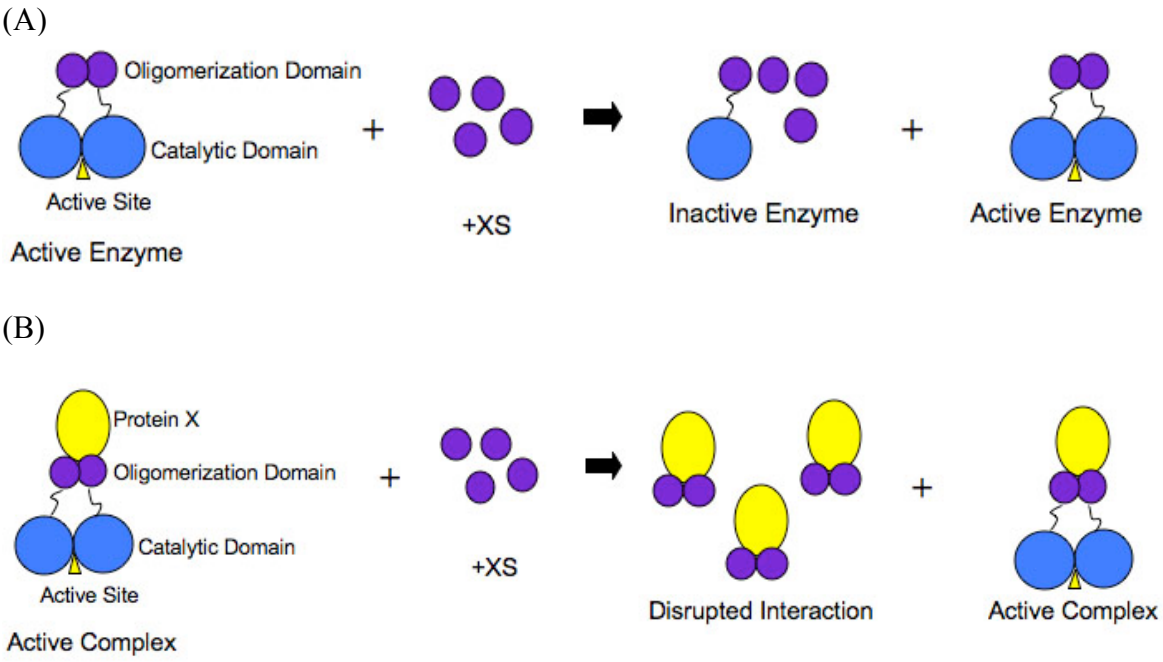

Figure 4.1: Proposed Targets for Self-Assembling Fragments. (A) Fragments containing oligomerization domains, and (B) Protein target X disruption with the self-assembling fragments.

The *dnaX* gene produces two polypeptides, τ and γ, due to a ribosomal frameshift at codons 429-430 (Flower and McHenry, 1990). Both products are members of the DNA Polymerase III holoenzyme and are involved in the DNA elongation step of replication, but only τ is essential (Blinkova *et al.*, 1993; Kodaira *et al.*, 1983). Two conditional mutations, *dnaX36* and *dnaX2016*, have been isolated and characterized *in vivo*. At the restricted temperature, these alleles are defective in DNA replication and as a result, the cells filament (Filip *et al.*, 1974; Henson *et al.*, 1979). This filamentation is due to induction of the SOS response and it is presumed that the inactivation of the tau/ gamma

destabilize the replication fork, leading to double stranded breaks (Skovgaard and Lobner-Olesen, 2005).

The C-terminal domain of τ has been shown to physically interact with the α subunit of DNA Polymerase III and is responsible for dimerizing the two core polymerases (Studwell-Vaughan and O'Donnell, 1991). The γ subunit contains the first two-thirds of the τ polypeptide (from residues 1-431), but lacks τ's C-terminal domain. It has been shown that the gamma subunit is the main component of the β clamp loader, and although both τ and γ contain domain III, only γ is bound to χ, ψ, δ, and δ' *in vivo* (Glover and McHenry, 2000; Jeruzalmi *et al.*, 2001b).

Of the 4,300 protein-encoding genes found in *E. coli*, only about 300 of those genes are essential (Baba *et al.*, 2006). Traditionally, methods for defining protein functions have included isolating mutants or deletions in the gene of interest and characterizing the

specific phenotypes for each mutation. Large-scale deletions projects have sought to ramp up this characterization, but approximately 1,700 proteins are still uncharacterized (Baba *et al.*, 2006; Gerdes *et al.*, 2003).

Large-scale phenotypic screens seek to identify conditions under which these functions are required for growth. Previous attempts to generate conditional media-dependent phenotypes have been rather successful. Gerdes *et al*., 2003 used transposon mutagenesis to identify genes essential for growth in LB. They found 620 proteins of unknown function to be essential, but 3,126 were dispensible for growth when deleted. Also, Ito *et al.,* 2005 used phenotypic microarrays to test whether 1400 deletions metabolize 95 different carbon sources. Of the 700 deletions that encoded proteins of unknown functions, approximately 230 showed metabolic defects on at least one carbon source. Using the protein fragments, we will try to generate media-specific phenotypes that can be studied further.

Materials and Methods

Bacterial Strains and Plasmids

Table 4.1: Bacterial Strains Used in Chapter IV.

Strain	Genotype	Reference
MB1927	MB1547 λ *cI*^{IND} *sulA::lacZ*	Mike Benedik
MG1655	F$^-$, λ$^-$, *rph-1*	Blattner *et al.*, 1997
DS908	MG1655 λ *cI*^{IND} *sulA::lacZ*	this study
AZ49	MG1655/ pJM187	this study
AZ102	MG1655/ pAZ9	this study
AZ436	MG1655/ pAZ211	this study
AZ437	MG1655/ pAZ212	this study
AZ438	MG1655/ pAZ213	this study
AZ439	MG1655/ pAZ215	this study
AZ440	MG1655/ pAZ216	this study
AZ441	MG1655/ pAZ217	this study
AZ442	MG1655/ pAZ222	this study
AZ443	MG1655/ pAZ223	this study
AZ444	MG1655/ pAZ224	this study
AZ445	MG1655/ pAZ228	this study
AZ446	MG1655/ pAZ229	this study
AZ450	MG1655/ pAZ214	this study
AZ451	MG1655/ pAZ219	this study
AZ452	MG1655/ pAZ220	this study
AZ453	MG1655/ pAZ227	this study
AZ454	MG1655/ pAZ218	this study
AZ455	MG1655/ pAZ221	this study
AZ457	MG1655/ pAZ225	this study
AZ1167	DS908/ pJM187	this study
AZ1168	DS908/ pAZ9	this study

Table 4.2: Plasmids Used in Chapter IV.

Plasmid Name	Description	Relevant Marker	Reference
pJM187	**Gcn4** LZ in pBAD-DEST49	ampicillin	this study
pAZ9	**DnaX247-455** in pBAD-DEST49	ampicillin	this study
pAZ211	**YbaO89-191** in pBAD-DEST49	ampicillin	this study
pAZ212	**YbbN163-296** in pBAD-DEST49	ampicillin	this study
pAZ213	**YbdG255-415** in pBAD-DEST49	ampicillin	this study
pAZ214	**YcaP102-230** in pBAD-DEST49	ampicillin	this study
pAZ215	**YceH172-215** in pBAD-DEST49	ampicillin	this study
pAZ216	**YdhT186-270** in pBAD-DEST49	ampicillin	this study
pAZ217	**YebT749-879** in pBAD-DEST49	ampicillin	this study
pAZ218	**YfaY216-400** in pBAD-DEST49	ampicillin	this study
pAZ219	**YfeC54-119** in pBAD-DEST49	ampicillin	this study
pAZ220	**YfeD79-130** in pBAD-DEST49	ampicillin	this study
pAZ221	**YfhK230-496** in pBAD-DEST49	ampicillin	this study
pAZ222	**YjeF215-515** in pBAD-DEST49	ampicillin	this study
pAZ223	**YgeV263-592** in pBAD-DEST49	ampicillin	this study
pAZ225	**YnaI227-343** in pBAD-DEST49	ampicillin	this study
pAZ227	**YphG466-735** in pBAD-DEST49	ampicillin	this study
pAZ228	**YqjI122-207** in pBAD-DEST49	ampicillin	this study
pAZ229	**YtfL266-447** in pBAD-DEST49	ampicillin	this study
pBAD-DEST49	P_{BAD} His-Patch Thioredoxin Gateway vector/ pUC origin	ampicillin	Invitrogen

Growth Conditions

Plating Dilutions for DnaX247-455

Overnight cultures were grown for about 16 hours in 2 ml LB + 200 µg/ml ampicillin + 0.1% D-fucose in a rotating rollerdrum at 37˚C. Bacterial strains and plasmids used in this study are listed in Tables 4.1 and 4.2, respectively. For plating dilutions, LB plates containing 200 µg/ml ampicillin + either 0.2% L-arabinose (inducer) or 0.1% D-fucose (anti-inducer) were used to test the various strains. Cultures were serially diluted 1:10 into 1x M9 salts using mulitchannel pipettes. Cells were spotted onto the plates using a

48-or 96-pronged replicator (Boekel). This instrument applies 5-10 µl of culture onto the plates. Plates were allowed to dry and then incubated at 37˚C overnight. Both colony morphology and plating efficiency were documented for these experiments

Growth Conditions for DnaX247-455 in Liquid Culture

Overnight cultures were inoculated with a single colony and grown in 2 ml M9 salts + 0.1 mM $CaCl_2$ + 1 mM $MgSO_4$ + 0.2% D-fructose + 5 µg/ml thiamine + 0.1% Casamino acids + 50 µg/ml uridine + 200 µg/ml ampicillin in 16 x 150 mm at 37˚C (Miller, 1972). Overnight cultures were then diluted 1:100 into 10 ml of fresh M9 + additives. At OD_{600} = 0.2, the fusions proteins were induced by adding L-arabinose to a final concentration of 0.2%. Cells were grown to an OD_{600} of 0.4 in a New Brunswick Gyrotory Water Bath Shaker Model G76 at a shaker speed of 6 (~210 rpm) and diluted 1:40 into fresh prewarmed M9 + additives + 0.2% L-arabinose. Cells were allowed to grow to 0.4 again before another 1:40 dilution (two series of dilutions total).

Y-gene Plating Dilutions

Overnight cultures were grown for about 16 hours in 2 ml of LB, M9 + CAA, Tryptone, or M9 + 0.5x LB with 200 µg/ml ampicillin and 0.1% D-fucose in a rotating rollerdrum at 37˚C. Bacterial strains and plasmids used in this study are listed in Tables 4.1 and 4.2, respectively. Cultures were serially diluted 1:10 into 1x M9 salts using a multichannel pipettor. Cells were spotted onto the plates using a 48-or 96-pronged replicator (Boekel). This instrument applies 5-10 µl of culture onto the plates. Plates were

allowed to dry and then incubated at 37˚C overnight. Both colony morphology and plating efficiency were documented for these experiments

Cloning Procedures

dnaX and the various y-gene fragments were amplified from the plasmids described in Marino *et al*., 2004 using the PCR primers *forward-attB1* (GGGGACAAGTTT-GTACAAAAAAGCAGGCTACAAGGACGACGATGACAAG) and *reverse-attB2* (GGGGACCACTT-TGTACAAGAAAGCTGGGTCTTTCGGGCTTTGTTAGCAG). The DNA fragments were cloned into the expression vector pBAD-DEST49 using the Gateway Cloning Technology (Invitrogen).

Microscopy

Cell Fixation

Cells were fixed by adding 0.19 volumes of 16% paraformaldehyde to aliquots of culture. Cells were allowed to stand at room temperature for 30 minutes and then placed on ice for up to 3 hours. Cells were then pelleted gently at 3.3xg in a tabletop centrifuge for 3 minutes. The supernant was removed and the cells were washed 3 times in ice-cold 1X PBS. After the final wash, the pellet was resuspended in 250-500 µl of 1x PBS (dependent upon the size of pellet) and stored at 4˚C in the dark.

Fluorescence

Coverslips were coated with 0.01% poly-L-lysine, washed 3 times with MilliQ water, then rinsed with 100% ethanol and dried. Cells (30 µl) were placed on the coverslip and allowed to sit for 3 minutes. Dabbing the edge of the coverslip to a paper towel and dipping the coverslip into 1x PBS removed the excess culture. The coverslips with the sample facing up were allowed to air dry for 5 minutes on a paper towel. 3 µl of DAPI (3 µg/ml) was added before the coverslips were inverted onto slides with 3 µl Anti-Fade mounting medium (Invitrogen).

Images were captured using a Zeiss AxioPhot 2 microscope at 100x magnification and images were processed using AxioVision software. Phase contrast and DNA were visualized using DIC and DAPI filters with 20-50 ms and 110-200 ms exposure times respectively.

Beta-Galactosidase Assays for SulA Induction

Cells were grown as described above, except only one 1:40 dilution into fresh media was needed. β-galactosidase assays were done in triplicate as described in Miller, 1972.

Results

Identification of Dominant Negative Phenotypes

Previously, our lab had identified *E. coli* protein fragments that could self-assemble when fused to the DNA-binding domain of the lambda cI repressor (Marino-Ramirez *et al.*, 2004); these fragments identify putative oligomerization domains in *E. coli* proteins. If the fragments reflect the normal oligomerization of the proteins from which they come, their overexpression might lead to the formation of mixed oligomers containing fragments bound to full-length subunits. In cases where function is dependent on oligomerization, this should yield a dominant negative phenotype, as modeled in Figure 4.1A.

Initially we determined whether we could recapitulate known phenotypes. Several self-assembling fragments were chosen to test for negative dominance in overexpression experiments. DnaX and ParC are essential and were chosen because their mutant phenotypes have been very well characterized (Hansen *et al.*, 1984; Kato *et al.*, 1988). The other proteins were chosen because mutants in these genes exhibit phenotypes that are easily scored (Munch-Petersen *et al.*, 1972; Kuhn and Somerville, 1971; Bruce *et al.*, 1984; Miller *et al.*, 1999). The phenotypes used to score the strains are described in Table 4.3.

Table 4.3: Description of Mutant Phenotypes.

Fragment	Mutant Phenotype	Reference
Gcn4 LZ	no known phenotype in *E.coli*	
DnaX247-485	lethal	Henson *et al*., 1979
ParC333-485	lethal	Kato *et al*., 1988
DeoR70-252	inosine as an improved C- source	Munch- Petersen *et al*., 1972
Lrp16-164	growth on D-Leucine	Kuhn *et al*., 1971
PspA99-195	resistance to hypoxanthine + sulfanilamide	Bruce *et al*., 1984
MutS789-853	increased rate to Lac+ reversion	Miller *et al*., 1999

The fragments listed above were cloned into a vector that expressed them as C-terminal fusions of a mutant thioredoxin (TRX). The expression of this construct was under control of the *araBAD* promoter, as shown in Figure 4.2.

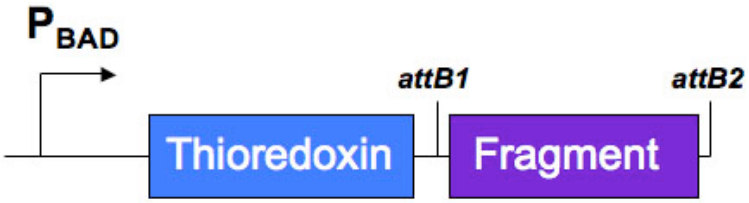

Figure 4.2: Expression Construct of the Thioredoxin Fragments.

Plating efficiency of cells expressing these fusions was compared to cells overexpressing similar fusions to protein fragments known to self-assemble (Figure 4.3). The leucine zipper domain of the yeast transcription factor GCN4 (Gcn4 LZ) was used as a control. Gcn4 LZ overexpression does not detectably affect growth.

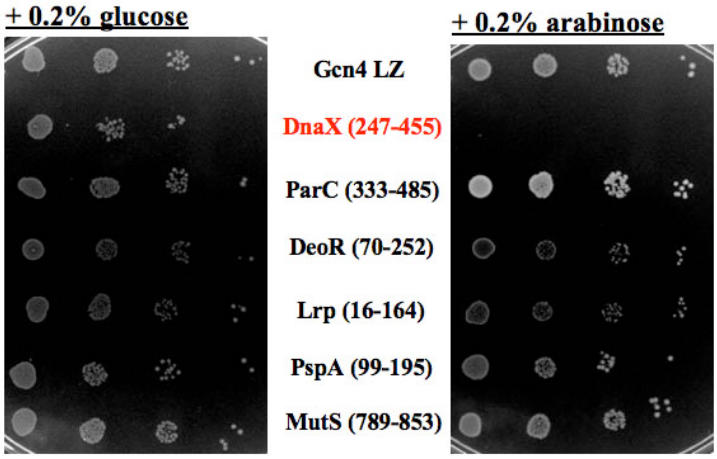

Figure 4.3: Arabinose-Dependent Plating Defect for DnaX247-455.

Upon induction of the TRX fusions, only the DnaX247-455 fragment demonstrated a lethal phenotype. All the other fragments, including ParC333-485, have plating efficiencies similar to that of the Gcn4 LZ control. Although the short ParC fragment does not cause a lethal phenotype, its overexpression does cause a septation phenotype that is characterized further in Chapter 3. Longer ParC fragments were lethal when overexpressed (Chapter II). We were unable to detect the protein-specific phenotypes listed for DeoR, Lrp, PspA, and MutS fragments overexpressed and therefore these were not studied further.

Characterization of the DnaX247-455 Phenotype

Growth Rate

To examine the deleterious expression of DnaX247-455, its expression in liquid culture was monitored (Figure 4.4).

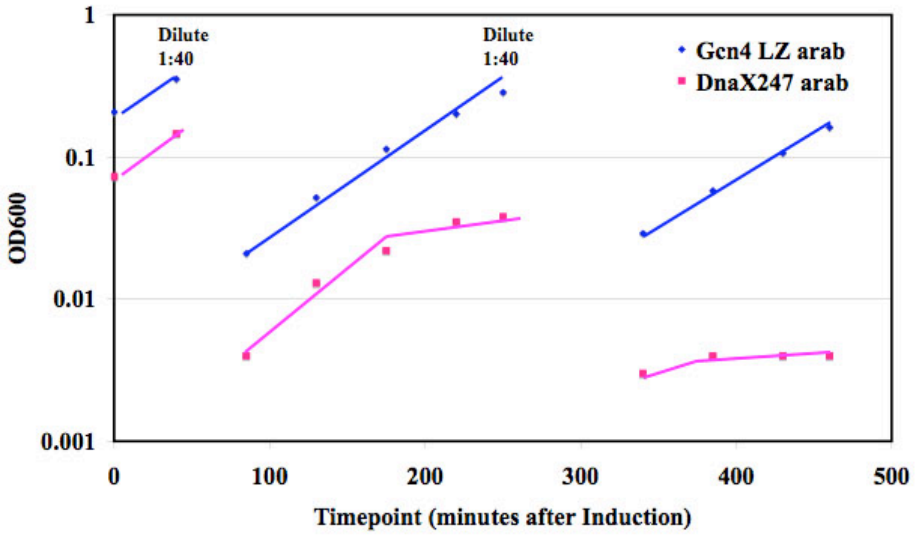

Figure 4.4: Lethality of DnaX247-455 Expression. The growth rate of the DnaX247-455 decreases while the Gcn4 growth rate is consistent.

The strain overexpressing the DnaX247-455 fragment exhibits a diminishing growth rate throughout the course of the induction. This is similar to the growth of the *dnaX* (*ts*)

mutants after the temperature shift to 42˚C (Henson *et al.*, 1979). Although replication stops immediately or within a generation, depending on the temperature used, cell mass continues to increase as the cells filament. In order to determine if the cells overexpressing DnaX247-455 are filamenting as well, I examined them under the microscope (Figure 4.5). Since the decrease in growth rate starts after the first dilution, we looked at the cells before this point.

DnaX247-455-Dependent Filamentation

After 30 minutes of induction, the culture contains cells of various lengths (Figure 4.5A). The filaments are over 10 cell-lengths long, indicating that the expression of the fragment is leaky even in the absence of L-arabinose. Moreover, the scarce amount of DNA in each of these filaments is consistent with a defect in replication. The filamentation phenotype caused by the *dnaX2016 (ts)* allele has been reported to be caused by SOS induction (Skovgaard and Lobner-Olesen, 2005). To determine whether SOS is causing the filamentation seen in strains overexpressing DnaX247-455, induction of the SOS-dependent cell division inhibitor *sulA* was investigated.

(A)

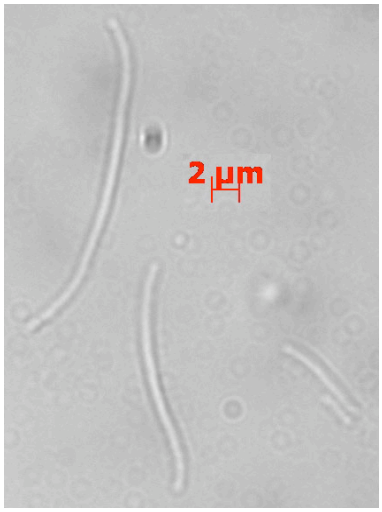

(B)

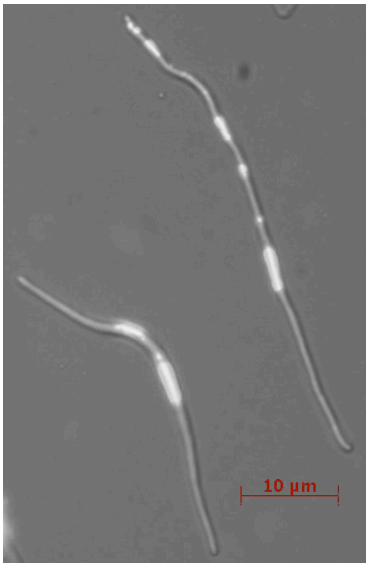

Figure 4.5: Cellular and Nucleoid Morphology of Cells Expressing DnaX247-455. The culture contains cells of various cell lengths (A). The distribution of DNA within filaments expressing DnaX247-455 is shown in (B).

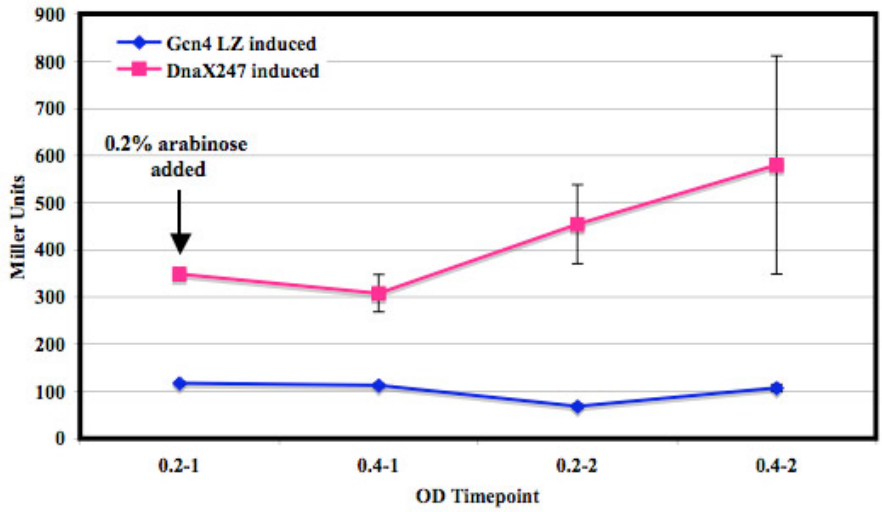

Figure 4.6: SulA Induction Profile of DnaX247-455. Expression of the DnaX247-455 fragment induces *sulA*. Cells expressing Gcn4 experience no such induction.

DnaX247-455 Expression Induces SulA

As shown in Figure 4.6, the overexpression of the DnaX247-455 fragment induces *sulA*, while overexpression of the Gcn4 LZ did not. These results coincide with those reported for the *dnaX2016 (ts)* phenotype, indicating that DnaX fragment-dependent filamentation is caused by induction of the SOS response. The high basal level of *sulA* expression at t = 0 minutes after induction also supports leaky expression of the vector

Irreversibility of the DnaX247-455 Lethality

Many temperature-sensitive phenotypes (i.e. *parC1215* or *parE10*) are reversible upon return to the permissive temperature (Adams *et al.*, 1992). To determine whether the toxic phenotype of the DnaX247-455 fragment is reversible once the inducer has been removed, cells were washed and plated on fucose at different times after induction. The recovery time-course is shown in Figure 4.7.

Before induction, both the DnaX247-455 fucose and arabinose samples plate equally well (Figure 4.7). Approximately 10 minutes after the fragment is induced, cell viability starts to decrease. The ability to form colonies is completely abolished at any timepoint after 60 minutes while the plating efficiency of the uninduced sample is stable. Thus, expression of the DnaX247-455 fragment leads to an irreversible loss of cell viability.

These reconstruction of the defects of the *dnaX (ts)* alleles shows that protein fragment overexpression may be used to generate phenotypes similar to those of the known mutant. In the next section, we generate media-specific phenotypes for proteins of unknown function.

(A)

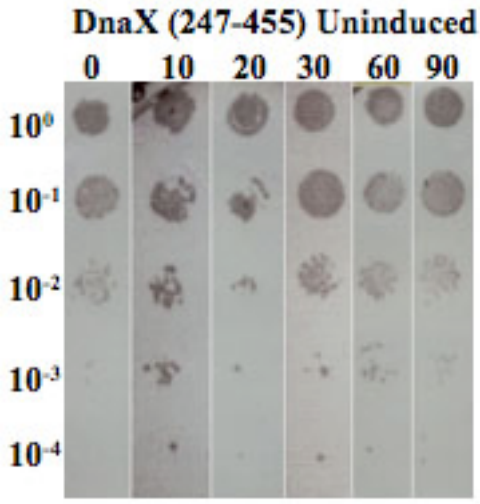

(B)

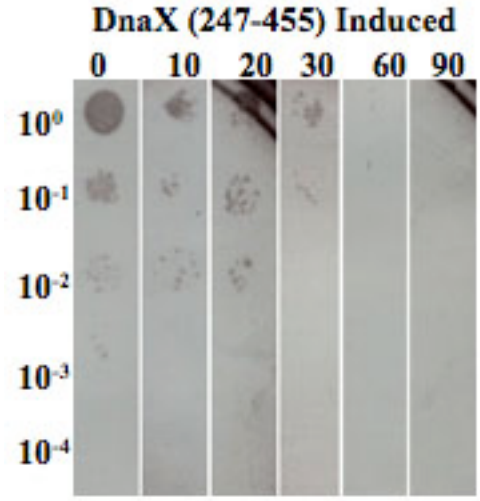

Figure 4.7: DnaX247-455 Recovery Time Course. (A) Recovery of cells containing the uninduced DnaX247-455 plasmid. (B) Recovery results of cells expressing the DnaX247-455. Numbers above indicate the time after induction (in minutes).

Y -gene Negative Dominance

Although fragment expression only gives a dominant negative phenotype some of the time, screening for fragment expression phenotypes could still provide insight into gene function in the subset of cases where inhibition occurs. There are approximately 1700 genes whose functions have not been determined (Ito *et al.*, 2005). Hypothetical functions for some proteins have been assigned based on inferred homology, expression patterns, the presence or absence of domains, and the presence of critical residues within those domains. Several studies have used gene deletions or transposon mutagenesis to shed light on the functions of unknown proteins, but the conditions under which these strains were tested only yielded phenotypes for a small fraction of the total (Baba *et al.*, 2006; Gerdes *et al.*, 2003). Attempts to identify the functions of all proteins have gotten closer, using phenotypic microarrays to sample a variety of conditions, but the functions of a large number of proteins remain elusive (Ito *et al.*, 2005).

The λ cI repressor screen for proteins that self-assemble found 76 genes that encoded proteins of unknown function (Marino-Ramirez *et al.*, 2004). These Y-gene fragments were used as dominant effectors to discover conditions under which loss of function is noticed. Fragments under 60% of the total protein length were cloned as described above (Figure 4.2). The overexpressed region of these proteins, their hypothetical functions, any putative domains from PFam or InterPro, and predicted transmembrane segments generated from TMHMM are depicted in Figure 4.8 (Daley *et al.*, 2005).

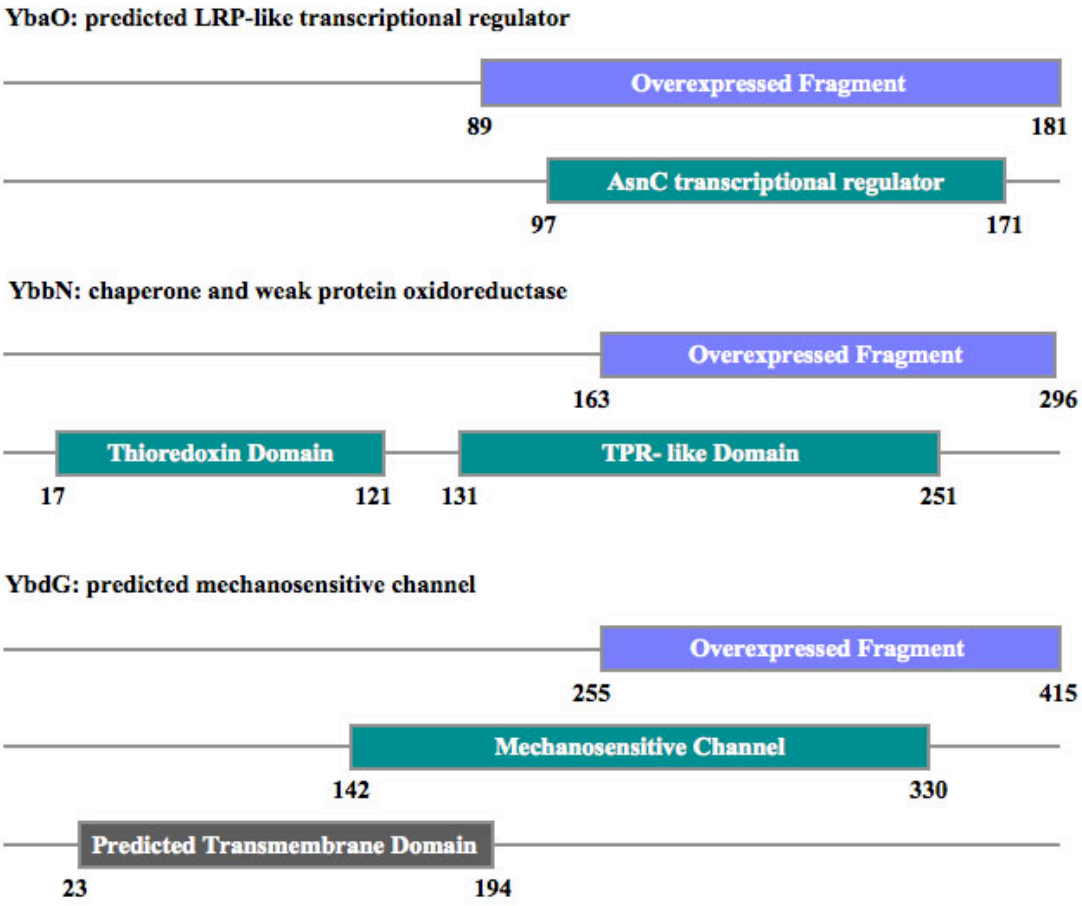

Figure 4.8: Predicted Domains of Proteins of Unknown Function. Regions of proteins identified from Marino-Ramirez *et al*., 2004 used in this experiment are in blue. The locations of putative domains found in PFam and InterPro are teal, and regions of the full-length predicted to be transmembrane domains (TMDs) are shown in gray.

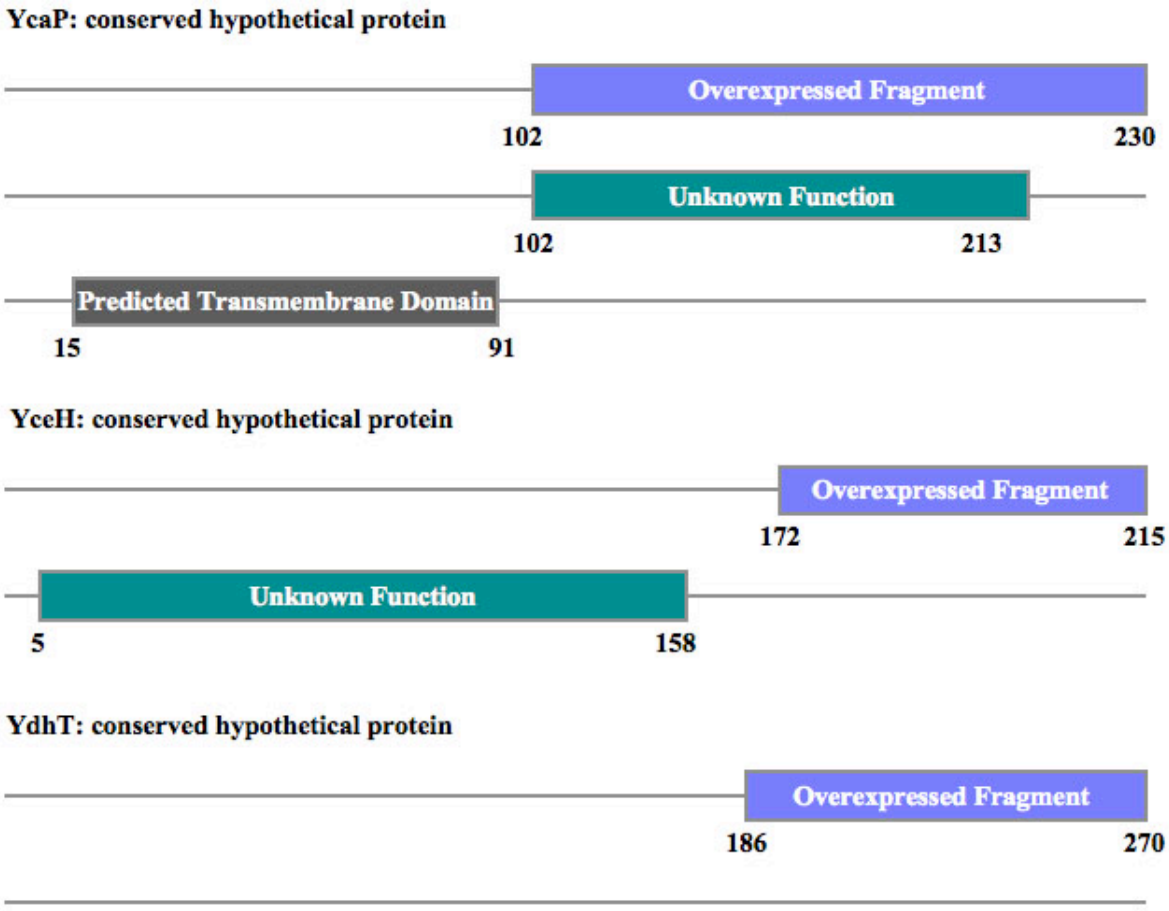

Figure 4.8 (cont'd): Predicted Domains of Proteins of Unknown Function. Regions of proteins identified from Marino-Ramirez *et al*., 2004 used in this experiment are in blue. The locations of putative domains found in PFam and InterPro are teal, and regions of the full-length predicted to be transmembrane domains (TMDs) are shown in gray.

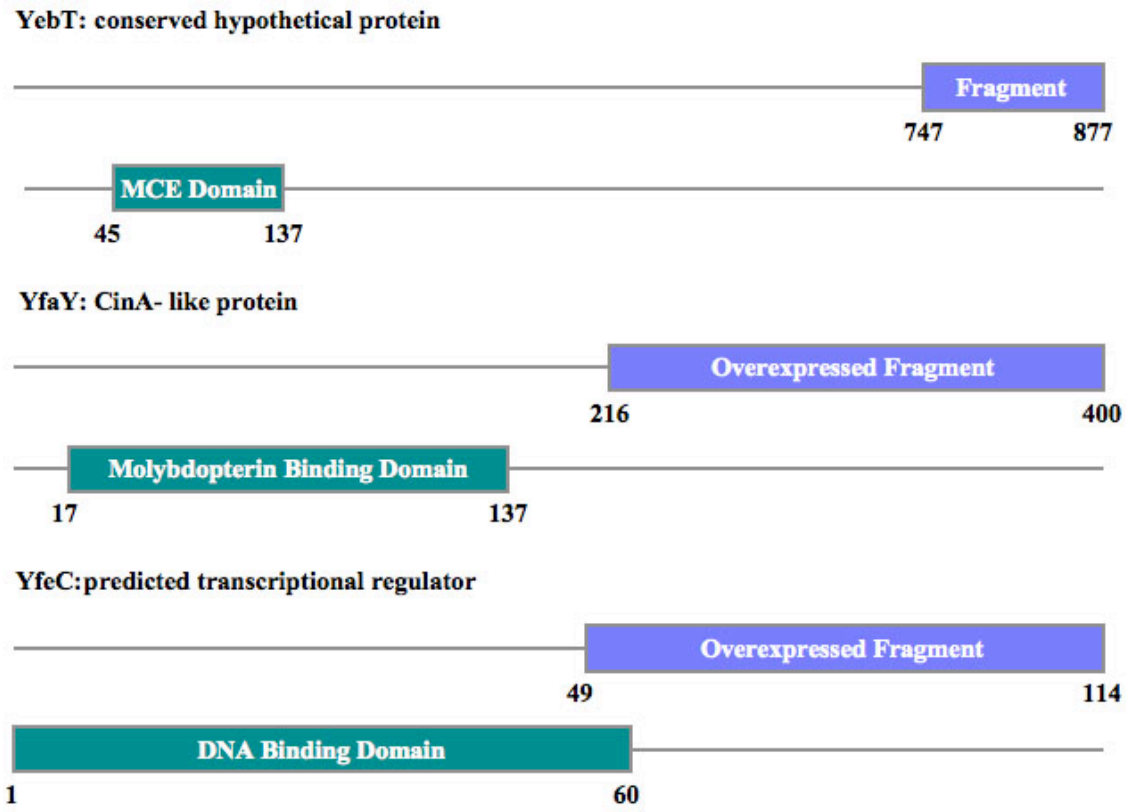

Figure 4.8 (cont'd): Predicted Domains of Proteins of Unknown Function. Regions of proteins identified from Marino-Ramirez *et al*., 2004 used in this experiment are in blue. The locations of putative domains found in PFam and InterPro are teal, and regions of the full-length predicted to be transmembrane domains (TMDs) are shown in gray.

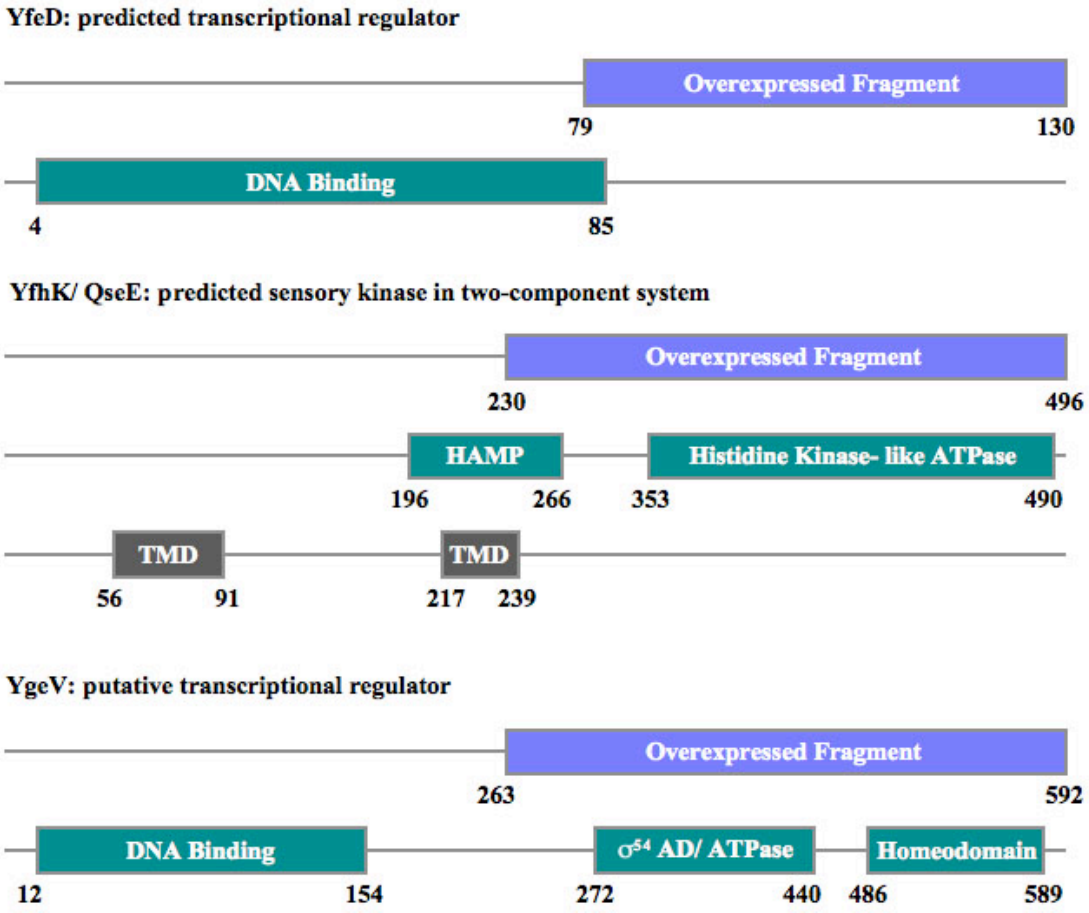

Figure 4.8 (cont'd): Predicted Domains of Proteins of Unknown Function. Regions of proteins identified from Marino-Ramirez *et al*., 2004 used in this experiment are in blue. The locations of putative domains found in PFam and InterPro are teal, and regions of the full-length predicted to be transmembrane domains (TMDs) are shown in gray.

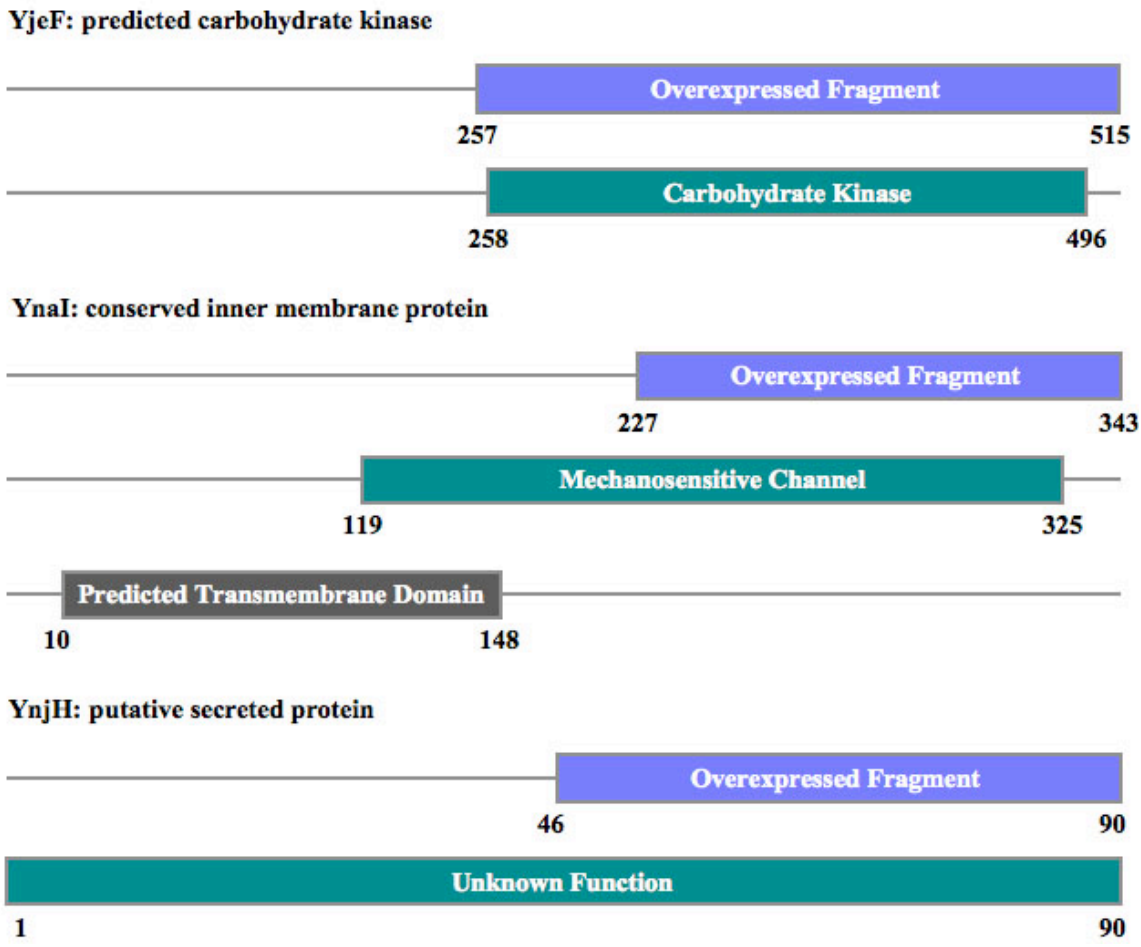

Figure 4.8 (cont'd): Predicted Domains of Proteins of Unknown Function. Regions of proteins identified from Marino-Ramirez *et al*., 2004 used in this experiment are in blue. The locations of putative domains found in PFam and InterPro are teal, and regions of the full-length predicted to be transmembrane domains (TMDs) are shown in gray.

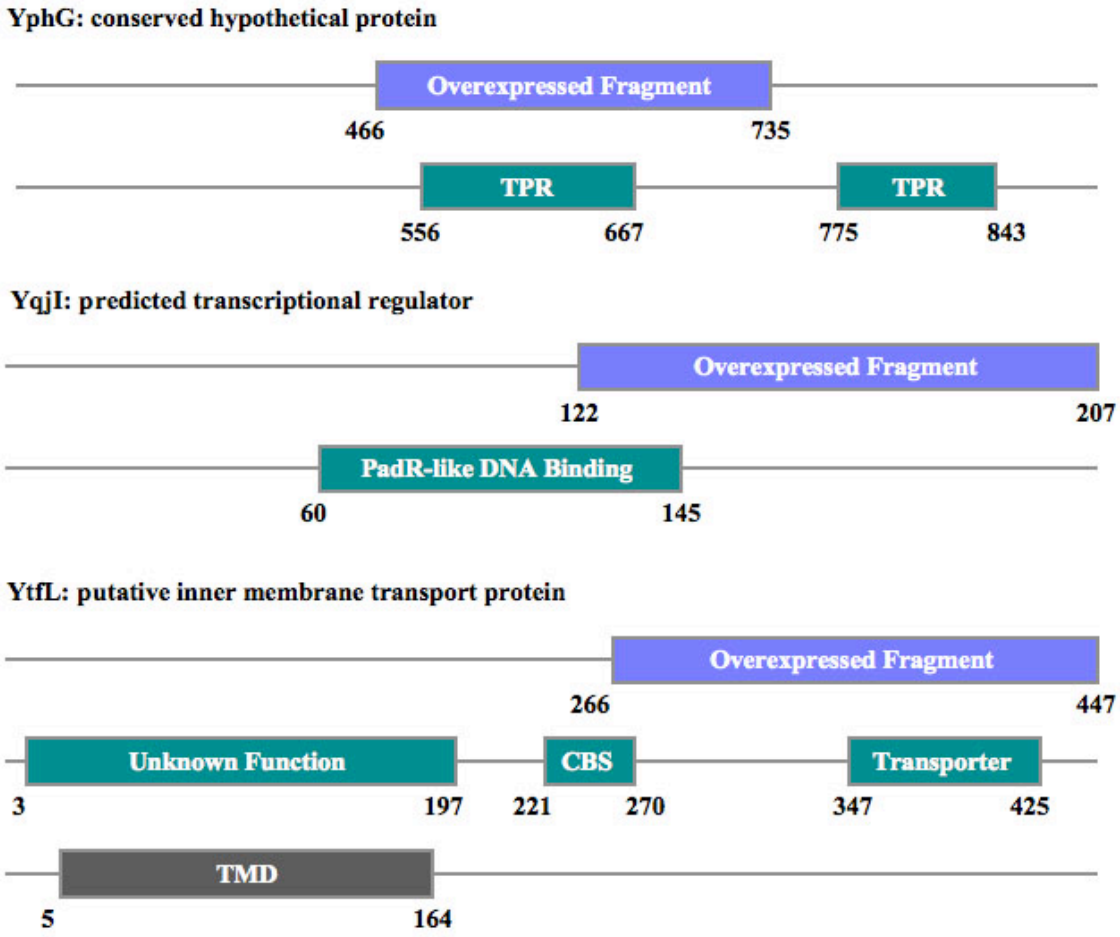

Figure 4.8 (cont'd): Predicted Domains of Proteins of Unknown Function. Regions of proteins identified from Marino-Ramirez *et al*., 2004 used in this experiment are in blue. The locations of putative domains found in PFam and InterPro are teal, and regions of the full-length predicted to be transmembrane domains (TMDs) are shown in gray.

The protein fragments displayed above were tagged with a His-Patch Thioredoxin and expressed under the control of the *araBAD* promoter. These strains were plated on various media + 0.2% D-glucose (control) or 0.2% L-arabinose (inducer) to find arabinose-dependent growth inhibition. Plating efficiencies were calculated and compared to the controls. Table 4.4 shows the results of these plating experiments. For comparison, the phenotypes of the full-length overexpression and the deletions plated on LB are also shown (Kitagawa *et al.*, 2005; Baba *et al.*, 2006).

As shown above, the majority of expressed fragments are localized to the C-terminal end of the protein. We looked to see if these regions are predicted to have secondary or tertiary structure in PFam and InterPro, and found that eleven of the fragments have putative structure. In the five fragments that are predicted to be membrane-associated (YbdG, YcaP, YfhK, YnaI, and YtfL), the region expressed does not overlap with the predicted membrane-spanning region.

Table 4.4: Media Dependence of Y-Fragment Overexpression Studies.

	Fragment Overexpression Plated on :				Full Length	Knockout
Fragment	**LB**	**M9 + CAA**	**M9 + LB**	**Tryptone**	**LB**	**LB**
Controls						
Gcn4 LZ	++	++	++	+	**nd**	**nd**
DnaX247-455	---	---	---	---	---	**essential**
No Growth Defects						
YbaO89-181	++	++	++	++	**nd**	**nonessential**
YcaP102-230	++	++	++	++	---	**nonessential**
YceH172-215	++	+	++	++	---	**nonessential**
YdhT186-270	++	++	++	+	---	**nonessential**
YjeF215-515	++	+	++	+	+	**nonessential**
YnjH49-90	++	+	++	++	---	**nonessential**
YphG466-735	++	++	++	++	++	**nonessential**
YtfL266-447	++	++	+	++	---	**nonessential**
Growth Defects on M9 + CAA only						
YbdG255-415	++	---	+	++	---	**nonessential**
YfaY216-400	++	---	+	++	---	**nonessential**
YfeD79-130	++	-	++	++	---	**nonessential**
YfhK230-496	++	---	+	++	---	**nonessential**
YnaI227-343	++	---	+	++	---	**nonessential**
YqjI122-207	+	---	+	++	++	**nonessential**
Growth Defects on M9 + CAA but not on M9 + 0.5x LB						
YgeV263-592	+	---	++	---	---	**nonessential**
Growth Defects on M9, Tryptone, and M9 + LB						
YbbN163-296	++	---	---	---	---	**nonessential**
YebT749-879	++	---	---	---	---	**nonessential**
Growth Defects on All Media						
YfeC54-119	---	---	---	---	---	**nonessential**

The fragments were tested on various media to look for growth defects and were grouped based on the severity of the phenotype. Overall, 10 fragments of the 18 tested exhibited a growth defect on at least one type of medium.

YbdG, YfaY, YfeD, YfhK, YnaI, and YqjI

The first class, consisting of YbdG, YfaY, YfeD, YfhK, YnaI, and YqjI, encompasses fragments that demonstrated growth inhibition on M9 + Casamino acids only. Growth of these six strains improved when the M9 was supplemented with 0.5x LB instead of Casamino acids as the peptide source and was fully restored on Tryptone.

YgeV

The second class includes YgeV. The overexpression of this protein yielded a growth defect on M9 + CAA that was completely restored at 0.5x LB, but tryptone was not able to properly restore growth. This result indicates that the phenotype of YgeV263-592 may require a vitamin, cofactor, nucleotide, or other component supplied in LB.

YbbN and YebT

The third class, which includes YbbN and YebT, exhibits fragment-dependent toxicity on most media tested, except LB. Not only was growth of these two fragments defective on M9 + CAA, but neither M9+ 0.5x LB nor tryptone could restore the plating efficiency of these fragments.

YfeC

The only fragment that showed a media-independent overexpression phenotype was YfeC. This fragment yielded an arabinose-dependent plating defect regardless of media.

Discussion

Overexpression of self-assembling protein fragments caused phenotypes for a subset of the fragments tested here. For those whose overexpression yielded an effect, there are several mechanisms by which these fragments may be eliciting a phenotype. First, the fragment may be interacting with its endogenous full-length counterpart to form an inactive hetero-multimer. This mechanism is expected to give a partial or complete loss of function resembling the phenotype of a knockout mutant. Second, the fragment might compete with the endogenous full-length protein for binding to another normal target protein or a compound in the cell. Third, the fragment could be involved in an abnormal interaction or activity. For example, the fragment might lack a regulatory domain, yielding a constitutively active mutant protein. These mechanisms are not mutually exclusive.

Failure to see a mutant phenotype upon fragment expression is not inconsistent with the ability of the fragments to form homo-multimers. The interaction may not hinder the target's function or that function is not required for growth under the conditions tested. Also, if the fragment does not interfere with the regions of the protein necessary for

function, then no effect would be expected. Lastly, if the fragment binds to its endogenous full-length counterpart and no effect is seen, then function may be independent of oligomerization.

DnaX247-455

The overexpression of DnaX247-455 caused filamentation, a nucleoid defect, and induction of *sulA*, similar to the effects seen with the temperature-sensitive alleles *dnaX36* and *dnaX2016* (Henson *et al.*, 1979; Skovgaard and Lobner-Olesen, 2005). This region of the protein has been shown to house the oligomerization domain for both τ and γ (Marino-Ramirez *et al.*, 2004; Glover and McHenry, 2000). As shown in Figure 4.9, the same 247-455 region of the DnaX protein overlaps with most of the δ δ' χ ψ binding region of the γ subunit and some of the DnaB binding region present only in τ (Gao and McHenry, 2001). This means that the fragment phenotype may be due to interactions with τ, γ, or any of these other proteins alone or in combination.

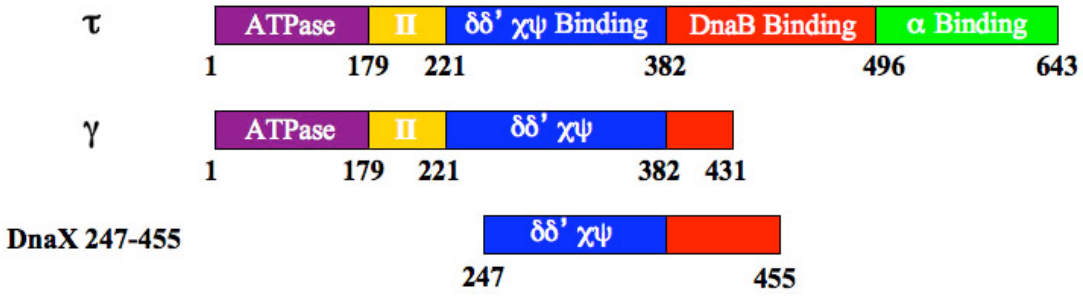

Figure 4.9: Heterogeneous Protein Interactions for DnaX. Protein interactions were mapped onto the two different proteins encoded by the *dnaX* gene. DnaX247-455 indicates the region overexpressed in this study. Domain III is also the oligomerization domain for both the τ and γ subunits.

The *dnaX36* and *dnaX2016* (*ts*) alleles are defective in DNA replication at the restrictive temperature and as a result, the cells filament (Henson *et al.*, 1979; Filip *et al.*, 1974). It is hypothesized that in these mutants, shifting to the restrictive temperature causes the replication forks to become destabilized and double stranded breaks (DSBs) result if the stalled forks are not repaired in a timely manner (Seigneur *et al.*, 1998; Michel, 2000). In the absence of a functional clamp loader, the cells will be unable to perform recombinational repair of these DSBs and will die.

If DnaX247-455 overexpression acts similarly to the *dnaX* (*ts*) alleles, this could explain the irreversibility of the phenotype. The induction of the SOS response even in the presence of basal expression of the fragment is consistent with this idea. However,

because the clamp loader complex is thought to be a processive component of the DNA polymerase III holoenzyme (Kim *et al.*, 1996a; Wu *et al.*, 1992), preexisting replication forks should be immune to disruption by coassembly of the DnaX fragment into the complex.

There are several possible models for how the DnaX fragment could be lethal that are consistent with processive clamp loaders. For example, aberrant clamp loader complexes might assemble at initiation and manifest lethality only when new forks are initiated. If the fragment replaced one molecule of τ, there could be loss of coordination between leading and lagging strand synthesis (Kim *et al.*, 1996a). Alternatively, the fragment could inactivate new clamp loaders and prevent the transition from initiation to elongation altogether. This could still lead to an SOS response; SOS is induced at the restrictive temperature in *dnaC2* (*ts*) mutants (Lobner-Olesen *et al.*, 2008). DnaC is required for initation and replication restart, but not for elongation.

Another possibility is that in addition to the clamp loaders in the holoenzyme complex, a second population of clamp loader complexes is needed for replication elongation, perhaps to unload β clamps from newly replicated DNA. If the fragment depleted this population, then elongating forks might run out of clamps to load. Mutations in *dnaN*, which encodes the clamp protein β, also induce the SOS response (Sutton, 2004).

Further characterization of the effects of the fragment might thus yield interesting insights about DNA metabolism.

Proteins of Unknown Function

The overexpression of the various y-protein fragments yielded a variety of media-specific plating defects. In total, 10 of the 18 fragments demonstrated a reduced plating efficiency on minimal M9 medium supplemented with Casamino acids (CAA). The fragments were grouped into several categories based on the severity of the inhibition.

YbdG, YfaY, YfeD, YfhK, YnaI, and YqjI

Six fragments inhibit growth on M9, but not other media. This group consists of YbdG, YfaY, YfeD, YfhK, YnaI, and YqjI. The ability of fragment-expressing cells to grow on LB, M9 mixed with LB, or on tryptone suggest that overexpression of the fragments creates an auxotrophy. The complex nature of tryptone and yeast extract makes it difficult to identify the nature of that auxotrophy.

Also, a large-scale functional analysis using phenotypic microarrays identified carbon source metabolic defects for *ybdG* and *ynaI*. Both deletions were unable to utilize acetate as a carbon source, but *ynaI* experienced additional defects on N-acetyl-D-glucosamine and α-glucose-1-phosphate.

YbbN, YebT, YfeC, and YgeV

The remaining four fragments have more complex patterns of growth on the different media.

YgeV

YgeV is annotated as a putative σ^{54}-dependent transcription factor, based on a predicted N-terminal DNA binding domain and a central predicted σ^{54} activation domain (AD) and the C-terminal region of YgeV is annotated as a homeodomain. Cells expressing the YgeV fragment grow on LB and M9+LB, but not on M9 or tryptone. This suggests that fragment expression interferes with the biosynthesis of something that is present in the yeast extract component of LB. The fragment encompasses the putative activation and homeodomains of YgeV, but lacks the putative DNA binding domain. Overexpression of the fragment could potentially cause inappropriate regulation of YgeV-regulated transcription, either by acting as a dominant negative inhibitor of YgeV DNA binding, or transcriptional activation of σ^{54}-dependent promoters from solution (Ninfa *et al.*, 1987; Popham *et al.*, 1989).

Transcriptional profiling experiments have shown that expression of *ygeV* is significantly upregulated in response to the quorum sensing signal AI-2 (DeLisa *et al.*, 2001). These results taken together with what is known above suggest that YgeV may regulate genes involved quorum sensing regulation via σ^{54}-dependent transcription.

YfeC

YfeC is also annotated as a putative transcription factor with an N-terminal DNA-binding domain. The overexpressed fragment consists of the C-terminal 62 amino acids of the protein, which only slightly overlap the predicted DNA binding domain. Transcriptional regulators either activate or repress expression of genes. If endogenous YfeC is an activator, then the fragment may be reducing/inhibiting expression of a necessary product. However, if it acts as a repressor, then fragment expression is causing the inappropriate expression of a product. The overexpression phenotype of YfeC is toxic on LB in this study while the deletion of this gene is viable under similar conditions. This example shows that the overexpression phenotype is more interesting than the phenotype for the corresponding knock-out.

Previous studies identified *yfeC* as a gene whose expression is activated by CRP *in vitro* (Zheng *et al.*, 2004), suggesting that YfeC may be involved in regulating carbon source metabolism. This raises the possibility that YfeC fragment lethality is due to the presence of arabinose in the media as an inducer. In the presence of arabinose, mutants of L-ribulose 5-phosphate 4-epimerase (*araD*) accumulate toxic quantities of L-ribulose 5-phosphate (Englesberg *et al.*, 1962). We cannot currently eliminate the unlikely possibility that the YfeC fragment somehow interferes with *araD* expression or activity.

YebT and YbbN

Overexpression of the YebT or YbbN fragments causes a perplexing set of media-dependent growth defects, where cells expressing the fragments plate on LB but not M9, M9 + 0.5x LB, or tryptone.

YebT orthologs are only found in a subset of the proteobacteria. YebT has been shown to have striking similarity to PqiB, a paraquat inducible protein, at both the N-and the C-terminal ends and was found to be upregulated by *luxS*, the enzyme that produces AI-2 (Wang *et al.*, 2005). YbbN has been shown to be a chaperone and a weak oxidoreductase (Caldas *et al.*, 2006; Kthiri *et al.*, 2008). The overexpressed C-terminus of YbbN was annotated as a tetratricopeptide repeat (TPR) domain, which is a conserved 34-amino acid motif generally annotated as a protein-protein interaction domain (Andrade *et al.*, 2001). Its expression was found to be upregulated close to 10-fold within 5 minutes of induction of a plasmid-borne *rpoH*, indicating a role in the general stress response (Zhao *et al.*, 2005). This role is further supported by the observation that *ybbN* is induced in stationary phase and in response to the DNA-damaging agent mitomycin C (Khil and Camerini-Otero, 2002). The *ybbN* deletion strain is unable to metabolize acetate (Ito *et al.*, 2005). Thus, YbbN may be a chaperone for a protein involved in acetate metabolism.

Comparison to Other Studies

For the majority of the proteins tested, the phenotypes exhibited by the fragments did not coincide with the previously described full-length overexpression phenotypes (Kitagawa *et al.*, 2005). This may reflect differences in the conditions used for overexpression of the full-length protein and the fragments. First, the vector from which the full-length proteins were induced has an IPTG-inducible *T5-lac*$^{+}$ promoter, which is a stronger promoter than the *araBAD* promoter used in this study. The higher expression from $P_{T5\text{-}lac+}$ may explain why 2,149 full-length proteins showed severe growth defects out of a total the 3,301 proteins tested. Second, 50% of those ORFs causing severe growth defects are attributed to membrane proteins or proteins predicted to have membrane spanning domains (Kitagawa *et al.*, 2005). Several fragments expressed in this study are derived from proteins predicted to have membrane-spanning domains (YbdG, YcaP, YfhK, YnaI, YtfL), but the fragments overexpressed lack the regions predicted to associate with the membrane (Figure 4.8). Due to the different expression vectors, it should also be noted that the conditions under which these studies were done were not identical. The fragments expressed in this study were induced with arabinose while the full-length protein overexpressions described in Kitagawa *et al*., 2005 were induced with IPTG.

Accumulation of the appropriately-sized band on SDS gels indicates that the fragment is not being degraded (data not shown). These fragments were identified based on their ability to self-assemble so they have been successfully expressed as C-terminal fusions

previously (Marino-Ramirez *et al.*, 2004). The motifs that form oligomerization domains often do not appear in domain prediction, so the failure to predict a fold is not proof one does not exist. However, since many of the protein fragments do not overlap with predicted domains, it is possible that the proteins are misfolded and sequestered into inclusion bodies. We do not believe inclusion bodies account for the observed cases of growth inhibition. *E.coli* is the host for the most widely used expression systems for recombinant protein purification. It tolerates inclusion bodies quite well and their presence is not generally toxic (Maisonneuve *et al.*, 2008). It should be noted that 60% of the fragments expressed in this study that exhibit growth defects do overlap with areas of predicted tertiary structure.

Several studies have tested deletion strains to find conditions that lead to growth defects (Ito *et al.*, 2005; Winterberg *et al.*, 2005). In these genome-wide studies, growth defects were encountered for no more than 30% of the y-genes tested. Even in the full-length overexpression study, phenotypes were shown for approximately 30% of the total cytosolic proteins tested (Kitagawa *et al.*, 2005). Here, we report phenotypes for 55% of the proteins tested. This higher percentage can be attributed to the occurrence of multiple *in vivo* targets. The excess fragment may have several different targets in the cell from which to elicit an effect: (1) the endogenous full-length protein, (2) a binding partner X, or (3) DNA/ RNA target. It is also important to note that any combination of the possibilities listed may be occurring concurrently. As a result, physical and genetic interactions may be identified. The overexpression of the soluble regions of predicted

membrane proteins allow for those interactions to be characterized, similar to that of the FtsK CTD protein (Bigot *et al.*, 2004).

Overall, overexpressing protein fragments of unknown functions identified conditional media-specific phenotypes that have not been identified in previous studies using full-length protein overexpression or deletions (Baba *et al.*, 2006; Kitagawa *et al.*, 2005).

CHAPTER V

CONCLUSIONS AND FUTURE DIRECTIONS

In this study, new phenotypes were characterized in order to bring insight into the biology and regulation of replication, chromosome segregation, and septation as well as identifying conditions under which proteins of unknown function may be studied.

Protein Interactions

Protein interactions are required in every physiological process and at every level of cellular function. All physiological processes in the cell rely on protein interactions of some kind, be they with nucleic acids, membranes, small molecules, or other proteins. The observation that at least 35% of proteins function in stable complexes reflects the evolutionary benefit to working in a group. Studying the interactions between proteins allow for a deeper understanding of the physiological processes and cellular functions in which they are involved.

Negative Dominance

The ability to isolate conditional mutations is a valuable genetic tool that results in the inducible inactivation of a function. This is especially valuable for essential genes, but conditional mutants are also used for ordering genes in pathways (Jarvik and Botstein, 1973). The resulting phenotype allows the processes involving that gene to be characterized.

Conditional mutants are usually thought of in terms of temperature sensitive and cold sensitive alleles. However, *ts* and *cs* mutants are not available for all essential genes, and for those genes with mutations, all molecules in the population usually exhibit the defect. Negative dominance provides an alternative genetic tool for generation of conditional phenotypes. Strain construction using negative dominant mutants is convenient because the mutant protein is provided *in trans* and is expressed from a plasmid vector. Unlike *ts* and *cs* mutants, expression of dominant negative proteins often only reduces the activity in a fraction of the population. This is beneficial when studying the functions of essential genes, as seen in the cases of DnaX and ParC, since partially reducing the function of a complex allows for new aspects of the physiological process to be discovered.

There are factors inherent within the design of negative dominance that may make the phenotypes difficult to interpret. First, due to the nature of fragment induction, there is a delay between when the fragments start being expressed and onset of the phenotype. The fragment must accumulate to a critical concentration in the cell before it incorporates into the complex and renders an effect. When using a thermo-labile or cold-labile mutant, the phenotype is present within a doubling or so after the temperature shift. Second, although most of the fragments tested here consist of interaction domains only, the dominant negative phenotype may be due to an interaction with other proteins in the cell rather than with the intended target or targets. This can lead to disparities between the dominant negative phenotype and the phenotypes of pure loss-of-function

mutants such as deletions. However, the complexity of the dominant negative phenotypes can present additional opportunities to reveal interesting biology.

In this study, we used self-assembling protein fragments to disrupt homo-and hetero-oligomeric complex formation for ParC, DnaX, and proteins of unknown function. Disruption of the interactions in which the proteins participate allows for the characterization of protein complexes and their heterogeneous interactions *in vivo*. Using the fragments also allows these phenotypes to be mapped onto the structure. My studies illustrate both the complexities and benefits of the dominant negative approach.

ParC333-485 Septation Phenotype

Expression of the ParC333-485 fragment exhibits a mild chaining phenotype in a subset of the cells. These chains extend to about 3-6 cells in length and a mutation in *recA* suppresses this phenotype. Although a direct interaction with XerCD has not been reported, the *recA*-dependence of the phenotype indicates that the Xer-mediated resolution of chromosome dimers is affected.

Resolution of chromosome dimers has been shown to require the C-terminal domain of FtsK (Steiner *et al.*, 1999). This observation suggests that the cell implements a checkpoint designed to couple chromosome segregation and septation. This ensures that each daughter cell receives an accurate, complete copy of the genome. In this study, the ParC333-485 fragment activates the checkpoint that delays the final constriction of the

ring. The specific interactions mediating this response are still unknown, but the *recA*-dependence of the phenotype implicates a functional interaction with XerCD.

Several mechanisms may account for the ParC333-485-mediated delay in septation. First, the checkpoint may be imposed due to the continuous interactions of FtsK with Topo IV, or XerCD. In this manner, Topo IV, XerCD, and FtsK may interact transiently to form a "segregation supercomplex." Upon completion of replication, active Topo IV is formed to unlink catenanes and XerCD resolves chromosome dimers, if any are present. After the chromosomes are completely separated, the termini migrate away from midcell and the septum closes. A second mechanism could be that Topo IV and XerCD interact with the same region of the FtsK CTD one complex at a time. In this mechanism, Topo IV and XerCD would eventually dissociate from FtsK in order for the other to bind. Therefore, after both proteins have left, the septal ring can constrict unimpeded. Third, a constant interaction between FtsK and XerCD may allow the final constriction. In all cases, the ParC333-485 fragment would be interfering with FtsK, XerCD, or both and would result in the inability to resolve chromosome dimers.

ParC206-752 and ParC332-752 Nucleoid Segregation Phenotype

Shifting the *parC1215 (ts)* to the nonpermissive temperature inactivates all complexes very efficiently, resulting in filamented cells with a single mass of intertwined chromosomes located in the center as well as numerous smaller anucleate cells. The fragment overexpression mimics the former component of the *parC1215* phenotype, but

lacks the anucleate cells. While cells harboring the *parC1215 (ts)* allele still exhibit functional septation machinery at the nonpermissive temperature, the cells expressing the ParC206-752 and the ParC332-752 fragment do not form regular septa. This filamentation of these cells is not due to *sulA* induction (data not shown). Therefore, this observation may be due to the interference of the ParC fragments with septal ring proteins or proteins involved in division site selection, such as MinCDE or SlmA proteins.

The proteins encoded by the *minB* operon and *slmA* locus are involved in selecting the site of Z-ring formation. MinCDE is a cell division inhibition system that prevents polymerization of FtsZ at the poles while SlmA inhibits septum formation in regions of the cell containing DNA (Bernhardt and de Boer, 2005; Meinhardt and de Boer, 2001). Even if the fragment phenotype represents what is occurring at early timepoints in the *parC1215 (ts)* mutant, it still would not explain the complete cessation of cell division. The site for the new cell division event is selected before the current round of cell division is complete (Addinall *et al.*, 1997). Therefore, the fragment overexpression may provide a means in which to study interactions between the regulators of cell division and nucleoid-associated proteins.

ParC is localized to the replication fork during replication and is released only after the DNA Polymerase III holoenzyme dissociates at the terminus. At this time, ParC is free to interact with ParE, forming the functional Topo IV complex (Espeli *et al.*, 2003b).

However, this is not the only active Topo IV in the cell; there are other functional Topo IV complexes available for cohesion, unknotting, and supercoiling maintenance.

Topo IV has more independent roles in the cell than any other topoisomerase in the cell. It is involved in decatenation, supercoiling maintenance, chromosome cohesion, and unknotting. The varied nucleoid phenotypes within the ParC206-752 and ParC332-752 filaments may resemble the nucleoid structure of the *parC1215 (ts)* early in its inactivation. If the fragments are unable to infiltrate into preexisting complexes then decatenation may be the first process affected by the fragment, since new Topo IV complexes form at *dif* (Espeli *et al.*, 2003b). As the inert complexes diffuse throughout the cytoplasm, other activities may be affected.

DnaX247-455 Irreversible Growth Defect

The DnaX247-455 fragment expression generates an SOS-dependent filamentation phenotype with a replication defect. Many aspects of the fragment phenotype, like cell filamentation, SOS induction, and abnormal nucleoid organization are consistent with the phenotype of the *dnaX (ts)* alleles. However, the presumed mechanism of negative dominance makes it somewhat surprising that the phenotypes are so similar.

During replication initiation, the DNA Polymerase III holoenzyme is assembled onto the DNA at the origin. Once the replisome is intact, many of the main proteins do not dissociate from the complex until it reaches the terminus region of the chromosome.

Among these processive subunits are the dnaX-encoded tau and the gamma subunits of the clamp loader (Kim *et al.*, 1996b; Wu *et al.*, 1992). Since neither tau nor gamma subunits dissociate from the replisome during elongation, overexpression of the DnaX247-455 would be expected to act at initiation only. However, *dnaA*ts mutants, which block initiation, do not induce the SOS response (Skovgaard and Lobner-Olesen, 2005).

A resolution to this problem is suggested by the phenotype of *dnaC* mutants. DnaC is responsible for loading the helicase onto the single-stranded origin during initiation of replication (Davey *et al.*, 2002) but DnaC is not needed for elongation. The inability to recruit DnaC leaves the origin available to bind RecA, resulting in induction of the SOS response (Lobner-Olesen *et al.*, 2008). DnaX247-455 expression might be expected to interfere with holoenzyme assembly via interactions with either tau or gamma, thereby leaving similar regions of single-stranded DNA at *oriC*.

During elongation, replication forks may stall at spontaneous or induced DNA damage. These types of blocks are present approximately 18% of the time under normal conditions (Maisnier-Patin *et al.*, 2001). In order to salvage the round of replication, origin-independent restart must occur. This may be done either by restarting the existing holoenzyme, or disassembling the original and building anew (Courcelle *et al.*, 1997). However, the fraction of cases that require complete reassembly is unknown. If the holoenzyme must be reassembled at the stalled fork, the DnaX247-455 fragment may

interfere with this assembly. Therefore, use of the fragment can provide information about how often the stalled replication forks require reassembly of the holoenzyme.

Proteins of Unknown Function

Several genome-scale attempts have been made to elucidate y-gene function (Baba *et al.*, 2006; Gerdes *et al.*, 2003). These screens were able to decipher some functions, but a large portion of proteins are still unknown. First, the conditions under which the strains are grown do not require the function of the unknown gene product. In order to define conditions that require the functions of these proteins, phenotypic arrays have been implemented (Ito *et al.*, 2005; Winterberg *et al.*, 2005).

A subset of fragments from proteins of unknown function were found to exhibit media-specific plating defects. The overexpression of the protein fragments yielded effects that were not seen by other overexpression or deletion experiments, even under similar growth conditions (Baba *et al.*, 2006; Kitagawa *et al.*, 2005). In theory, only a subset of the proteins from the total population *in vivo* were partially or fully inactivated in this study. This may make the cell less able to cope with the growth condition, and as a result a phenotype would occur.

REFERENCES

Adams, D.E., Shekhtman, E.M., Zechiedrich, E.L., Schmid, M.B., and Cozzarelli, N.R. (1992) The role of topoisomerase IV in partitioning bacterial replicons and the structure of catenated intermediates in DNA replication. *Cell* **71**: 277-288.

Addinall, S.G., Cao, C., and Lutkenhaus, J. (1997) FtsN, a late recruit to the septum in *Escherichia coli*. *Mol Microbiol* **25**: 303-309.

Andrade, M.A., Perez-Iratxeta, C., and Ponting, C.P. (2001) Protein repeats: structures, functions, and evolution. *J Struct Biol* **134**: 117-131.

Arifuzzaman, M., Maeda, M., Itoh, A., Nishikata, K., Takita, C., Saito, R., Ara, T., Nakahigashi, K., Huang, H.C., Hirai, A., Tsuzuki, K., Nakamura, S., Altaf-Ul-Amin, M., Oshima, T., Baba, T., Yamamoto, N., Kawamura, T., Ioka-Nakamichi, T., Kitagawa, M., Tomita, M., Kanaya, S., Wada, C., and Mori, H. (2006) Large-scale identification of protein-protein interaction of *Escherichia coli* K-12. *Genome Res* **16**: 686-691.

Aussel, L., Barre, F.X., Aroyo, M., Stasiak, A., Stasiak, A.Z., and Sherratt, D. (2002) FtsK is a DNA motor protein that activates chromosome dimer resolution by switching the catalytic state of the XerC and XerD recombinases. *Cell* **108**: 195-205.

Baba, T., Ara, T., Hasegawa, M., Takai, Y., Okumura, Y., Baba, M., Datsenko, K.A., Tomita, M., Wanner, B.L., and Mori, H. (2006) Construction of *Escherichia coli* K-12 in-frame, single-gene knockout mutants: the Keio collection. *Mol Syst Biol* **2**: 2006 0008.

Bahng, S., Mossessova, E., Nurse, P., and Marians, K.J. (2000) Mutational analysis of *Escherichia coli* topoisomerase IV. III. Identification of a region of *parE* involved in covalent catalysis. *J Biol Chem* **275**: 4112-4117.

Bates, D., and Kleckner, N. (2005) Chromosome and replisome dynamics in *E. coli*: loss of sister cohesion triggers global chromosome movement and mediates chromosome segregation. *Cell* **121**: 899-911.

Begg, K.J., Dewar, S.J., and Donachie, W.D. (1995) A new *Escherichia coli* cell division gene, *ftsK*. *J Bacteriol* **177**: 6211-6222.

Bellon, S., Parsons, J.D., Wei, Y., Hayakawa, K., Swenson, L.L., Charifson, P.S., Lippke, J.A., Aldape, R., and Gross, C.H. (2004) Crystal structures of *Escherichia coli* topoisomerase IV ParE subunit (24 and 43 kilodaltons): a single residue dictates differences in novobiocin potency against topoisomerase IV and DNA gyrase. *Antimicrob Agents Chemother* **48**: 1856-1864.

Bernhardt, T.G., and de Boer, P.A. (2003) The *Escherichia coli* amidase AmiC is a periplasmic septal ring component exported via the twin-arginine transport pathway. *Mol Microbiol* **48**: 1171-1182.

Bernhardt, T.G., and de Boer, P.A. (2004) Screening for synthetic lethal mutants in *Escherichia coli* and identification of EnvC (YibP) as a periplasmic septal ring factor with murein hydrolase activity. *Mol Microbiol* **52**: 1255-1269.

Bernhardt, T.G., and de Boer, P.A. (2005) SlmA, a nucleoid-associated, FtsZ binding protein required for blocking septal ring assembly over chromosomes in *E. coli*. *Mol Cell* **18**: 555-564.

Bigot, S., Corre, J., Louarn, J.M., Cornet, F., and Barre, F.X. (2004) FtsK activities in Xer recombination, DNA mobilization and cell division involve overlapping and separate domains of the protein. *Mol Microbiol* **54**: 876-886.

Bigot, S., Saleh, O.A., Cornet, F., Allemand, J.F., and Barre, F.X. (2006) Oriented loading of FtsK on KOPS. *Nat Struct Mol Biol* **13**: 1026-1028.

Bigot, S., Saleh, O.A., Lesterlin, C., Pages, C., El Karoui, M., Dennis, C., Grigoriev, M., Allemand, J.F., Barre, F.X., and Cornet, F. (2005) KOPS: DNA motifs that control *E. coli* chromosome segregation by orienting the FtsK translocase. *EMBO J* **24**: 3770-3780.

Bigot, S., Sivanathan, V., Possoz, C., Barre, F.X., and Cornet, F. (2007) FtsK, a literate chromosome segregation machine. *Mol Microbiol* **64**: 1434-1441.

Blakely, G., Colloms, S., May, G., Burke, M., and Sherratt, D. (1991) *Escherichia coli* XerC recombinase is required for chromosomal segregation at cell division. *New Biol* **3**: 789-798.

Blakely, G., May, G., McCulloch, R., Arciszewska, L.K., Burke, M., Lovett, S.T., and Sherratt, D.J. (1993) Two related recombinases are required for site-specific recombination at *dif* and *cer* in *E. coli* K-12. *Cell* **75**: 351-361.

Blattner, F.R., Plunkett, G., 3rd, Bloch, C.A., Perna, N.T., Burland, V., Riley, M., Collado-Vides, J., Glasner, J.D., Rode, C.K., Mayhew, G.F., Gregor, J., Davis, N.W., Kirkpatrick, H.A., Goeden, M.A., Rose, D.J., Mau, B., and Shao, Y. (1997) The complete genome sequence of *Escherichia coli* K-12. *Science* **277**: 1453-1462.

Blinkova, A., Hervas, C., Stukenberg, P.T., Onrust, R., O'Donnell, M.E., and Walker, J.R. (1993) The *Escherichia coli* DNA polymerase III holoenzyme contains both products of the *dnaX* gene, tau and gamma, but only tau is essential. *J Bacteriol* **175**: 6018-6027.

Bonne, L., Bigot, S., Chevalier, F., Allemand, J.F., and Barre, F.X. (2009) Asymmetric DNA requirements in Xer recombination activation by FtsK. *Nucleic Acids Res* **37**: 2371-2380.

Brendler, T., Sawitzke, J., Sergueev, K., and Austin, S. (2000) A case for sliding SeqA tracts at anchored replication forks during *Escherichia coli* chromosome replication and segregation. *EMBO J* **19**: 6249-6258.

Bruce, I., Hardy, J., and Stacey, K.A. (1984) Potentiation by purines of the growth-inhibitory effects of sulphonamides on *Escherichia coli* K-12 and the location of the gene which mediates this effect. *J Gen Microbiol* **130**: 2489-2495.

Bush, J.W., and Markovitz, A. (1973) The Genetic Basis for Mucoidy and Radiation Sensitivity in *capR* (*lon*) Mutants of *E. coli* K-12. *Genetics* **74**: 215-225.

Butland, G., Peregrin-Alvarez, J.M., Li, J., Yang, W., Yang, X., Canadien, V., Starostine, A., Richards, D., Beattie, B., Krogan, N., Davey, M., Parkinson, J., Greenblatt, J., and Emili, A. (2005) Interaction network containing conserved and essential protein complexes in *Escherichia coli*. *Nature* **433**: 531-537.

Caffrey, D.R., Somaroo, S., Hughes, J.D., Mintseris, J., and Huang, E.S. (2004) Are protein-protein interfaces more conserved in sequence than the rest of the protein surface? *Protein Sci* **13**: 190-202.

Caldas, T., Malki, A., Kern, R., Abdallah, J., and Richarme, G. (2006) The *Escherichia coli* thioredoxin homolog YbbN/Trxsc is a chaperone and a weak protein oxidoreductase. *Biochem Biophys Res Commun* **343**: 780-786.

Capiaux, H., Lesterlin, C., Perals, K., Louarn, J.M., and Cornet, F. (2002) A dual role for the FtsK protein in *Escherichia coli* chromosome segregation. *EMBO Rep* **3**: 532-536.

Carr, K.M., and Kaguni, J.M. (2002) *Escherichia coli* DnaA protein loads a single DnaB helicase at a DnaA box hairpin. *J Biol Chem* **277**: 39815-39822.

Chen, C.R., Malik, M., Snyder, M., and Drlica, K. (1996) DNA gyrase and topoisomerase IV on the bacterial chromosome: quinolone-induced DNA cleavage. *J Mol Biol* **258**: 627-637.

Corbett, K.D., Schoeffler, A.J., Thomsen, N.D., and Berger, J.M. (2005) The structural basis for substrate specificity in DNA topoisomerase IV. *J Mol Biol* **351**: 545-561.

Courcelle, J., Carswell-Crumpton, C., and Hanawalt, P.C. (1997) *recF* and *recR* are required for the resumption of replication at DNA replication forks in *Escherichia coli*. *Proc Natl Acad Sci USA* **94**: 3714-3719.

Cui, Y., Petrushenko, Z.M., and Rybenkov, V.V. (2008) MukB acts as a macromolecular clamp in DNA condensation. *Nat Struct Mol Biol* **15**: 411-418.

Daley, D.O., Rapp, M., Granseth, E., Melen, K., Drew, D., and von Heijne, G. (2005) Global topology analysis of the *Escherichia coli* inner membrane proteome. *Science* **308**: 1321-1323.

Davey, M.J., Fang, L., McInerney, P., Georgescu, R.E., and O'Donnell, M. (2002) The DnaC helicase loader is a dual ATP/ADP switch protein. *EMBO J* **21**: 3148-3159.

Deibler, R.W., Rahmati, S., and Zechiedrich, E.L. (2001) Topoisomerase IV, alone, unknots DNA in *E. coli*. *Genes Dev* **15**: 748-761.

DeLisa, M.P., Wu, C.F., Wang, L., Valdes, J.J., and Bentley, W.E. (2001) DNA microarray-based identification of genes controlled by autoinducer 2-stimulated quorum sensing in *Escherichia coli*. *J Bacteriol* **183**: 5239-5247.

Diez, A.A., Farewell, A., Nannmark, U., and Nystrom, T. (1997) A mutation in the *ftsK* gene of *Escherichia coli* affects cell-cell separation, stationary-phase survival, stress adaptation, and expression of the gene encoding the stress protein UspA. *J Bacteriol* **179**: 5878-5883.

Englesberg, E., Anderson, R.L., Weinberg, R., Lee, N., Hoffee, P., Huttenhauer, G., and Boyer, H. (1962) L-Arabinose-sensitive, L-ribulose 5-phosphate 4-epimerase-deficient mutants of *Escherichia coli*. *J Bacteriol* **84**: 137-146.

Espeli, O., Lee, C., and Marians, K.J. (2003a) A physical and functional interaction between *Escherichia coli* FtsK and topoisomerase IV. *J Biol Chem* **278**: 44639-44644.

Espeli, O., Levine, C., Hassing, H., and Marians, K.J. (2003b) Temporal regulation of topoisomerase IV activity in *E. coli*. *Mol Cell* **11**: 189-201.

Espeli, O., Nurse, P., Levine, C., Lee, C., and Marians, K.J. (2003c) SetB: an integral membrane protein that affects chromosome segregation in *Escherichia coli*. *Mol Microbiol* **50**: 495-509.

Fernandez De Henestrosa, A.R., Ogi, T., Aoyagi, S., Chafin, D., Hayes, J.J., Ohmori, H., and Woodgate, R. (2000) Identification of additional genes belonging to the LexA regulon in *Escherichia coli*. *Mol Microbiol* **35**: 1560-1572.

Filip, C.C., Allen, J.S., Gustafson, R.A., Allen, R.G., and Walker, J.R. (1974) Bacterial cell division regulation: characterization of the *dnaH* locus of *Escherichia coli*. *J Bacteriol* **119**: 443-449.

Flower, A.M., and McHenry, C.S. (1990) The gamma subunit of DNA polymerase III holoenzyme of *Escherichia coli* is produced by ribosomal frameshifting. *Proc Natl Acad Sci USA* **87**: 3713-3717.

Gao, D., and McHenry, C.S. (2001) tau binds and organizes *Escherichia coli* replication proteins through distinct domains. Domain IV, located within the unique C terminus of tau, binds the replication fork, helicase, DnaB. *J Biol Chem* **276**: 4441-4446.

Geissler, B., and Margolin, W. (2005) Evidence for functional overlap among multiple bacterial cell division proteins: compensating for the loss of FtsK. *Mol Microbiol* **58**: 596-612.

Gerdes, S.Y., Scholle, M.D., Campbell, J.W., Balazsi, G., Ravasz, E., Daugherty, M.D., Somera, A.L., Kyrpides, N.C., Anderson, I., Gelfand, M.S., Bhattacharya, A., Kapatral, V., D'Souza, M., Baev, M.V., Grechkin, Y., Mseeh, F., Fonstein, M.Y., Overbeek, R., Barabasi, A.L., Oltvai, Z.N., and Osterman, A.L. (2003) Experimental determination and system level analysis of essential genes in *Escherichia coli* MG1655. *J Bacteriol* **185**: 5673-5684.

Gerding, M.A., Ogata, Y., Pecora, N.D., Niki, H., and de Boer, P.A. (2007) The trans-envelope Tol-Pal complex is part of the cell division machinery and required for proper outer-membrane invagination during cell constriction in *E. coli*. *Mol Microbiol* **63**: 1008-1025.

Glover, B.P., and McHenry, C.S. (2000) The DnaX-binding subunits delta' and psi are bound to gamma and not tau in the DNA polymerase III holoenzyme. *J Biol Chem* **275**: 3017-3020.

Goodsell, D.S., and Olson, A.J. (2000) Structural symmetry and protein function. *Annu Rev Biophys Biomol Struct* **29**: 105-153.

Gordon, G.S., and Wright, A. (2000) DNA segregation in bacteria. *Annu Rev Microbiol* **54**: 681-708.

Graham, J.E., Sivanathan, V., Sherratt, D.J., and Arciszewska, L.K. (2010) FtsK translocation on DNA stops at XerCD-*dif*. *Nucleic Acids Res* **38**: 72-81.

Grainge, I., Bregu, M., Vazquez, M., Sivanathan, V., Ip, S.C., and Sherratt, D.J. (2007) Unlinking chromosome catenanes *in vivo* by site-specific recombination. *EMBO J* **26**: 4228-4238.

Gruger, T., Nitiss, J.L., Maxwell, A., Zechiedrich, E.L., Heisig, P., Seeber, S., Pommier, Y., and Strumberg, D. (2004) A mutation in *Escherichia coli* DNA gyrase conferring quinolone resistance results in sensitivity to drugs targeting eukaryotic topoisomerase II. *Antimicrob Agents Chemother* **48**: 4495-4504.

Hale, C.A., and de Boer, P.A. (2002) ZipA is required for recruitment of FtsK, FtsQ, FtsL, and FtsN to the septal ring in *Escherichia coli*. *J Bacteriol* **184**: 2552-2556.

Hansen, E.B., Atlung, T., Hansen, F.G., Skovgaard, O., and von Meyenburg, K. (1984) Fine structure genetic map and complementation analysis of mutations in the *dnaA* gene of *Escherichia coli*. *Mol Gen Genet* **196**: 387-396.

Hardy, C.D., and Cozzarelli, N.R. (2003) Alteration of *Escherichia coli* topoisomerase IV to novobiocin resistance. *Antimicrob Agents Chemother* **47**: 941-947.

Heidrich, C., Templin, M.F., Ursinus, A., Merdanovic, M., Berger, J., Schwarz, H., de Pedro, M.A., and Holtje, J.V. (2001) Involvement of N-acetylmuramyl-L-alanine amidases in cell separation and antibiotic-induced autolysis of *Escherichia coli*. *Mol Microbiol* **41**: 167-178.

Hendricks, E.C., Szerlong, H., Hill, T., and Kuempel, P. (2000) Cell division, guillotining of dimer chromosomes and SOS induction in resolution mutants (*dif*, *xerC* and *xerD*) of *Escherichia coli*. *Mol Microbiol* **36**: 973-981.

Henson, J.M., Chu, H., Irwin, C.A., and Walker, J.R. (1979) Isolation and characterization of *dnaX* and *dnaY* temperature-sensitive mutants of *Escherichia coli*. *Genetics* **92**: 1041-1059.

Herskowitz, I. (1987) Functional inactivation of genes by dominant negative mutations. *Nature* **329**: 219-222.

Hiasa, H., and Marians, K.J. (1992) Differential inhibition of the DNA translocation and DNA unwinding activities of DNA helicases by the *Escherichia coli* Tus protein. *J Biol Chem* **267**: 11379-11385.

Hojgaard, A., Szerlong, H., Tabor, C., and Kuempel, P. (1999) Norfloxacin-induced DNA cleavage occurs at the *dif* resolvase locus in *Escherichia coli* and is the result of interaction with topoisomerase IV. *Mol Microbiol* **33**: 1027-1036.

Hu, Z., and Lutkenhaus, J. (2000) Analysis of MinC reveals two independent domains involved in interaction with MinD and FtsZ. *J Bacteriol* **182**: 3965-3971.

Hyrien, O. (2000) Mechanisms and consequences of replication fork arrest. *Biochimie* **82**: 5-17.

Ishino, F., Park, W., Tomioka, S., Tamaki, S., Takase, I., Kunugita, K., Matsuzawa, H., Asoh, S., Ohta, T., Spratt, B.G., and et al. (1986) Peptidoglycan synthetic activities in membranes of *Escherichia coli* caused by overproduction of penicillin-binding protein 2 and RodA protein. *J Biol Chem* **261**: 7024-7031.

Ito, M., Baba, T., and Mori, H. (2005) Functional analysis of 1440 *Escherichia coli* genes using the combination of knock-out library and phenotype microarrays. *Metab Eng* **7**: 318-327.

Jaffe, A., D'Ari, R., and Hiraga, S. (1988) Minicell-forming mutants of *Escherichia coli*: production of minicells and anucleate rods. *J Bacteriol* **170**: 3094-3101.

Jarvik, J., and Botstein, D. (1973) A genetic method for determining the order of events in a biological pathway. *Proc Natl Acad Sci USA* **70**: 2046-2050.

Jeruzalmi, D., O'Donnell, M., and Kuriyan, J. (2001a) Crystal structure of the processivity clamp loader gamma (gamma) complex of *E. coli* DNA polymerase III. *Cell* **106**: 429-441.

Jeruzalmi, D., Yurieva, O., Zhao, Y., Young, M., Stewart, J., Hingorani, M., O'Donnell, M., and Kuriyan, J. (2001b) Mechanism of processivity clamp opening by the delta subunit wrench of the clamp loader complex of *E. coli* DNA polymerase III. *Cell* **106**: 417-428.

Kamada, K., Ohsumi, K., Horiuchi, T., Shimamoto, N., and Morikawa, K. (1996) Crystallization and preliminary X-ray analysis of the *Escherichia coli* replication terminator protein complexed with DNA. *Proteins* **24**: 402-403.

Kang, S., Han, J.S., Park, J.H., Skarstad, K., and Hwang, D.S. (2003) SeqA protein stimulates the relaxing and decatenating activities of topoisomerase IV. *J Biol Chem* **278**: 48779-48785.

Kato, J., Nishimura, Y., Imamura, R., Niki, H., Hiraga, S., and Suzuki, H. (1990) New topoisomerase essential for chromosome segregation in *E. coli*. *Cell* **63**: 393-404.

Kato, J., Nishimura, Y., Yamada, M., Suzuki, H., and Hirota, Y. (1988) Gene organization in the region containing a new gene involved in chromosome partition in *Escherichia coli*. *J Bacteriol* **170**: 3967-3977.

Keyer, K., Gort, A.S., and Imlay, J.A. (1995) Superoxide and the production of oxidative DNA damage. *J Bacteriol* **177**: 6782-6790.

Khil, P.P., and Camerini-Otero, R.D. (2002) Over 1000 genes are involved in the DNA damage response of *Escherichia coli*. *Mol Microbiol* **44**: 89-105.

Khodursky, A.B., and Cozzarelli, N.R. (1998) The mechanism of inhibition of topoisomerase IV by quinolone antibacterials. *J Biol Chem* **273**: 27668-27677.

Khodursky, A.B., Peter, B.J., Schmid, M.B., DeRisi, J., Botstein, D., Brown, P.O., and Cozzarelli, N.R. (2000) Analysis of topoisomerase function in bacterial replication fork movement: use of DNA microarrays. *Proc Natl Acad Sci USA* **97**: 9419-9424.

Kim, S., Dallmann, H.G., McHenry, C.S., and Marians, K.J. (1996a) Tau couples the leading-and lagging-strand polymerases at the *Escherichia coli* DNA replication fork. *J Biol Chem* **271**: 21406-21412.

Kim, S., Dallmann, H.G., McHenry, C.S., and Marians, K.J. (1996b) Tau protects beta in the leading-strand polymerase complex at the replication fork. *J Biol Chem* **271**: 4315-4318.

Kitagawa, M., Ara, T., Arifuzzaman, M., Ioka-Nakamichi, T., Inamoto, E., Toyonaga, H., and Mori, H. (2005) Complete set of ORF clones of *Escherichia coli* ASKA library (a complete set of *E. coli* K-12 ORF archive): unique resources for biological research. *DNA Res* **12**: 291-299.

Kodaira, M., Biswas, S.B., and Kornberg, A. (1983) The *dnaX* gene encodes the DNA polymerase III holoenzyme tau subunit, precursor of the gamma subunit, the *dnaZ* gene product. *Mol Gen Genet* **192**: 80-86.

Kruse, T., Moller-Jensen, J., Lobner-Olesen, A., and Gerdes, K. (2003) Dysfunctional MreB inhibits chromosome segregation in *Escherichia coli*. *EMBO J* **22**: 5283-5292.

Kthiri, F., Le, H.T., Tagourti, J., Kern, R., Malki, A., Caldas, T., Abdallah, J., Landoulsi, A., and Richarme, G. (2008) The thioredoxin homolog YbbN functions as a chaperone rather than as an oxidoreductase. *Biochem Biophys Res Commun* **374**: 668-672.

Kuempel, P.L., Henson, J.M., Dircks, L., Tecklenburg, M., and Lim, D.F. (1991) *dif*, a *recA*-independent recombination site in the terminus region of the chromosome of *Escherichia coli*. *New Biol* **3**: 799-811.

Kuhn, J., and Somerville, R.L. (1971) Mutant strains of *Escherichia coli* K-12 that use D-amino acids. *Proc Natl Acad Sci USA* **68**: 2484-2487.

Lobner-Olesen, A., Slominska-Wojewodzka, M., Hansen, F.G., and Marinus, M.G. (2008) DnaC inactivation in *Escherichia coli* K-12 induces the SOS response and expression of nucleotide biosynthesis genes. *PLoS One* **3**: e2984.

Lopez, C.R., Yang, S., Deibler, R.W., Ray, S.A., Pennington, J.M., Digate, R.J., Hastings, P.J., Rosenberg, S.M., and Zechiedrich, E.L. (2005) A role for topoisomerase III in a recombination pathway alternative to RuvABC. *Mol Microbiol* **58**: 80-101.

Lowe, J., Ellonen, A., Allen, M.D., Atkinson, C., Sherratt, D.J., and Grainge, I. (2008) Molecular mechanism of sequence-directed DNA loading and translocation by FtsK. *Mol Cell* **31**: 498-509.

Madabhushi, R., and Marians, K.J. (2009) Actin homolog MreB affects chromosome segregation by regulating topoisomerase IV in *Escherichia coli*. *Mol Cell* **33**: 171-180.

Maisnier-Patin, S., Nordstrom, K., and Dasgupta, S. (2001) Replication arrests during a single round of replication of the *Escherichia coli* chromosome in the absence of DnaC activity. *Mol Microbiol* **42**: 1371-1382.

Maisonneuve, E., Fraysse, L., Moinier, D., and Dukan, S. (2008) Existence of abnormal protein aggregates in healthy *Escherichia coli* cells. *J Bacteriol* **190**: 887-893.

Maki, H., Maki, S., and Kornberg, A. (1988) DNA Polymerase III holoenzyme of *Escherichia coli*. IV. The holoenzyme is an asymmetric dimer with twin active sites. *J Biol Chem* **263**: 6570-6578.

Marians, K.J., Minden, J.S., and Parada, C. (1986) Replication of superhelical DNAs *in vitro*. *Prog Nucleic Acid Res Mol Biol* **33**: 111-140.

Marino-Ramirez, L., Minor, J.L., Reading, N., and Hu, J.C. (2004) Identification and mapping of self-assembling protein domains encoded by the *Escherichia coli* K-12 genome by use of lambda repressor fusions. *J Bacteriol* **186**: 1311-1319.

Marszalek, J., and Kaguni, J.M. (1994) DnaA protein directs the binding of DnaB protein in initiation of DNA replication in *Escherichia coli*. *J Biol Chem* **269**: 4883-4890.

Meinhardt, H., and de Boer, P.A. (2001) Pattern formation in *Escherichia coli*: a model for the pole-to-pole oscillations of Min proteins and the localization of the division site. *Proc Natl Acad Sci USA* **98**: 14202-14207.

Mercer, K.L., and Weiss, D.S. (2002) The *Escherichia coli* cell division protein FtsW is required to recruit its cognate transpeptidase, FtsI (PBP3), to the division site. *J Bacteriol* **184**: 904-912.

Michel, B. (2000) Replication fork arrest and DNA recombination. *Trends Biochem Sci* **25**: 173-178.

Miller, J.H. (1972) *Experiments in Molecular Genetics*. Cold Spring Harbor, NY: Cold Spring Harbor Laboratory Press.

Miller, J.H., Suthar, A., Tai, J., Yeung, A., Truong, C., and Stewart, J.L. (1999) Direct selection for mutators in *Escherichia coli*. *J Bacteriol* **181**: 1576-1584.

Munch-Petersen, A., Nygaard, P., Hammer-Jespersen, K., and Fiil, N. (1972) Mutants constitutive for nucleoside-catabolizing enzymes in *Escherichia coli* K-12. Isolation, characterization and mapping. *Eur J Biochem* **27**: 208-215.

Neylon, C., Brown, S.E., Kralicek, A.V., Miles, C.S., Love, C.A., and Dixon, N.E. (2000) Interaction of the *Escherichia coli* replication terminator protein (Tus) with DNA: a model derived from DNA-binding studies of mutant proteins by surface plasmon resonance. *Biochemistry* **39**: 11989-11999.

Niki, H., Jaffe, A., Imamura, R., Ogura, T., and Hiraga, S. (1991) The new gene *mukB* codes for a 177 kd protein with coiled-coil domains involved in chromosome partitioning of *E. coli*. *EMBO J* **10**: 183-193.

Ninfa, A.J., Reitzer, L.J., and Magasanik, B. (1987) Initiation of transcription at the bacterial *glnAp2* promoter by purified *E. coli* components is facilitated by enhancers. *Cell* **50**: 1039-1046.

Nooren, I.M., and Thornton, J.M. (2003) Structural characterisation and functional significance of transient protein-protein interactions. *J Mol Biol* **325**: 991-1018.

Nurse, P., Levine, C., Hassing, H., and Marians, K.J. (2003) Topoisomerase III can serve as the cellular decatenase in *Escherichia coli*. *J Biol Chem* **278**: 8653-8660.

Osawa, M., Anderson, D.E., and Erickson, H.P. (2009) Curved FtsZ protofilaments generate bending forces on liposome membranes. *EMBO J* **28**: 3476-3484.

Peng, H., and Marians, K.J. (1993) *Escherichia coli* topoisomerase IV. Purification, characterization, subunit structure, and subunit interactions. *J Biol Chem* **268**: 24481-24490.

Perals, K., Cornet, F., Merlet, Y., Delon, I., and Louarn, J.M. (2000) Functional polarization of the *Escherichia coli* chromosome terminus: the *dif* site acts in chromosome dimer resolution only when located between long stretches of opposite polarity. *Mol Microbiol* **36**: 33-43.

Peter, B.J., Arsuaga, J., Breier, A.M., Khodursky, A.B., Brown, P.O., and Cozzarelli, N.R. (2004) Genomic transcriptional response to loss of chromosomal supercoiling in *Escherichia coli*. *Genome Biol* **5**: R87.

Pichoff, S., and Lutkenhaus, J. (2002) Unique and overlapping roles for ZipA and FtsA in septal ring assembly in *Escherichia coli*. *EMBO J* **21**: 685-693.

Pisabarro, A.G., Prats, R., Vaquez, D., and Rodriguez-Tebar, A. (1986) Activity of penicillin-binding protein 3 from *Escherichia coli*. *J Bacteriol* **168**: 199-206.

Popham, D.L., Szeto, D., Keener, J., and Kustu, S. (1989) Function of a bacterial activator protein that binds to transcriptional enhancers. *Science* **243**: 629-635.

Priyadarshini, R., de Pedro, M.A., and Young, K.D. (2007) Role of peptidoglycan amidases in the development and morphology of the division septum in *Escherichia coli*. *J Bacteriol* **189**: 5334-5347.

Priyadarshini, R., Popham, D.L., and Young, K.D. (2006) Daughter cell separation by penicillin-binding proteins and peptidoglycan amidases in *Escherichia coli*. *J Bacteriol* **188**: 5345-5355.

Raskin, D.M., and de Boer, P.A. (1999) Rapid pole-to-pole oscillation of a protein required for directing division to the middle of *Escherichia coli*. *Proc Natl Acad Sci USA* **96**: 4971-4976.

RayChaudhuri, D., Gordon, G.S., and Wright, A. (2000) How does a bacterium find its middle? *Nat Struct Biol* **7**: 997-999.

Recchia, G.D., Aroyo, M., Wolf, D., Blakely, G., and Sherratt, D.J. (1999) FtsK-dependent and -independent pathways of Xer site-specific recombination. *EMBO J* **18**: 5724-5734.

Riley, M., Abe, T., Arnaud, M.B., Berlyn, M.K., Blattner, F.R., Chaudhuri, R.R., Glasner, J.D., Horiuchi, T., Keseler, I.M., Kosuge, T., Mori, H., Perna, N.T., Plunkett, G., 3rd, Rudd, K.E., Serres, M.H., Thomas, G.H., Thomson, N.R., Wishart, D., and Wanner, B.L. (2006) *Escherichia coli* K-12: a cooperatively developed annotation snapshot--2005. *Nucleic Acids Res* **34**: 1-9.

Rothstein, R., Michel, B., and Gangloff, S. (2000) Replication fork pausing and recombination or "gimme a break". *Genes Dev* **14**: 1-10.

Saleh, O.A., Perals, C., Barre, F.X., and Allemand, J.F. (2004) Fast, DNA-sequence independent translocation by FtsK in a single-molecule experiment. *EMBO J* **23**: 2430-2439.

Scheffers, D.J., de Wit, J.G., den Blaauwen, T., and Driessen, A.J. (2002) GTP hydrolysis of cell division protein FtsZ: evidence that the active site is formed by the association of monomers. *Biochemistry* **41**: 521-529.

Seigneur, M., Bidnenko, V., Ehrlich, S.D., and Michel, B. (1998) RuvAB acts at arrested replication forks. *Cell* **95**: 419-430.

Seitz, H., Weigel, C., and Messer, W. (2000) The interaction domains of the DnaA and DnaB replication proteins of *Escherichia coli*. *Mol Microbiol* **37**: 1270-1279.

Skovgaard, O., and Lobner-Olesen, A. (2005) Reduced initiation frequency from *oriC* restores viability of a temperature-sensitive *Escherichia coli* replisome mutant. *Microbiology* **151**: 963-973.

Steiner, W., Liu, G., Donachie, W.D., and Kuempel, P. (1999) The cytoplasmic domain of FtsK protein is required for resolution of chromosome dimers. *Mol Microbiol* **31**: 579-583.

Steiner, W.W., and Kuempel, P.L. (1998a) Cell division is required for resolution of dimer chromosomes at the *dif* locus of *Escherichia coli*. *Mol Microbiol* **27**: 257-268.

Steiner, W.W., and Kuempel, P.L. (1998b) Sister chromatid exchange frequencies in *Escherichia coli* analyzed by recombination at the *dif* resolvase site. *J Bacteriol* **180**: 6269-6275.

Studwell-Vaughan, P.S., and O'Donnell, M. (1991) Constitution of the twin polymerase of DNA polymerase III holoenzyme. *J Biol Chem* **266**: 19833-19841.

Sugino, A., Higgins, N.P., and Cozzarelli, N.R. (1980) DNA gyrase subunit stoichiometry and the covalent attachment of subunit A to DNA during DNA cleavage. *Nucleic Acids Res* **8**: 3865-3874.

Sunako, Y., Onogi, T., and Hiraga, S. (2001) Sister chromosome cohesion of *Escherichia coli*. *Mol Microbiol* **42**: 1233-1241.

Sutton, M.D. (2004) The *Escherichia coli dnaN159* mutant displays altered DNA polymerase usage and chronic SOS induction. *J Bacteriol* **186**: 6738-6748.

Takata, M., Guo, L., Katayama, T., Hase, M., Seyama, Y., Miki, T., and Sekimizu, K. (2000) Mutant DnaA proteins defective in duplex opening of *oriC*, the origin of chromosomal DNA replication in *Escherichia coli*. *Mol Microbiol* **35**: 454-462.

Ursinus, A., and Holtje, J.V. (1994) Purification and properties of a membrane-bound lytic transglycosylase from *Escherichia coli*. *J Bacteriol* **176**: 338-343.

Wang, L., Li, J., March, J.C., Valdes, J.J., and Bentley, W.E. (2005) *luxS*-dependent gene regulation in *Escherichia coli* K-12 revealed by genomic expression profiling. *J Bacteriol* **187**: 8350-8360.

Wang, L., and Lutkenhaus, J. (1998) FtsK is an essential cell division protein that is localized to the septum and induced as part of the SOS response. *Mol Microbiol* **29**: 731-740.

Wang, X., Reyes-Lamothe, R., and Sherratt, D.J. (2008) Modulation of *Escherichia coli* sister chromosome cohesion by topoisomerase IV. *Genes Dev* **22**: 2426-2433.

Winterberg, K.M., Luecke, J., Bruegl, A.S., and Reznikoff, W.S. (2005) Phenotypic screening of *Escherichia coli* K-12 Tn5 insertion libraries, using whole-genome oligonucleotide microarrays. *Appl Environ Microbiol* **71**: 451-459.

Wissel, M.C., and Weiss, D.S. (2004) Genetic analysis of the cell division protein FtsI (PBP3): amino acid substitutions that impair septal localization of FtsI and recruitment of FtsN. *J Bacteriol* **186**: 490-502.

Woldringh, C.L., Mulder, E., Huls, P.G., and Vischer, N. (1991) Toporegulation of bacterial division according to the nucleoid occlusion model. *Res Microbiol* **142**: 309-320.

Wu, C.A., Zechner, E.L., Hughes, A.J., Jr., Franden, M.A., McHenry, C.S., and Marians, K.J. (1992) Coordinated leading-and lagging-strand synthesis at the *Escherichia coli* DNA replication fork. IV. Reconstitution of an asymmetric, dimeric DNA polymerase III holoenzyme. *J Biol Chem* **267**: 4064-4073.

Yates, J., Zhekov, I., Baker, R., Eklund, B., Sherratt, D.J., and Arciszewska, L.K. (2006) Dissection of a functional interaction between the DNA translocase, FtsK, and the XerD recombinase. *Mol Microbiol* **59**: 1754-1766.

Yokochi, T., Kato, J., and Ikeda, H. (1996) DNA nicking by *Escherichia coli* topoisomerase IV with a substitution mutation from tyrosine to histidine at the active site. *Genes Cells* **1**: 1069-1075.

Yu, X.C., Weihe, E.K., and Margolin, W. (1998) Role of the C terminus of FtsK in *Escherichia coli* chromosome segregation. *J Bacteriol* **180**: 6424-6428.

Zechiedrich, E.L., Khodursky, A.B., Bachellier, S., Schneider, R., Chen, D., Lilley, D.M., and Cozzarelli, N.R. (2000) Roles of topoisomerases in maintaining steady-state DNA supercoiling in *Escherichia coli*. *J Biol Chem* **275**: 8103-8113.

Zechiedrich, E.L., Khodursky, A.B., and Cozzarelli, N.R. (1997) Topoisomerase IV, not gyrase, decatenates products of site-specific recombination in *Escherichia coli*. *Genes Dev* **11**: 2580-2592.

Zhao, K., Liu, M., and Burgess, R.R. (2005) The global transcriptional response of *Escherichia coli* to induced sigma 32 protein involves sigma 32 regulon activation followed by inactivation and degradation of sigma 32 *in vivo*. *J Biol Chem* **280**: 17758-17768.

Zheng, D., Constantinidou, C., Hobman, J.L., and Minchin, S.D. (2004) Identification of the CRP regulon using *in vitro* and *in vivo* transcriptional profiling. *Nucleic Acids Res* **32**: 5874-5893.

VITA

Name:	Adrienne Elizabeth Zweifel
Address:	Dept. of Biochemistry and Biophysics, Texas A&M University, 2128 TAMU, College Station, TX 77843-2128
Email Address:	azweifel@gmail.com
Education:	B.S., Biochemistry, University of Missouri-Columbia, 2001 Ph.D., Biochemistry, Texas A&M University, 2010